HIGH PRESSURE VAPOUR-LIQUID EQUILIBRIUM DATA OF FLUOROCHEMICAL SYSTEMS FOR VARIOUS TEMPERATURES USING A NEW STATIC APPARATUS

by:

Mulamba Marc Tshibangu

[B. Eng. (Chem.)]

University of Lubumbashi (D R Congo)

In fulfillment of the degree of Master of Science, Faculty of Engineering,
School of Chemical Engineering, University of KwaZulu-Natal

Supervisor: Prof. Deresh Ramjugernath

Co-supervisors: Dr. Paramespri Naidoo and Dr. Christophe Coquelet

April 2010

DECLARATION

I, Mulamba Marc Tshibangu, declare that:

(i) The research reported in this dissertation, except where otherwise indicated, is my original work.

(ii) This dissertation has not been submitted for any degree or examination at any university.

(iii) This dissertation does not contain other person's data, pictures, graphs or other information, unless specifically acknowledged as being sourced from other persons.

(iv) This dissertation does not contain other person's writing, unless specifically acknowledged as being sourced from other researchers. Where other written sources have been quoted then:

a) Their words have been re-written but the general information attributed to them has been referenced;

b) Where their exact words have been used, their writing has been placed inside quotation marks, and referenced.

(v) Where I have reproduced a publication of which I am an author or co-author I have indicated in detail which part of the publication was actually written by myself alone and have fully referenced such publications:

(vi) This dissertation does not contain text, graphics or tables copied and pasted from the internet, unless specifically acknowledged, and the source are detailed in the dissertation and in the References sections.

_____ _____

MM Tshibangu (candidate) Date

As the candidate's supervisor I agree/ do not agree to the submission of this dissertation.

_____ _____

Prof. D. Ramjugernath Date

ACKNOWLEDGEMENTS

I would like to take this opportunity and extend my heartfelt gratitude to different people and organization that aided in the completion of this work.

- First and foremost, Jesus-Christ, my Lord and savior, who makes a way where there seems to be no way.

- My supervisor and co-supervisors Professor D. Ramjugernath, Doctor P. Naidoo and Doctor C. Coquelet, respectively. Their expert knowledge, tireless support and wisdom are acknowledged. It has been a real blessing working with them.

- The technical staff of the School of Chemical Engineering, Kelly Robertson, Ken Jack, Lindinkosi Mkize and Ayanda Khanyile for their comprehension and availability when needed.

- To the National Research Foundation for financial support.

- To my colleagues in the Thermodynamic Research Unit and friends: Jim Chiyen, Xavier Courtial, Kaniki Tumba, Caleb Narasigadu, Samuel Iwarere, Magret Tadie, Serge Mapan, Youdeshne Perumal, Christian & Helen Mulol, Joseph Bwapwa, Francois Kabulu, Tresor Kalambayi, Betty Kasonde, Sandra Tshibangu and Babbis Kashironge.

- Last but not least, to my lovely and wonderful parents for their prayer, love and support: my father, Kayembe Tshikala and my mum, Ngalula Malu.

ABSTRACT

The thermodynamic knowledge of accurate phase equilibrium data plays an important role in the design and optimization of separation processes in chemical and engineering industries. Vapour-liquid equilibrium data are essential for the design of efficient separation processes such as distillation.

The presented research study is mainly focused on the vapour-liquid equilibrium data measurement of fluorochemical and hydrocarbon binary systems at various temperatures and at high pressures.

A new static analytical apparatus was constructed and commissioned for the measurement of accurate and precise vapour-liquid equilibrium data at temperatures and absolute pressures ranging from low temperatures to 323.15 K and 0 to 10 MPa respectively. The new apparatus incorporates the ROLSI ^{TM} sampler, a sampling technique developed by the CEP/TEP laboratory in Fontainebleau, France.

Isothermal high pressure VLE data were measured for three binary systems comprising of hexafluoroethane (R116) + propane, HFPO + propane and ethane + octafluoropropane (R218).

The R116 + propane system at 263.15 K was measured as a test system using the new static apparatus. These measurements helped to confirm the functioning of the experimental apparatus. The reliability and the reproducibility of the experimental procedure were also checked. The data obtained were in excellent agreement with data in the literature. Thereafter, measurements of previously unmeasured systems were undertaken.

Isothermal vapour-liquid equilibrium data measurements for the ethane + octafluoropropane system were performed at five isotherms with temperatures and pressures ranging from 264.05 to 308.04 K and 0.298 to 4.600 MPa respectively. The five isotherms constitute new experimental data.

The HFPO + propane system was also investigated and vapour-liquid equilibrium data were measured at three isotherms (283.05, 303.05 and 323.05 K) with pressures ranging from 0.437 to 2.000 MPa. The data measured also constitute a set of a new HPVLE data.

The uncertainties in the measurement for both systems were within ± 0.09 K, ± 0.0016 MPa and less than 2% for temperatures, pressures and mole fractions, respectively.

All experimental data were correlated via the direct method using the Peng-Robinson equation of state with the Mathias-Copeman alpha function and the Wong-Sandler mixing rules incorporating the NRTL activity coefficient model.

The consistency of the measured VLE data was tested using the Van Ness point test which yielded few points of difference between the measured and calculated data, suggesting a low error rate.

TABLE OF CONTENTS

LIST OF FIGURES

LIST OF PHOTOGRAPHS

CHAPTER FOUR: EXPERIMENTAL APPARATUS

LIST OF TABLES

CHAPTER FIVE: EXPERIMENTAL PROCEDURE

CHAPTER SIX: RESULTS AND DISCUSSION

NOMENCLATURE

Symbols

a	Parameter, cubic equation of state
a	Parameter, Tsonopoulos correlation
a_i	Activity, pure species i
A	Parameter, empirical equations
b	Parameter, cubic equation of state
B	Second virial coefficient
C	Third virial coefficient
C	Parameter, empirical equations
C_i	Adjustable parameters (Peng-Robinson EoS)
D	Fourth virial coefficient
f_i	Fugacity, pure species i
G	Molar or specific Gibbs free energy
ΔG	Gibbs-energy change of mixing
H_i	Enthalpy, species i in solution
k_{ij}	Binary interaction parameter
l	Parameter in the UNIQUAC liquid-phase model
m	Parameter, Wilson's approach
M	Molar or specific value, extensive thermodynamic property

n	Number of moles
n_i	Number of moles, species i
P	Absolute pressure
q	Relative molecular surface
r	Relative molecular volume
R	Universal gas constant
S_i	Entropy, species i in solution
T	Absolute temperature
V	Molar or specific volume
x_i	Mole fraction, species i, liquid phase
y_i	Mole fraction, species i, liquid phase
z	Co-ordination number
Z	Compressibility factor

Greek letters

α	Function, cubic equation of state
α	The non-random parameter in the NRTL liquid-phase model
Γ_i	Integration constant
γ_i	Activity coefficient, species i in solution
λ	Energetic interaction terms for the Wilson equation
μ_i	Chemical potential, species i
τ	Adjustable parameter in the NRTL liquid-phase model

θ	Area fraction in the UNIQUAC liquid-phase model
Φ_i	Ratio of fugacity coefficients and Poynting correction factor
ϕ_i	Fugacity coefficient, pure species i
Ω	Constant, cubic equation of state
Λ	Adjustable parameter
ω	Acentric factor

Superscripts

E	Denotes excess thermodynamic property
id	Denotes value for an ideal solution
l	Denotes liquid phase
sat	Property evaluated at the Saturation pressure of the component
v	Denotes vapour phase

Subscript*s*

c	Critical property
exp	Denotes an experimental value
i, j	Component identification
ij	Interaction between components i and j
r	Reduced property

Overbars

¯	Partial molar property
^	Property of component in a mixture

Abbreviation*s*

AAD	Average Absolute Deviation
ASOG	Analytical solution of groups
BIASU	
CFC	Chlorofluorocarbons
ENSMP	Ecole Superior des Mines de Paris
EoS	Equation of State
FID	Flame ionization detector
FEI	Fluorochemical Expansion Initiative
GC	Gas chromatograph
GWP	Global Warming Potential
HFPO	Hexafluoropropylene oxide
HPVLE	High-pressure vapour-liquid equilibrium
LPVLE	Low-pressure vapour-liquid equilibrium
NRTL	Non-Random Two-Liquid activity coefficient model
PR	Peng-Robinson
PRMCWS	Peng-Robinson-Mathias-Copeman-Wong-Sandler
PT	Pressure-Temperature
PVT	Pressure-Volume-Temperature

PV	Pressure-Volume
ROLSI	Rapid Online Sampler Injector
RTD	Resistance thermometer detector
SRK	Soave-Redlich-Kwong
TCD	Thermal conductivity detector
TEP	Thermodynamique des équilibres des phases
UNIQUAC	Universal QUasi-Chemical Activity coefficient model
UNIFAC	UNIQUAC functional-group activity coefficient model
VLE	Vapour-liquid equilibrium
WSMR	Wong and Sandler mixing rule

CHAPTER

ONE

INTRODUCTION

Over 25 years a drastic annual loss of the earth's protective ozone layer has been noticed above Antarctica and the same phenomenon has been detected more recently above the Arctic. Intense research attributed the effect primarily to the long atmospheric lifespan of man-made chlorinated compounds such as chlorofluorohydrocarbons (CFCs) [Rowland and Molina, 1974]. CFCs however have applications in a very wide domain of the chemical industry, for example in refrigeration system, air conditioners, propellants in aerosols and solvents.

In 1987, a modification of the Montréal protocol was signed which prohibited the use of chlorofluorohydrocarbons (CFCs) because of their effects on ozone. Since then there has been a growing interest in the search for more effective and environmentally ozone-friendly replacements with very low Global Warming Potential (GWP). Alternatives have included hydrocarbons, fluorinated hydrocarbons and mixtures of theses.

Fluorinated hydrocarbons have chemical stability and relatively low toxicity and have met the criteria of the modified Montréal protocol [Francisco and Maricq, 1996]. Unfortunately, their thermophysical properties differ from the CFCs. Measurement of thermophysical properties for pure components and mixtures of fluorinated compounds is thus greatly needed.

To promote research in the chemical sector, The Republic of South Africa has recently launched a program to fully beneficiate fluorspar (CaF_2) whereby manufacture of fluorinated compounds takes place. This has led to the establishment of the Fluorochemical Expansion Initiative (FEI). In this regard, measurement, interpretation and modelling of vapour-liquid equilibrium (VLE) data and thermophysical properties for systems containing fluorochemicals commenced in the Thermodynamic Research Unit of the School of Chemical Engineering at the University of KwaZulu Natal.

Accurate VLE data are a prerequisite for the design and optimization of unit operations in the chemical, petrochemical and gas processing industry.

Theoretical prediction of these data has proven sufficient in the preliminary stage of design but accurate experimental VLE data is still necessary for the final design, especially for non-ideal systems. Furthermore, the development of prediction methods and the improvement of existing equations of state require accurate experimental VLE data.

This research project is therefore focused on the construction and commissioning of a new static analytical apparatus capable of accurate measurement of vapour-liquid equilibrium (VLE) for fluorinated hydrocarbon systems at temperatures ranging from low temperatures up to 373.15 K and absolute pressures ranging from 0 up to 10 MPa.

Isothermal vapour-liquid equilibrium data (VLE) were measured and presented for three binary systems:

- Hexafluoroethane (R116) (1) + propane (2) at 263.15 K and pressures ranging from 0.328 up to 1.180 MPa.
- Octafluoropropane (R218) (1) + ethane (2) at five temperatures ranging from 264.05 to 308.04 K and pressures ranging from 0.298 up to 4.600 MPa.
- Hexafluoropropylene oxide (HFPO) (1) + Propane (2) at three temperatures 283.05, 303.05 and 323.05 K and pressures ranging from 0.437 up to 2.00 MPa.

The measured VLE data were correlated via a direct method using the Peng-Robinson equation of state (EoS) with the Mathias-Copeman alpha function and Wong-Sandler mixing rule incorporating the NRTL activity coefficient model.

This dissertation documents the objectives and results of the research as follows:

In the first chapter, the research project and its goals are introduced.

In the second chapter, experimental techniques for the investigation of the high pressure vapour-liquid equilibrium data will be described.

The third chapter will present a survey on the theoretical aspects of high pressure vapour-liquid equilibria.

The fourth and fifth chapters will describe in detail the experimental equipment and the operating procedures.

The sixth chapter will present the data, modelling and discussion of the experimental results.

The seventh chapter will present the conclusion.

Finally, recommendations will be presented in the eighth chapter.

CHAPTER

TWO

DESCRIPTION OF EXPERIMENTAL TECHNIQUES IN HPVLE

2.1 Introduction

An understanding of the thermodynamics of high-pressure phase equilibrium data of pure components and mixtures plays an essential role in various domains of chemical engineering. These data are regarded as one of the most important types of information for the efficient design of various separation and purification processes.

For most substances consisting of pure species or of different species in mixtures, most thermodynamic properties of interest have been measured by various methods. However, a large disparity has frequently been noticed between different data measured for the same system in the same conditions. In the other hand, the theories of phase equilibria have developed models to interpolate as well as extrapolate limited experimental data and to predict data for systems that have not previously been investigated. However, this method does not always provide reliable outputs since certain systems cannot be predicted by theories or models. Additionally, molecular simulation, which seems to be a powerful tool, can also fail to predict some systems.

Though very time-consuming and difficult to obtain, experimental data is still critically important in the chemical engineering sector. “Theory suggests but experimental decides” (Izaak M. Kolthoff).

This chapter, therefore, presents a brief summary of diverse experimental techniques for HPVLE data measurement. The classification of these techniques is not always easy because different basic principles can be combined in different ways [Richon, 2003].

The selection of methods, as well as apparatus for undertaking HPVLE data measurements depends largely on the physical properties for the systems being investigated: temperature, pressure, vapour pressure, component stability, material compatibility, measurement accuracy and safety [Uusi-Kyyny, 2004]. Numerous equipments have been designed and constructed and others modified depending on the envisioned application.

2.2 Classification of experimental methods

The classification of experimental methods for HPVLE measurement depends firstly on how the coexisting phases in equilibrium are determined (analytical methods and synthetic methods) and secondly on the working regime (static methods and dynamic methods).

In analytical or direct-sampling methods, the exact overall composition of the system investigated does not need to be known. The system temperature and pressure are regulated to bring about phase separation. At the equilibrium state, a sample from each of the phases is withdrawn using a sampling device and analyzed by suitable methods such as gas chromatography or mass spectrometry. The greatest challenge concerning this method is the withdrawal and sampling of true and representative samples. A small change in either the system temperature or pressure may disturb the equilibrium state and result in erroneous results.

In the synthetic or indirect method, a mixture of known composition is prepared and then its behaviour observed as a function of temperature and pressure. There is no need for sample analysis since the phase composition of the mixture can be easily calculated from the initial loading quantities. However, the challenges associated in analyzing the equilibrium mixture is replaced by challenges in synthesis of the mixture.

Raal and Mühlbauer [1994] state that the classification of techniques for HPVLE measurement depends on whether the liquid, vapour or both phases are circulated through the equilibrium cell. If any phase is in circulation, then this is known as the dynamic method. Otherwise, the method is defined as static.

Figure 2.1 shows clearly the division as well as the sub-divisions of different classes of HPVLE equipment.

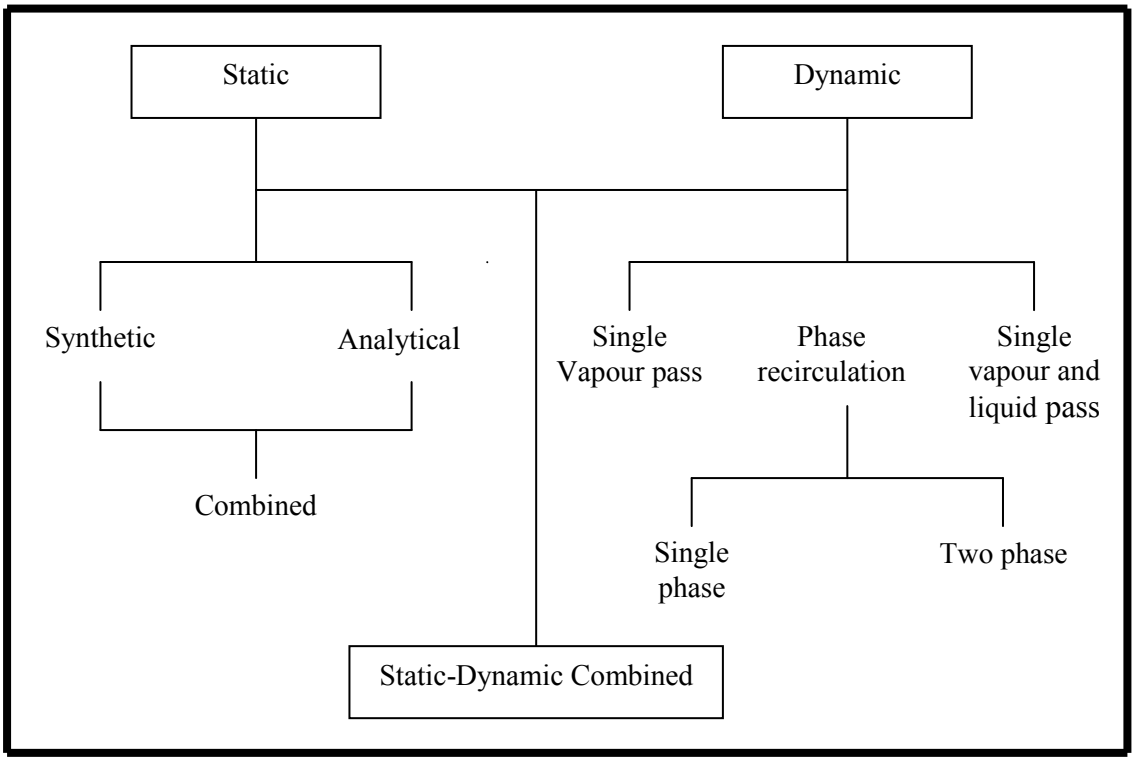

Figure 2.1: **Division and sub-division of different classes of HPVLE equipments [Raal and Mühlbauer, 1998]**

2.3 Principal features of HPVLE experimental equipment

The main features of HPVLE experimental apparatus using either static or dynamic methods are presented as follows. The apparatus consists of some or all of the following features:

An equilibrium cell or chamber where liquid and vapour phases attain equilibrium with each other.

A temperature-controlled environment in which the cell is housed. This is vital for isothermal measurements. Thermo-regulated environment such as liquid baths [Coquelet, 2003] and air baths [Ramjugernath 2000] are frequently used.

A mechanism for mixing and agitating the cell contents in order to promote contact between the phases, shorten the equilibration time. Static methods use internal stirrers, mechanical rocking of the equilibrium cell or piston devices. Dynamic methods use the recirculation of both the liquid and vapour phase throughout the equilibrium cell. The combination of internal stirrer and vapour recirculation is also reported in the dynamic methods [Inomata et al., 1989].

The analytical method requires an appropriate device for sample analysis. The analysis can be done either in-situ (spectroscopy, photometry or refractive indexes) or externally (gas chromatography).

The synthetic method does not require any device for sample analysis. Phase composition of the mixture can be calculated from knowledge of the initial loading quantities.

Accurate devices for pressure and temperature measurement. These have to be intermittently calibrated against a standard to determine any deviation and to correct for any errors.

2.4 Challenges associated with HPVLE experimentation

Raal and Mühlbauer [1994] have reviewed the challenges frequently encountered in obtaining accurate experimental HPVLE data. These include:

2.4.1 Degassing of the liquid component

It is vitally important to ensure that the liquid component is free of any dissolved gas. This may compete with the more volatile component in the liquid phase and therefore result in considerable error in composition analysis. The degassing of the liquid component can be undertaken either in-situ or prior to loading into the equilibrium cell.

2.4.2 Obtaining a true isothermal condition of the equilibrium cell

Obtaining a true isothermal condition of the equilibrium cell is both challenging and crucial. Raal and Mühlbauer [1998] reported that a slight vertical temperature gradient within the equilibrium cell will result in a state of non-equilibrated phase composition. A variation of 0.2 – 0.5 K is acceptable as a good indication of temperature uniformity. To prevent the temperature gradient, the following recommendations are suggested.

Insertion of the two platinum probes into the wall of the equilibrium cell at levels corresponding to the vapour and the liquid phase. Additionally, ensure that the equilibrium cell is placed entirely within the bath.

The environment housing the equilibrium cell and its surroundings should be adiabatic. Aluminium foil may be used to cover the top of the liquid bath whilst copper or Fibrefrax Duraback may be used for the air bath. Mühlbauer [1990] reported the use of these materials as insulation in his work.

Generally heaters are used as add-on to the environment housing the equilibrium cell. These may radiate heat directly onto the equilibrium cell and therefore create local hot spots. This may be prevented by the use of deflection shields.

Elimination of anything on the equipment that may serve as conductive paths to or from the equilibrium cell. Attention should be paid to attachments or fittings, all of which should be kept at the same temperature as the environment housing the equilibrium cell.

2.4.3 Attainment of equilibrium

Equilibrium is defined as a static condition in which no changes occur in the macroscopic properties of a system over time. This implies a balance of all potentials that may cause change [Smith et al., 2001]. The equilibration time depends on the system and on the method used. In the dynamic methods, recirculation is used as a mixing method and promotes contact between the phases. The equilibration time is short taking just a few minutes. In the static methods, the equilibration time generally takes longer, generally in the order of hours. High stirring rates result in greater contact of phases and shorten the time to attain the equilibrium. As equilibrium approaches, the rate of change becomes infinitesimal. Equilibrium is thus assumed when no changes are observable in the measurable properties of the system. Temperature, pressure and phase composition give a good indication of an equilibrium state. For isothermal measurement, equilibrium is assumed if the fluctuation in the measured pressure is less than a fixed percentage of the measured value for a certain amount of time. For isothermal measurement, a change in pressure of less than 0.05% over half an hour is a sufficient condition for equilibrium having been obtained [Fredenslund et al., 1973]. Stability in refractive index of the coexisting phases is also reported as indicator of the equilibrium condition [Besserer and Robinson, 1971], [Karla and Robinson, 1986] and [Freitag and Robinson, 1971]. Various authors reported other conditions, for example [Ramjugernath et al., 2000] stated that for isothermal condition, equilibrium is assumed when the total pressure remains constant to within ± 10 kPa for 10 minutes of rapid stirring.

2.4.4 Temperature and pressure measurement

Accurate temperature can be measured by a diverse array of sensors. All of them infer temperature by sensing some change in a physical characteristic. The engineer is likely to come into contact with thermocouples, resistive temperature devices and bimetallic devices to name a few. For temperature measurements in the range of -200 ˚C to 850 ˚C, resistive temperature devices such as platinum resistance thermometers are preferable while for temperatures above 850 ˚C, thermocouples are the most common. All temperature

measurement devices are carefully and periodically calibrated against a reference one. Further information on high-accuracy temperature measurement devices can be found in Perry and Green [1984].

Many techniques have been developed for the measurement of pressure. Among these, temperature compensated pressure transducers and bourdon-type pressure gauges have been favoured and are still preferred for very accurate pressure measurement in VLE data. However, the choice of a suitable temperature compensated pressure transducer always depends on its accuracy and temperature compensation. The pressure measurement devices must be intermittently calibrated against a reference pressure transducer to determine any deviation and correct for any errors. The reference pressure transducer is generally calibrated by the supplier.

2.4.5 Avoiding disturbance of equilibrium during sampling

Once equilibrium has been reached, a representative sample of each phase inside the equilibrium cell is withdrawn and sent to the GC for composition analysis (only, of course in methods that involve sample analysis outside the equilibrium cell).

The sampling of phases by withdrawal has never been an easy task. This becomes serious when it disturbs the equilibrium state. The two challenges associated with the sampling and the withdrawal procedures are:

- The volume of the withdrawn sample which result in a change of the overall volume.
- The change of the overall volume associated with either the sampling or the withdrawal device utilized.

The sample volume is generally determined by the analytical method employed but the ideal is to have it as small as possible. The GC calibration has proven to be an attractive analytical instrument since it requires small sample size.

The change in volume of the system may cause a pressure drop inside the equilibrium cell, affect the phase composition of one phase or another, etc and therefore disturbs the equilibrium state. Several procedures have been implemented to minimize this effect with varying degrees of success. Besserer and Robinson [1971] and Wagner and Wichterle [1987] reported pressure fluctuations of 0.1 to 0.01 bar in their sampling procedure. A large equilibrium cell was used to overcome some of the difficulties brought about by the sampling method. This was shown to be inadequate since it consumes large quantities of chemicals. Sagara et al. [1975], Ashcroft et al. [1983], Klink et al. [1987] and Mühlbauer [1990] also reported the use of large equilibrium cells. The use of variable volume equilibrium cells to compensate for the change in pressure

was also reported [Nasir et al., 1981] [Staby and Mollerup, 1991]. Other sampling techniques can be found in literature such as detachable sampling devices or microcells [Legret et al., 1981] [Dohrn et al., 1993]; sampling rods [Rogers and Prausnitz, 1970] [Nakayama et al., 1987]; sampling method using capillaries [Wagner and Wichterle 1987] [Matos et al., 1989], [Guilbot et al., 2000]; sampling technique using a six-port GC sampling valve [Raal and Ramjugernath, 1998] [Ramjugernath, 2000].

Baba-Ahmed et al. [1999] and Guilbot et al. [2000] reported the use of a Rapid Online Sampling Injector (ROLSI ^{TM}) for sample withdrawal. This sampling technique was developed specially for sampling of high pressure fluids. The ROLSI ^{TM} sampler can be directly connected to a chemical reactor, an equilibrium cell or a process line for an adjustable sample size ranging from 0.01 mg to a few mg. It allows in situ removal of repeatable and representative samples which can be analyzed without any contamination or disturbance of the medium. Compared to other sampling techniques, the ROLSI ^{TM} seems to overcome the difficulties of sample withdrawal based methods. Various authors have used the ROLSI ^{TM} sampler and acknowledged it as a good choice in the framework of sampling in a wide range of temperatures and pressures.

2.4.6 Accurate analysis of the withdrawn sample

Accurate analysis of the coexisting phases in equilibrium can be done either in-situ or externally. For external analysis, gas chromatography has proven to be an excellent method for binary and multicomponent mixtures [Ramjugernath, 2000]. A number of detectors are used in gas chromatography, the most common being the flame ionization detector (FID) and thermal conductivity detector (TCD). Both work over a wide range of concentrations. While FIDs can only detect organic compounds (depending on the number of C-H bonds), TCDs detect both organic and non-organic compounds. Detectors are periodically calibrated using either the internal standardization or the direct injection method.

2.5 Dynamic and Static methods

This section presents a brief survey of the dynamic and static methods as experimental techniques for high-pressure vapour-liquid equilibrium data measurement. The purpose is not to fully describe the two methods but rather, to put more focus on the static methods since it will be of service to this project.

2.5.1 Dynamic methods

In dynamic methods, the recirculation or flow of the fluid phases through the equilibrium cell achieves a mixing of phases in the system under investigation. With this method, special care must be taken to ensure the circulating phase is in equilibrium. Samples are taken into the circulation line through valves. Before composition analysis, the mixture is given some time without stirring, rocking or recirculation for the separation of the phases. What is unique about this method is the ease of sampling of phases in equilibrium. Also, the equilibration is short.

According to Raal and Mühlbauer [1998], dynamic methods are divided into two categories: Phase pass/ continuous flow methods and phase recirculation / semi-flow methods. Each category can further be subdivided into two sub-categories depending on how the phases are fed into the equilibrium cell. Figure 2.1 summarizes the different categories in the dynamic methods.

Numerous authors have reported the use of experimental dynamic methods for the investigation of phase equilibria for different systems. For additional details on dynamic methods, the reader is referred to: Galacia Luna et al [1994], Bouchot and Richon [1998], Raal and Mühlbauer [1998], Fredenslund et al. [1973], Dorau et al. [1983], Weber et al. [1984], Freitag and Robinson [1986], Kim et al. [1986], Muirbrook and Prausnitz [1965], Kubota et al. [1983] and Shibata and Sandler [1989].

2.5.2 Static methods

Since we have chosen the static analytic method as the preferred experimental method for HPVLE data measurement, this method will be emphasized in this section.

According to Raal and Mühlbauer [1998], static methods are divided into three main classes depending on how the compositions of the two coexisting phases are determined, analytical and synthetic methods. Figure 2.2 shows clearly the division as well as the subdivision of the static methods.

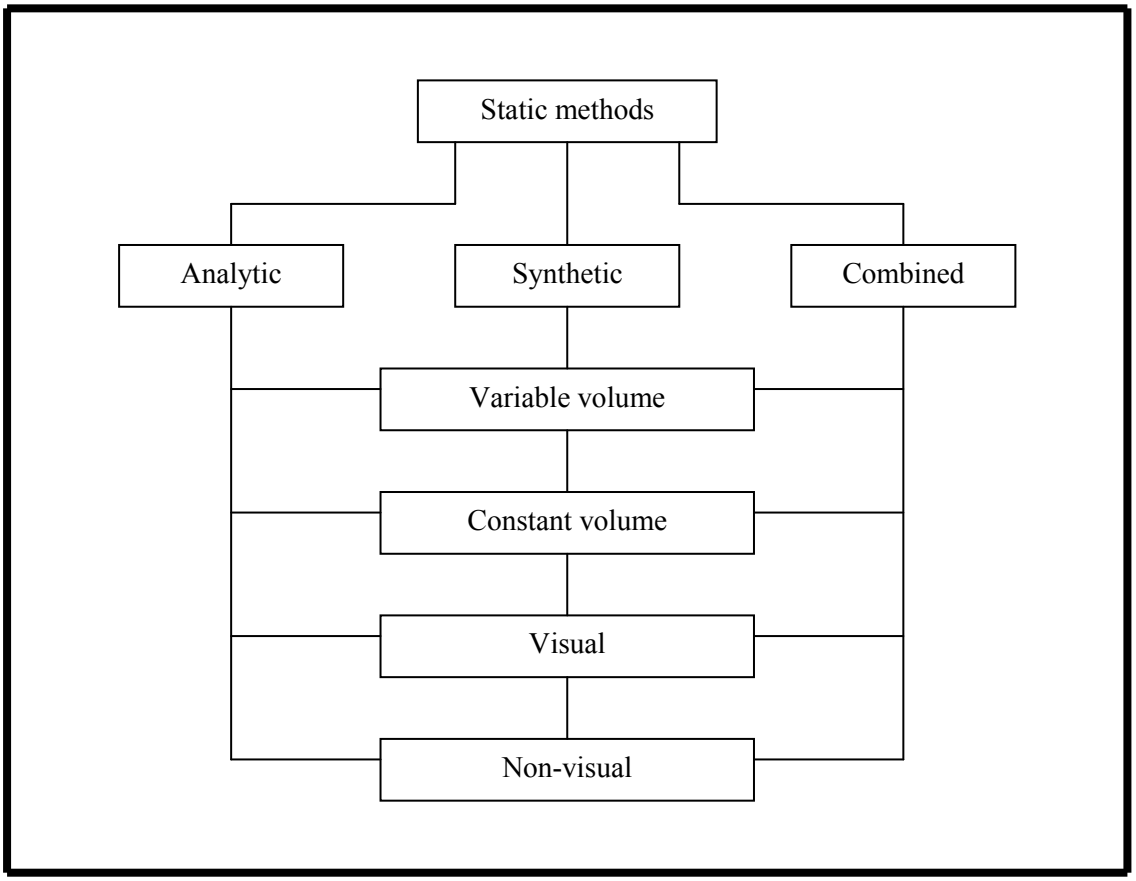

Figure 2.2: Division and subdivision of the static methods

[Raal and Mühlbauer, 1998]

2.5.2.1 Synthetic method

The principle of this method is based upon preparing a mixture of known composition and then observing its behaviour as a function of temperature and pressure. This observation can be carried out either visually or non-visually. The temperature and pressure of the homogeneous phase inside the equilibrium is adjusted until a phase separation occurs. As soon as the phase separation starts, the system temperature and pressure are noted. After the appearance of the second phase, the procedure is repeated for a range of temperatures and pressures during the entire experiment. There is no need for sample analysis since the phase composition of the mixture can be easily calculated from the initial loading quantities.

The synthetic method whereby the temperature is varied at constant pressure is known as the method of temperature variation and P (T) isopleths are generated while the reverse is known as the method of pressure variation and T (P) isopleths are generated.

The final results of the synthetic experiments, pressure versus mole fraction and temperature versus mole fraction phase diagrams, must be obtained by cross plotting from the two isopleths [Raal and Mühlbauer, 1994].

The advantage of this method is that sampling and therefore the use of analytic devices is not required. The data measurements can be done even near the critical conditions and with very simple equipment. The main disadvantage of this method is in the synthesis of the mixture.

In this method, the features of different equilibrium cells are taken into account.

Variable volume cell

High pressure VLE data using the synthetic variable volume cell offers flexibility in measurement. Variable volume cells are characterized by a change in volume provided by bellows or pistons. The experiment requires the visual observation of a dew or bubble point as well as pure saturated liquid molar volumes or mixtures of known composition. Different compressibility properties are also taken into account. Lesavre et al. [1981] and Fontalba et al. [1984] have reported this method in their work. Figure 2.3 illustrates the principle behind this method.

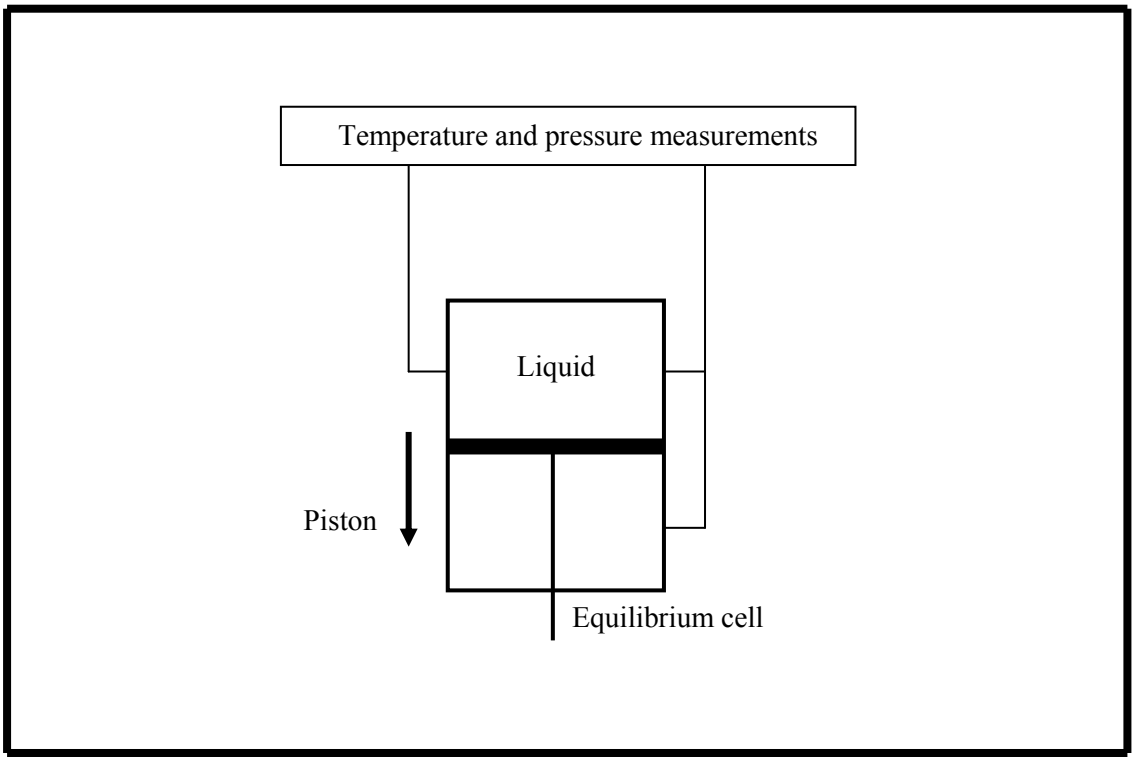

Figure 2.3: A schematic illustrating the principle of the synthetic variable volume cell [Raal and Mühlbauer, 1998]

Constant volume cell

In this method, the composition of the two coexisting phases in equilibrium is calculated using material balance and equilibrium thermodynamics. Additionally, saturated liquid and vapour are calculated using thermodynamic models. The principle behind this method is well described by Tanaka et al. [1993] and Legret et al. [1980].

If the total pressure is measured, the method is known as a total pressure method. This method is often used when the separation of phases is difficult because of the closeness of their densities. The application can also be extended for measurement at pressures up to 1 MPa.

2.5.2.2 Static analytic method

The static analytic method also known as the direct sampling method has an advantage over other static methods as it allows highly accurate data measurement as well as high precision in the VLE data. Further, it gives a representation of a truer equilibrium state. In this method the exact overall composition of the system investigated does not need to be known. The degassed components are enclosed into an equilibrium cell where the system temperature and pressure are regulated to bring about phase separation. Conditions are most often isothermal. Vigorous internal stirring of the cell contents is permitted to rapidly attain the equilibrium state and then a sample from each of the phases is withdrawn using a sampling device and analyzed by suitable methods such as gas chromatography or mass spectrometry.

A schematic illustrating the features of an apparatus using a static analytic method is shown in Figure 2.4.

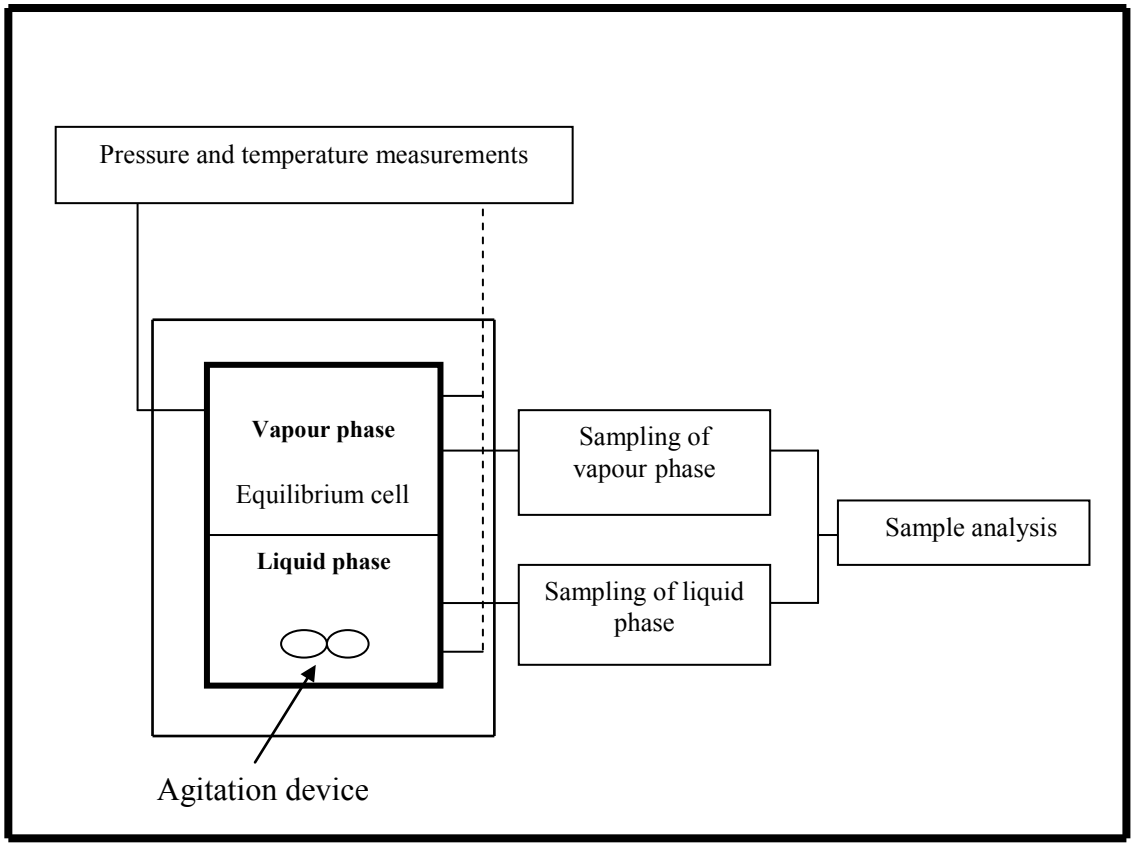

Figure 2.4: Schematic representation of a static analytic apparatus [Raal and Mühlbauer, 1998]

This method does however present certain problems to be solved, viz.

- The degassing of non volatile components.
- The time that is required to produce an isotherm and to calibrate analytical equipments.

A withdrawal device is required that ensures no disturbance of the equilibrium state takes place during sampling. Partial condensation of the vapour phase and/ or partial vaporisation of the liquid phase during sampling and sample transfer would cause a discrepancy between the results from the samples as analysed and actual condition in the equilibrium cell.

Some equilibrium cells have constant volume while others have variable volume. In addition, other features such as visual observations (sapphire windows) are incorporated to enhance the accuracy in the measurement.

Static analytic apparatus with a constant volume cell

Research has been undertaken and different solutions and apparatus have been proposed to remedy problems associated with the static analytic method.

Van Ness and Abott [1997] designed a static apparatus with a constant volume cell where the degassing process is achieved by the continuous flow of a liquid under vacuum conditions. Procedures involving freezing and melting cycles have also been proven to be successful for the degassing of non volatile components in the determination of VLE data [Bogatu et al., 2005].

At equilibrium, a sample of a certain volume is withdrawn and sent to the GC for analysis. This usually causes a pressure drop depending on the volume of the sample withdrawn and thus a disturbance of the equilibrium occurs. To prevent this, a variable volume cell in combination with a syringe pump is used. In addition, withdrawal of a sample proportional to the volume of the cell using capillaries and special valves is performed.

Coquelet [2003] and Valtz et al.[2002] have used and presented HPVLE apparati using special devices such as mobile and immobile pneumatic capillary samplers for taking small samples from coexisting phases in equilibrium without any perturbation.

The equipments described in Coquelet [2003] and Valtz et al. [2002] have proven successful for VLE data measurement of refrigerants for a wide range of pressures and temperatures. Numerous researchers have made use of them and VLE data have been reported. Valtz et al. [2002] used of the equipment described in his work and performed VLE data measurements for the propane + 1, 1, 1, 2, 3, 3, 3-heptafluoropropane (R227) system at temperatures ranging from 293.16 up to 353.18 K and pressures up to 3.4 MPa, Ramjugernath et al. [2009] used the equipment described in Coquelet [2003] for isothermal VLE data measurements for the Hexafluoroethane (R116) and Propane system at temperatures from (263 to 323) K.

Static analytic apparatus with a variable volume cell

The use of this apparatus in the investigation of HPVLE data measurement offers many advantages apart from the one described in the previous section. The variable volume of the cell is achieved either by the movement of a piston or by injecting a relatively small volume of an immiscible component into the system under investigation. With this apparatus, PVT data can also be obtained. Naidoo et al. [2008] presented a new high-pressure vapour-liquid equilibrium apparatus with a variable volume cell. Figure 2.5 shows schematically the variable volume equilibrium cell of the equipment used.

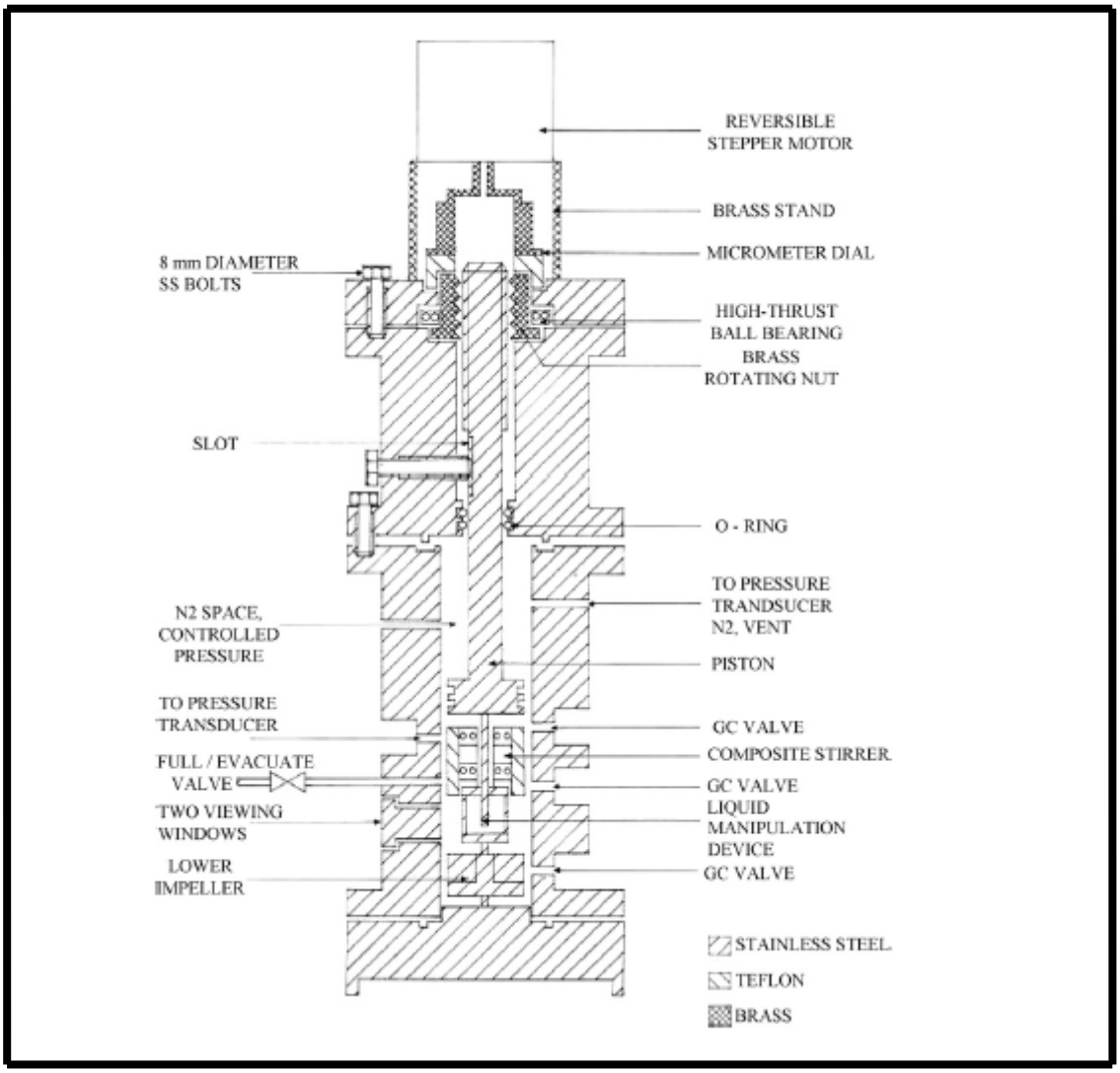

Figure 2.5: Variable volume equilibrium cell [Naidoo et al., 2008]

The variable volume static type high-pressure VLE apparatus [Naidoo, 2008] was designed, constructed, and tested on a certain defined number of binary systems. These included isothermal VLE data measurement for the Carbon dioxide + toluene system at temperatures from 283.25 to 391.45 K, Carbon dioxide + methanol at temperatures from 263.15 to 373.15 K and propane + 1-propanol at temperatures from 323.15 to 393.15 K.

The main drawback of this equipment is the relatively large volume of the cell. Previously this had been considered as an advantage as phases were not disturbed at equilibrium during the sampling procedure. The novel technique of sampling developed by Mines Paris Tech, [P. Guilbot et al., 1999], has shown this to be a flawed approach since it requires large amount of chemicals for a single run of experiments. Inclusion of equipment for homogenisation and sampling such as jet mixers is also cited as a disadvantage.

2.5.2.3 Combined method

Owing to the difficulties associated with static methods (static analytic and static synthetic methods), the combined method was developed. This method, also known as the static-synthetic method is a simple combination of features giving advantages of both the static analytic and static synthetic methods.

In static analytic method, withdrawal of samples of coexisting phases in equilibrium is a major problem since changing and disturbing the contents of the cell is likely to disturb the equilibrium state over time. The static synthetic method however does not require any sample withdrawal. Therefore, in the combined method, alteration of the equilibrium state is not experienced. Furthermore, the inaccuracy of the synthetic method in the region away from the critical state is no longer experienced, since the analytic option is preferred to the synthetic one.

In the combined method, components of the mixture are introduced separately and the composition is determined by weight. The volume of the cell is modified with a piston to reach bubble or dew points. At a fixed temperature, saturating properties (pressure and saturated molar volume) of the mixture are determined through the recording of pressure versus volume curves that display a priori the break point. Because of their versatility, most static combined equipment are equipped with viewing windows, stirring devices and provisions for determining the volume of the cell.

Several authors have reported the use of the static combined method. For further information on this method, the reader is referred to Slocum [1975], Legret et al. [1980], Huang et al. [1985], Stenby et al. [1993] and Kang and Lee [1996].

Conclusion

Different aspects of the dynamic and static methods have been briefly presented and discussed in this chapter. In this research project, a particular attention was drawn to the static method and in particular the static analytic method; although this method has some disadvantages, its advantages prevail over other static methods. The static analytic method gives a truer representation of the equilibrium state and allows highly accurate VLE data measurement. Several researchers have used equipments based on the static analytic method and found these equipments adequate for their work. Numerous examples are given throughout the chapter. Among these, the use of a “static-analytic” (constant volume) type apparatus by Ramjugernath et al. [2009]. These authors reported accurate VLE data measurement. For these reasons, the

static analytic method was chosen as the experimental technique for VLE data measurement in this project.

CHAPTER

THREE

THEORETICAL ASPECTS OF HIGH PRESSURE VAPOUR-LIQUID EQUILIBRIA

The most commonly encountered binary coexisting phases in industrial practice are vapour and liquid, although liquid/liquid, vapour/solid, and liquid/solid systems are also found. The theoretical methods that have been applied to describe, interpret and predict the liquid and vapour phase in equilibrium at high pressures are explained in this chapter.

A discussion of the modelling of pure components with equations of state and alpha functions for the calculation of vapour pressures will be presented.

Further, the modelling of binary mixtures will be presented along with liquid activity coefficient models and mixing rules.

Finally, the chapter will conclude with a discussion of some consistency tests for VLE data.

3.1. Pure components

3.1.1. Equations of state

Equations of state play an important role in chemical engineering design and they have assumed an expanding role in the study of the phase equilibria of fluids and fluid mixtures. They refer to mathematical relationships between two or more state functions associated with substances, such as its temperature, pressure, volume and internal energy.

Equations of state (EoS) were first used for pure components, then for mixtures of non-polar compounds and thereafter for slightly polar compounds. To date hundreds of EoS's have been proposed in available literature. Most equations of state can however be classified as belonging to one of three principal classes: empirical, theoretical and semi-empirical or semi-theoretical [Naidoo, 2004].

Empirical equations, appropriately named correlations, are obtained by fitting experimental data of a chosen system to a known multi parameter function. These equations have disadvantages as well as advantages. As a disadvantage, a large amount of experimental data is required and the outputs cannot be extended to mixtures. The main advantage is their accuracy in the limited range of the system.

Theoretical equations are general and are applicable to a wider range of systems obeying the given intermolecular potential model. However, only a specified interaction model that provides a fair representation of real fluids is qualified for such equations.

Semi-empirical equations are derived from a theoretically-based functional form of EoS. This class of EoS is very practical. Only a few adjustable quantities are required as parameters for representing experimental data.

Raal and Mühlbauer [1994, 1998] explicitly categorized the equations of state as follows:

1. The statistical-mechanical n-parameters virial EoS
2. The traditional thermodynamic cubic EoS
3. The modified traditional thermodynamic cubic EoS and the mixing rules
4. The complex EoS
5. The statistical thermodynamic perturbation theory EoS

These equations are intensively discussed in Sandler et al. [1994], Raal and Mühlbauer [1994] and Naidoo [1998]. The most popular are presented and discussed hereunder.

The Virial Equation of State

The statistical-mechanical studies of the forces between molecules lead to the virial equation of state. The general form of a virial EoS may be written as follows:

$$Z \equiv \frac{PV}{RT} = 1 + \frac{B}{V} + \frac{C}{V^2} + \frac{D}{V^3} + \ldots \tag{3-1}$$

An alternative expression for Z is:

$$Z \equiv \frac{PV}{RT} = 1 + B'P + C'P^2 + D'P^3 + \ldots \tag{3-2}$$

where Z is called the compressibility factor and B, C, D, etc., and B', C', D', etc., are called virial coefficients and are temperature dependants. Parameters B' and B are second virial coefficients; C' and C are third virial coefficients; etc.

From low to moderate pressures, the virial EoS can be assumed to adequately describe the vapour phase. Since, little is known about the third virial coefficient and beyond, the application of the entire equation is not possible to practical calculation. Therefore, the truncations of the virial are considered where the degree of truncation is a function of temperature and pressure.

In this regard, the virial equation of state has been applied mainly in its two-parameter form. This equation appears to provide accurate PVT behaviour at sub-critical temperatures and pressures up to 15 bars [Smith et al., 2001]. For non-ideal gas, the virial EoS truncated to two terms is useful in the calculation of number of moles. This was used during the GC calibration process for compounds of interest in this project (the reader is referred to appendix A for further details). This equation is represented as:

$$Z \equiv \frac{PV}{RT} = 1 + \frac{BP}{RT} \tag{3-3}$$

Where B is the second virial coefficient and is a function of temperature and composition. The second virial coefficient can be experimentally determined by various techniques. One of these techniques is outlined in Sandler et al. [1994]. However, experimental data for compounds of interest at desired conditions is not always easy if not impossible to obtain. Therefore, theoretical ways can solve the problem. Correlations have been developed on the determination of the second virial coefficient. If the accuracy in the prediction is closer to experimental results, correlations are favoured.

Several correlations have however been developed and are available in literature. Among the most popular are those presented by Pitzer and Curl [1957], Tsonopoulos [1974], Hayden and O'Connel [1975], Trakad and Danner [1977], Vetere [1998, 1991 and 1999], Weber [1994], etc. Some of the most commonly used correlations are presented hereunder.

The Pitzer and Curl correlation (1957)

Pitzer and Curl [1957] proposed an expression for the determination of the second virial coefficient of nonpolar components, which is a function of reduced temperature ($T_r=T/T_c$) and the acentric factor (ω) as follows:

$$\frac{BP_c}{RT_c} = f^{(0)}(T_r) + \omega f^{(1)}(T_r) \tag{3-4}$$

$$f^{(0)} = 0.1445 - 0.330/T_r - 0.1385/T_r^2 - 0.0121/T_r^3 \tag{3-5}$$

$$f^{(1)} = 0.073 - 0.46/T_r - 0.50/T_r^2 - 0.097/T_r^3 - 0.0073/T_r^8 \quad (3\text{-}6)$$

where B is the second virial coefficient, ω is an acentric factor, P_c and T_c are respectively the critical pressure and critical temperature and R is the universal gas constant. In equations (3.17-19), $f^{(0)}(T_r)$ is fitted from small spherical molecules (ω=0) such as argon and $f^{(1)}(T_r)$ is obtained from data for non polar molecules (ω≠0), such as butane or propane.

The Tsonopoulos correlation (1974)

A modification of the well-known Tsonopoulos correlation for the second virial coefficient was developed and proposed in 1974. This correlation is capable of calculating the second virial coefficient for non-polar substances, slightly polar substances and those exhibiting hydrogen bonding. Furthermore, two dependent parameters were introduced to account for non polar substances:

$$\frac{BP_c}{RT_c} = f^{(0)}(T_r) + \omega f^{(1)}(T_r) + f^{(2)}(T_r) \quad (3\text{-}7)$$

where $f^{(0)}(T_r)$ and $f^{(1)}(Tr)$ are defined as in the Pitzer and Curl correlation, and $f^{(2)}(T_r)$ is defined as:

$$f^{(2)}(T_r) = a/T_r^6 \quad (3\text{-}8)$$

In equations (3.7-8), T_r $(=T/T_c)$ is the reduced temperature, ω is the acentric factor, P_c and T_c are critical pressure and critical temperature and B is the second virial coefficient. $f^{(2)}$ was obtained from data for non hydrogen bonding polar molecules. Equations (3-9) and (3-10) are very important at reduced temperature less than unity for representing the behaviour of polar fluids.

$$a = -2.188*10^{-11}\mu_r^4 - 7.831*10^{-21}\mu_r^8 \quad (3\text{-}9)$$

$$\mu_r = \frac{\mu^2 P_c}{1.01325 T_c^2} \quad (3\text{-}10)$$

The parameter a is expressed as a function of the reduced dipole moment (μ_r). In equation (3-10), μ is defined as the dipole moment expressed in Debye (1D=3.33504*10^{-30} Cm), T_c is the critical temperature in Kelvin and P_c, the critical pressure in Pascal.

For the same reduced temperature and acentric factors, the second virial coefficients for polar compounds are more negative than those of non-polar compounds.

Cubic Equations of State (CEoS)

The general form of the traditional cubic EoS is based on the expression of pressure as the combination of two terms: a repulsion pressure and an attraction pressure.

$$P = P_{attraction} + P_{repulsion} \tag{3-11}$$

The repulsion pressure is usually represented by the van der Waals hard-sphere equation:

$$P_r = RT/(V-b) \tag{3-12}$$

where b is known as the van der Waals volume or co-volume related to the size of the hard sphere.

The attraction pressure is expressed as:

$$P_a = -a/g(V) \tag{3-13}$$

where *a* is defined as the measure of intermolecular attraction forces and *g (V)* a function of molar volume.

The general form of cubic equation of state thus becomes:

$$P = \frac{RT}{V-b} - \frac{a}{g(V)} \tag{3-14}$$

Van der Waals EoS (1873)

Proposed in 1873, the van der Waals equation of state was the first attempt to quantitatively take intermolecular forces into account in qualitatively describing properties of fluids over a wider range. The proposed equation is expressed as follow:

$$P = \frac{RT}{V-b} - \frac{a}{V^2} \tag{3-15}$$

In equation (3-15), apart from *P, V, T* and *R*, *a* is regarded as the attraction parameter and b, the effective molar volume. Parameters *a* and *b* are determined at the critical point. The procedure is detailed hereunder.

$$\left(\frac{\partial P}{\partial V}\right)_T = \left(\frac{\partial^2 P}{\partial V^2}\right)_T = 0 \tag{3-16}$$

Thus, we find:

$$a = \frac{27}{64}\frac{R^2 T_C^2}{P_C} \tag{3-17}$$

$$b = \frac{1}{8}\frac{RT_C}{P_C} \tag{3-18}$$

$$Z_c = \frac{PV_C}{RT_C} = 0.375 \tag{3-19}$$

The primary use of an equation of state is to predict phase equilibria. Compared to the ideal gas EoS which was found to have limited application under certain conditions, the van der Waals EoS has proven to solve several problems previously experienced. Among other benefits, the actual EoS does predict the formation of liquid phases. Accuracy in the prediction does however remain an important thing to consider. Although the van der Waals EoS could predict the formation of the liquid phase, sufficient accuracy was not necessarily achieved. Furthermore, there was no temperature-dependency of parameters of the van der Waals cubic EoS; this precluded its application to highly non-ideal systems. Consider the compressibility factor Z_c, the van der Waals CEoS predicts $Z_c = 0.375$ for all fluids while Z_c varies from 0.24 to 0.29 for different hydrocarbons. The inaccuracy in vapour pressure predictions is also included [Sandler et al., 1994]. Therefore, a number of much more accurate EoS's than the van der Waals EoS have been developed and the popular models will be discussed in the next sections.

Redlich Kwong EoS (1949)

Introduced in 1949, the Redlich Kwong equation of state was considered the first modification of the van der Waals equation of state. In this EoS, the parameter a in the van der Waals equation was given a square root of T and b was given as a dependency to the second term in the denominator. In mathematical form, this can be expressed as:

$$P = \frac{RT}{V-b} - \frac{a/\sqrt{T}}{V(V+b)} \tag{3-20}$$

In a way similar to the van der Waals EoS, parameters *a* and *b* are determined at the critical point

$$a = \Omega_a \frac{R^2 T_c^{\,2}}{P_c} \tag{3-21}$$

$$b = \Omega_b \frac{RT_c}{P_c} \tag{3-22}$$

$$\Omega_a = 0.42748 \tag{3-23}$$

$$\Omega_b = 0.008664 \tag{3-24}$$

$$Z_C = \frac{1}{3} \tag{3-25}$$

The Redlich-Kwong equation is adequate for nonpolar compounds and slightly polar compounds. It is of great use in the correlation of data over a wider range and provides a better representation in the critical zone (Z_c = 0.333) compared to the van der Waals EoS. Despite all the advantages cited, the Redlich-Kwong equation fails at some points. It performs poorly with respect to the liquid phase and consequently cannot be used to predict accurate vapour-liquid equilibrium data or to calculate properties of mixtures. To overcome this inconvenience, the use of a separate liquid-phase model is compulsory.

The Redlich-Kwong equation is suitable for calculations of vapour phases only when the reduced pressure is less than about one-half the reduced temperature.

Guess et al., [1991] states that the Redlich-Kwong EoS is generally successful for ideal systems and for simple fluids with Z_c = 0. For complex fluids with $Z_c \neq 0$, the accuracy is uncertain.

Soave-Redlich-Kwong EoS (1972)

In 1972, Soave proposed a modification to the Redlich-Kwong EoS to overcome some of its limitations. The temperature-dependence of the attraction term was modified to include the acentric factor. Mathematically this can be represented as:

$$P = \frac{RT}{V-b} - \frac{a(T,\omega)}{V(V+b)} \tag{3-26}$$

In equation (3-39), all the variables are defined in a similar way as for the previous cubic equations of state apart from ω which is defined as the acentric factor.

Due to modifications that came along with this equation, accurate prediction of properties of pure substances and mixtures is assured. Vapour pressure of a number of light hydrocarbons and several binary systems were calculated and compared with experimental data [Soave, 1972]. The Soave's modification agreed well with the experimental data and was able to correlate the phase equilibria at moderate and high pressures and in the critical region for non-polar and slightly polar fluids.

The main drawback of this equation is its failure to correlate phase equilibria for systems consisting of highly polar species or molecules that exhibit hydrogen bonding.

The two equations of state, Redlich-Kwong and Soave-Redlich-Kwong, usually generate satisfactory vapour densities but fail to generate satisfactory liquid densities [Mühlbauer and Raal, 1994].

Peng-Robinson Equation of State (1976)

The Peng-Robinson equation of state was developed in 1976 to improve predictive accuracy over that of the Soave-Redlich-Kwong EoS of liquid volumes and vapour pressures. The modification to the Soave-Redlich-Kwong EoS involved a different volume dependence, temperature dependence of *a* and reasonable accuracy near the critical region (This counts mostly for the compressibility factor and the liquid density).

Thus, the Peng-Robinson EoS is given by:

$$P = \frac{RT}{V-b} - \frac{a(T,\omega)}{V(V+b)+b(V-b)} \tag{3-27}$$

where the temperature dependence is given as:

$$a(T) = \Omega_a \frac{R^2 T_c^2}{P_c} \tag{3-28}$$

$$b(T) = \Omega_b \frac{RT_c}{P_c} \tag{3-29}$$

$$\Omega_b = 0.0778 \tag{3-30}$$

$$Z_c = 0.3074 \tag{3-31}$$

The Peng-Robinson EoS slightly improves the prediction of liquid volumes and predicts the compressibility factor Z_c equal to 0.304. This EoS is particularly accurate for predicting the properties of hydrocarbons and fluorochemicals, including the behaviour of mixtures and VLE data. Similar to the SRK EoS, the Peng-Robinson is not accurately applicable to highly polar molecules, hydrogen bonded fluids (especially water) and electrolytes. This equation usually gives results that are much closer to results obtained experimentally.

The Soave-Redlich-Kwong and the Peng-Robinson CEoS find a wide application in industry. The advantages of these equations are that they can easily correlate phase behaviour from pure components to multicomponent systems. Also, the Soave-Redlich-Kwong and the Peng-Robinson CEoS require little input information such as critical properties and acentric factors for generalized parameters. The computer time is relatively short and can produce good correlation for phase behaviour. The disadvantages of these equations are that they are not accurate in the critical region and that the calculated liquid volumes are not improved.

Other modifications to the cubic equation of state have been centered on the attractive term. These additions have improved the prediction of both the saturation pressure and the liquid volume. For more detail, the reader is referred to [Coquelet, 2003] and [Naidoo, 2004]

3.1.2 Alpha correlations

Proposed in 1873, the van der Waals EoS was the first cubic equation of state to predict the behaviour of gases and liquids. Its advantages and disadvantages have led researchers into much more convenient cubic equations of state. Many cubic equations of state have thus been developed and proposed. Researchers focused on the modification and improvement of the van der Waals EoS for better results. For thermodynamic properties of pure components, they were mainly concerned with vapour pressures.

From 1964 to 1966, Wilson proposed the introduction of alpha correlations in the Redlich-Kwong equation of state to reproduce the vapour pressure. The attractive term is newly expressed as:

$$a(T) = a(T_c)\alpha(T_r) \tag{3-32}$$

$$\alpha(T_r) = \left[T_r + (1.57 + 1.62\omega)(1 - T_r)\right] \tag{3-33}$$

In equations (3-32) and (3-33), *a* (T_c) is the value of the attractive term in the RK EoS at the critical point, $\alpha\ (T_r)$ is the alpha function, defined as a function of the reduced temperature T_r and the acentric factor ω.

The temperature dependence $\alpha\ (T_r)$ in equation (3-32) does not provide good enough representation of vapour pressure. This explains why the Wilson's alpha function did not acquire wide popularity.

Following Wilson's approach, Soave [1972] proposed an equation of the form:

$$\alpha(T_r) = \left[1 + m\left(1 - T_r^{1/2}\right)\right]^2 \tag{3-34}$$

The parameter *m* is obtained by forcing the equation to produce vapour pressure for non-polar compounds at $T_r = 0.7$ and is expressed as a function of ω, the acentric factor.

$$m = 0.480 + 1.57\omega - 0.175\omega^2 \tag{3-35}$$

The parameters in equations (3-34) and (3-35) were adjusted for vapour pressure corresponding to $T_r = 0.7$. This was derived from the definition of the acentric factor.

Originally, the acentric factor was used by Pitzer and Curl [1957] as an expression in an equation for the compressibility factor. It is defined as:

$$\omega = \log\left(P_r^{sat}\right)_{Simplefluid(T_r=0.7)} - \log\left(P_r^{sat}\right)_{T_r=0.7} \tag{3-36}$$

For most simple fluids P_r^{sat} at $T_r = 0.7$ is close to 0.1, therefore $\omega \approx 0$. Then, equation (3-36) becomes:

$$\omega = -1 - \log\left(P_r^{sat}\right)_{T_r=0.7} \tag{3-37}$$

In equations (3-36) and (3-37), $T_r = T/T_c$ is defined as the reduced temperature and $P_r{}^{sat} = P^{sat}/P_c$, the saturated reduced pressure.

The acentric factor accounts for characteristics of the molecular structure. A value of ω is obtained by using an accurate equation for $P_r^{sat}\ (T)$ along with the required critical properties. Values of ω are tabulated in many thermodynamic tables.

Soave's introduction of the new form of the alpha function improved predicted vapour pressures as compared to Wilson's contribution. Owing to its relative accuracy and simplicity, the Soave alpha function has been used and been considered as a standard in prediction of

thermodynamic properties. Despite the advantages that come along with this type of alpha function, it fails to reproduce accurately the vapour pressure at low reduced temperatures for heavy hydrocarbons which have large critical temperatures.

Other generalised alpha functions have been developed depending on the type of cubic equation of state. The development was based upon the experimental data for pure components. Hence, for the PR and the SRK EoS, the parameter *m* is respectively expressed as follows:

SRK EoS: $$m = 0.47830 + 1.6337\omega - 0.3170\omega^2 + 0.760\omega^3 \quad (3\text{-}38)$$

PR EoS: $$m = 0.374640 + 1.542260\omega - 0.26992\omega^2 \quad (3\text{-}39)$$

However, numerous investigators have tried to modify and improve Soave's alpha function for better results. The reader is referred to Coquelet [2003] and Moller [2008] for details of several other proposed alpha functions.

An example of a further developed alpha function is the three parameters Mathias-Copeman alpha function. It is expressed as follows:

$$\alpha(T) = \left[1 + C_1\left(1 - \sqrt{T_r}\right) + C_2\left(1 - \sqrt{T_r}\right)^2 + C_3\left(1 - \sqrt{T_r}\right)^3\right]^2 \quad (3\text{-}40)$$

if $T < T_c$

And

$$\alpha(T) = \left[1 + C_1\left(1 - \sqrt{T_r}\right)\right]^2 \quad (3\text{-}41)$$

if $T > T_c$

where C_1, C_2, C_3 are the adjustable parameters, T, the working temperature, T_c, the critical temperature and T_r, the reduced temperature.

Over the years, it has been noticed that the three- parameters Mathias-Copeman alpha reproduces more accurately vapour pressures of pure components than others.

3.1.3. Vapour pressure calculation

Consider a sealed vessel of constant volume that contains a liquid and its vapour. At certain temperatures, the molecules in the liquid phase will tend to evaporate to the vapour phase and the molecules in the vapour phase will tend to condense back into the liquid phase. With the

rate of condensation being equal to the rate of vaporisation, a state of dynamic equilibrium will be achieved.

The equilibrium vapour pressure is then defined as the pressure exerted by a vapour when the vapour is in equilibrium with its liquid phase at a defined temperature.

The equilibrium is defined as a static condition in which no changes occur in the macroscopic properties of a system with time. This implies a balance of all potentials that may cause change [Smith et al., 2001]. Mathematically this can be expressed as follows:

$$dG(T,P) = 0 \tag{3-42}$$

where G is the molar Gibbs free energy. The tendency for a reaction to reach an equilibrium state is driven by the Gibbs free energy. Thus, for a reversible reaction, when $\Delta G > 0$ the reverse reaction is said to be spontaneous, when $\Delta G < 0$, the forward reaction is said to be spontaneous and when $\Delta G = 0$, the system has reached the equilibrium state.

Consider a closed system consisting of two phases in equilibrium: a vapour and liquid phase. Equation (3-42) may be written as follows:

$$G^v(T,P) = G^l(T,P) \tag{3-43}$$

Whence

$$G(T,P) = \Gamma_i(T) + RT \ln f_i \tag{3-44}$$

In Equation (3-44), $\Gamma_i(T)$ is an integration constant at temperature T, f_i represents the fugacity of pure species *i.* It is the pressure value needed at a given temperature to make the properties of non-ideal gas satisfy the equation for an ideal gas.

Therefore, equation (3-44) may be written for species *i* as a saturated vapour

$$G^v(T,P) = \Gamma_i(T) + RT \ln f_i^v \tag{3-45}$$

and for species *i* as a saturated liquid at the same temperature:

$$G^l(T,P) = \Gamma_i(T) + RT \ln f_i^l \tag{3-46}$$

By difference,

$$G^v(T,P) - G^l(T,P) = RT \ln \frac{f_i^v}{f_i^l} \tag{3-47}$$

According to Equation (3-43),

$$G^v(T,P) - G^l(T,P) = 0 \tag{3-48}$$

therefore:

$$f_i^v(T,P) = f_i^l(T,P) = f_i^{sat}(T,P) \tag{3-49}$$

Equation (3-49) gives another mathematical expression of two phases in equilibrium. For two pure species coexisting liquid and vapour phases are in equilibrium when they have the same temperature, pressure and fugacity [Smith et al., 2005].

An alternative formulation is based on the corresponding fugacity coefficients (ϕ). This is expressed as:

$$\phi_i^v(T,P) = \phi_i^l(T,P) = \phi_i^{sat}(T,P) \tag{3-50}$$

Where

$$\phi = \frac{f(T,P)}{P} \tag{3-51}$$

Calculation of fugacity coefficients is done from the following expression:

$$\ln[\phi(T,P)] = Z - 1 - \ln(Z) + \frac{1}{RT}\int_{\infty}^{v}\left(\frac{RT}{v} - P\right)dV \tag{3-52}$$

To summarize pure species properties, phase diagrams are frequently used. The most well known phase diagrams include Pressure-Volume (PV) and Pressure-Temperature (PT). Figure 3-1 illustrates this clearly.

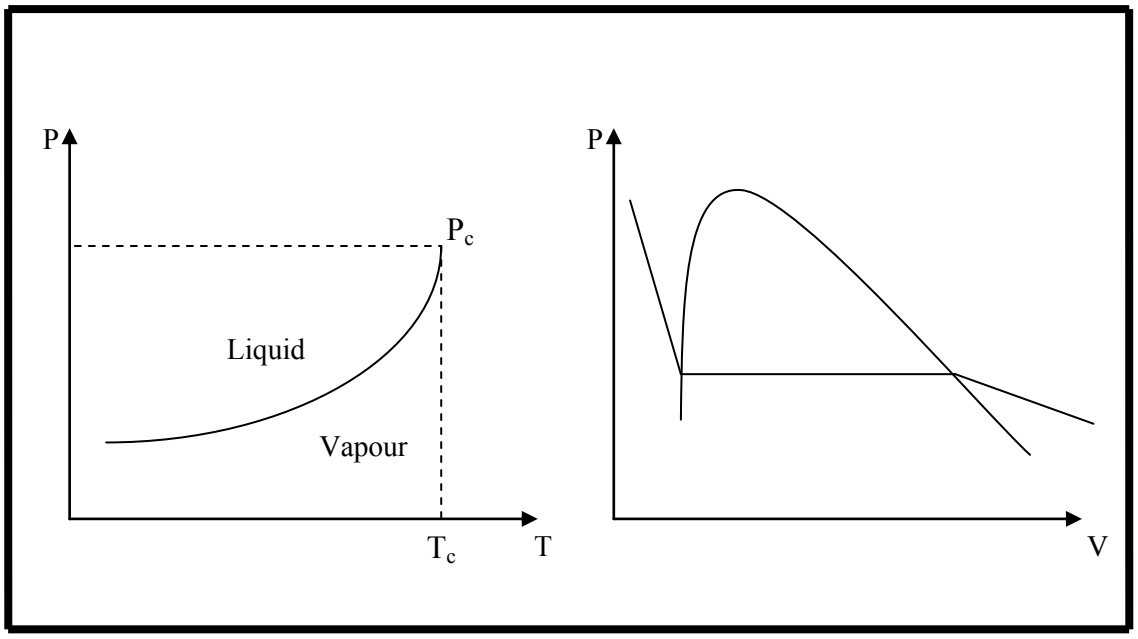

Figure 3-1: Equilibrium diagrams

3.2 Components in solution

In the chemical, petroleum, and pharmaceutical industries multicomponent fluid mixtures at varied conditions are the most commonly encountered systems and so, necessarily, most attention has been paid to the theories and models required to describe their behaviour.

In fact a mixture is a combination of two or more dissimilar substances that do not chemically combine and do not necessarily exist in fixed proportion to each other. Mixtures can be classified into three types: suspension mixtures, colloidal mixtures or solution, depending on how they are combined or can be separated.

Special care is paid to solutions since they are homogeneous mixtures where one substance is completely dissolved into another. In the phase equilibria studies, the engineer is most likely to deal with this type of mixture. Two types of solutions are most commonly considered: the ideal solution and the real solution. The ideal solution, a useful model, serves as a standard to which real solution behaviour can be compared. This is formalized by the introduction of excess properties.

Equation (3-53) establishes the behaviour of species in an ideal solution

$$\overline{G}_i^{id} = G_i + RT \ln x_i \tag{3-53}$$

where the superscript ^{id} denotes an ideal solution property, x_i represents the liquid mole fraction. For an ideal solution of gases, y_i will represent the vapour mole fraction.

Mathematical expressions for other thermodynamic properties for an ideal solution are calculated referring to Equation (3-53). Thus we have:

$$\overline{S}_i^{id} = S_i - R\ln x_i \tag{3-54}$$

$$\overline{V}_i^{id} = V_i \tag{3-55}$$

$$\overline{H}_i^{id} = H_i \tag{3-56}$$

The application of the summability relation ($M^{id} = \sum_i x_i \overline{M}_i^{id}$), to equations (3-54), (3-55), (3-56) yields:

$$S^{id} = \sum_i x_i S_i - R\sum_i x_i \ln x_i \tag{3-57}$$

$$V^{id} = \sum_i x_i V_i \tag{3-58}$$

$$H^{id} = \sum_i x_i H_i \tag{3-59}$$

In 1923, Lewis proposed a simple equation for the fugacity of species in an ideal solution. This is expressed mathematically as:

$$\hat{f}_i^{id} = x_i f_i \tag{3-60}$$

Equation (3-60) known as the Lewis/Randall rule expresses that the fugacity of species in an ideal solution is equal to the fugacity of pure species *i* in the same physical state as the solution and at the same temperature and pressure. It also shows that the fugacity of each species in an ideal solution is proportional to its mole fraction.

3.2.1 Excess properties

Excess properties are introduced in thermodynamics to measure any kind of deviation from the behaviour of ideal solution. More precisely, they are thermodynamic properties of solutions that are in excess of those of an ideal solution at the same temperature, pressure and composition [Prausnitz, 1999].

If M represents the molar value of any extensive thermodynamic property, an M^E is defined as the difference between the actual property value of a solution and the value it would have as an ideal solution at the same temperature, pressure and composition. Mathematically, this is expressed as:

$$M^E = M - M^{id} \tag{3-61}$$

Similar definitions hold for V^E, H^E, G^E and S^E, which are, respectively, excess volume, excess enthalpy, excess Gibbs energy and excess entropy. Thus,

$$V^E = V - V^{id} \tag{3-62}$$

$$H^E = H - H^{id} \tag{3-63}$$

$$G^E = G - G^{id} \tag{3-64}$$

$$S^E = S - S^{id} \tag{3-65}$$

For an ideal solution all excess properties are equal to zero. However, excess properties may be positive or negative. For example when the excess Gibbs energy is greater than zero, the solution exhibits a positive deviation from ideality or else the solution exhibits a negative deviation from ideality.

3.2.2 Activity and activity coefficients

An activity coefficient, γ, is a factor used in thermodynamics to account for deviations of a solution from the behaviour of an ideal solution. The activity coefficient of a component *i* at some temperature, pressure and composition is defined as the ratio of the activity of *i* to that of the concentration *i*, usually the mole fraction. It is expressed mathematically as follows:

$$\gamma_i = \frac{a_i}{x_i} \tag{3-66}$$

Activity coefficients are derived from excess Gibbs energies and are related as follows:

$$\ln \gamma_i = \left[\frac{\partial \left(nG^E / RT \right)}{n_i} \right]_{T,P,n_j} \tag{3-67}$$

In practice, the process is reversed and excess Gibbs energies are evaluated from known activity coefficients using the summability relation. Thus we have:

$$\frac{G^E}{RT} = \sum_i x_i \ln \gamma_i \tag{3-68}$$

Activity coefficients can be determined experimentally and are found from VLE data.

For a binary mixture the activity coefficients can be calculated from Equation (3-68) as follows:

$$\ln \gamma_1 = \frac{G^E}{RT} + x_2 \frac{d\left(G^E/RT\right)}{dx_1} \tag{3-69}$$

$$\ln \gamma_2 = \frac{G^E}{RT} - x_1 \frac{d\left(G^E/RT\right)}{dx_2} \tag{3-70}$$

As observed from equations (3-67) to (3-70), a mathematical relation for G^E as a function of composition is required to calculate the activity coefficient. As a result, models for the determination of G^E have been developed.

3.2.2.1 Activity coefficient models

As the variety of organic compounds of interest in chemical processing is very wide, and the number of mixtures is essentially uncountable, situations frequently arise in which engineers need to make activity coefficient predictions for systems, or at conditions, for which experimental data are not available. Accordingly, models based on the excess Gibbs energy have been developed and proposed over the years. Some of the well known models include: Margules (1895), Van Laar (1910), Wilson (1964), NRTL (Renon and Prausnitz, 1986) and UNIQUAC (Abrams and Prausnitz, 1975).

The first two models are known as the empirical models whereas the last three are known as the group contribution liquid-phase models.

3.2.2.2 Margules equation (1895)

In 1895, Margules proposed what are considered now as the oldest models but are still in common use today and show remarkable accuracy. The first model is the two-suffix (one parameter), and it may be written as follows:

$$G^E = Ax_1x_2 \tag{3-71}$$

where A is an empirical parameter with units of energy (*J/mol*), characteristic of component *1* and *2* and depends on the temperature.

The activity coefficients are given by:

$$\ln \gamma_1 = Ax_2^2 \tag{3-72}$$

$$\ln \gamma_2 = Ax_1^2 \tag{3-73}$$

The second model is the Margules three-suffix (two-parameter). For this model, the Gibbs molar energy may be written as follows:

$$\frac{G^E}{RT} = \left(A_{21}x_1 + A_{12}x_2\right)x_1x_2 \tag{3-74}$$

The activity coefficients are given by:

$$\ln \gamma_1 = \left[A_{12} + 2\left(A_{21} - A_{12}\right)x_1\right]x_2^2 \tag{3-75}$$

$$\ln \gamma_2 = \left[A_{21} + 2\left(A_{12} - A_{21}\right)x_2\right]x_1^2 \tag{3-76}$$

These models do not have a fundamental background; they should work for equal size molecules. No temperature dependency and no energetic interactions are taken into account for the system under investigation. The primary value of the Margules models lies in their ability to represent experimentally determined activity coefficients with only a few constants.

Later, another model was introduced by Margules. This included three temperature independent parameters and was named the four-suffix Margules equation. Excess Gibbs energy and activity coefficients are respectively expressed as follows:

$$\frac{G^E}{RT} = x_1x_2\left(A_{12}x_2 + A_{21}x_1 - Cx_1x_2\right) \tag{3-77}$$

$$\ln \gamma_1 = \left[A_{12} + 2\left(A_{21} - A_{12} - C\right)x_1 + 3Cx_1^2\right]x_2^2 \tag{3-78}$$

$$\ln \gamma_2 = \left[A_{21} + 2\left(A_{12} - A_{21} - C\right)x_2 + 3Cx_2^2\right]x_1^2 \tag{3-79}$$

This model has been used to reduce experimental VLE data for many systems and has proven to give good representation.

3.2.2.3 Van Laar equation (1910)

The Van Laar equation was originally proposed in 1910. It is based on the van der Waals EoS.

The excess Gibbs energy expression for the Van Laar model is:

$$\frac{G^E}{RT} = \frac{A_{12}A_{21}x_1x_2}{x_1A_{12} + x_2A_{21}} \tag{3-80}$$

Where A_{12} and A_{21} are two adjustable parameters in the model.

The activity coefficients for the Van Laar equation are expressed as follows

$$\ln \gamma_1 = A_{12}\left(\frac{A_{21}x_2}{A_{12}x_1 + A_{21}x_2}\right)^2 \tag{3-81}$$

$$\ln \gamma_2 = A_{21}\left(\frac{A_{12}x_2}{A_{12}x_1 + A_{21}}\right)^2 \tag{3-82}$$

In this model, the size difference between molecules is taken into account. As in the previous method, there is no temperature dependency.

The main problem with the Van Laar equation is its failure to describing highly non-ideal system. It also lacks a good representation of data for isothermal condition. The Van Laar equation can however be used for relatively simple non-polar solutions [Prausnitz et al., 1986].

Both the Margules and Van Laar equations have the merit of simplicity and provide flexibility in fitting VLE data for simple binary mixtures.

3.2.2.4 Wilson equation (1964)

In 1964, Wilson proposed a new model which is based on more advanced theories. Wilson considered energetic interactions between molecules which depend primarily on local composition.

The G^E model for the Wilson model is given by:

$$\frac{G^E}{RT} = -x_1 \ln\left(x_1 + \Lambda_{12}x_2\right) - x_2\left(x_1\Lambda_{21} + x_2\right) \tag{3-83}$$

$$\Lambda_{ji} = \frac{V_i}{V_j} \exp\left[-\frac{\lambda_{ji} - \lambda_{jj}}{RT} \right] \tag{3-84}$$

Where,

Λ_{12} and Λ_{21} are adjustable parameters, λ_{jj} and λ_{ji} are energetic interaction terms, V_j and V_i are the molar volumes at temperature T of pure liquids j and i.

The activity coefficients derived from Equations (3-86) and (3-87) are given by:

$$\ln \gamma_1 = -\ln(x_1 + \Lambda_{12} x_2) + x_2 \left(\frac{\Lambda_{12}}{x_1 + \Lambda_{12} x_2} - \frac{\Lambda_{21}}{\Lambda_{21} x_1 + x_2} \right) \tag{3-85}$$

$$\ln \gamma_2 = -\ln(x_2 + \Lambda_{21} x_1) - x_1 \left(\frac{\Lambda_{12}}{x_1 + \Lambda_{12} x_2} - \frac{\Lambda_{21}}{\Lambda_{21} x_1 + x_2} \right) \tag{3-86}$$

The Wilson equation has built-in temperature dependence for the adjustable parameters. This facilitates the parameter determination on local-composition models. The Wilson equation provides a good representation of the Gibbs energies for a variety of miscible mixtures, including systems that contain polar or associating compounds in alcohols. The major disadvantage that came with this model is its failure to predict limited miscibility for certain systems. To remedy the drawback, Prausnitz et al. [1986] suggested the use of the Wilson model only on systems that are completely miscible or for those limited regions of partially miscible systems where one liquid is present.

T-K Wilson model (1975)

In 1975, Tsuboka and Katayama successfully modified the Wilson (two-parameter) model into a model with three parameters called T-K Wilson model. It is expressed in terms of the G^E model as follows:

$$\frac{G^E}{RT} = x_1 \ln\left(\frac{x_1 + V_{12} x_2}{x_1 + \Lambda_{12} x_2} \right) + x_2 \ln\left(\frac{V_{12} x_1 + x_2}{\Lambda_{12} x_1 + x_2} \right) \tag{3-87}$$

Where

$$V_{ji} = \frac{V_i}{V_j} \tag{3-88}$$

The equation for activity coefficients are given by:

$$\ln \gamma_1 = \ln\left(\frac{x_1 + V_{12}x_2}{x_1 + \Lambda_{12}x_2}\right) + x_2\left(\beta - \beta_v\right) \tag{3-89}$$

$$\ln \gamma_2 = \ln\left(\frac{V_{12}x_1 + x_2}{\Lambda_{12}x_1 + x_2}\right) - x_1\left(\beta - \beta_v\right) \tag{3-90}$$

Where

$$\beta = \frac{\Lambda_{12}}{x_1 + \Lambda_{12}x_2} - \frac{\Lambda_{21}}{\Lambda_{21}x_1 + x_2} \tag{3-91}$$

$$\beta_v = \frac{V_{12}}{x_1 + V_{12}x_2} - \frac{V_{21}}{V_{21}x_1 + x_2} \tag{3-92}$$

The modification brought to the Wilson model permits the description of both miscible and partially miscible systems.

3.2.2.5 NRTL liquid-phase model

An improved liquid composition model known as the Non-Random Two Liquids (NRTL) was proposed by Renon and Prausnitz in 1986. The new model based on both the two liquid model of Scott [1956] and the assumption of non-randomness in the solution aimed to address deficiencies of the Wilson equation. This led to the following equations:

$$\frac{G^E}{RT} = x_1x_2\left(\frac{\tau_{21}G_{21}}{x_1 + G_{21}x_2} + \frac{\tau_{12}G_{12}}{G_{12}x_1 + x_2}\right) \tag{3-93}$$

Where,

$$\tau_{ji} = \frac{G_{ji} - G_{ii}}{RT} = \frac{\Delta G_{ji}}{RT} \tag{3-94}$$

$$G_{ji} = \exp\left(-\alpha_{ji}\tau_{ji}\right) \tag{3-95}$$

In Equations (3-93) and (3-95) τ_{ij} and τ_{ji} are adjustable parameters and $\alpha_{ji} = \alpha_{ij}$ the non-random parameter. According to Walas [1985] the values for α_{ij} vary from 0.2, 0.3 and 0.5 depending on the type of mixtures.

The activity coefficients are derived as:

$$\ln \gamma_1 = x_2^2 \left[\tau_{21} \left(\frac{G_{21}}{x_1 + G_{21} x_2} \right)^2 + \frac{\tau_{12} G_{12}}{\left(G_{12} x_1 + x_2 \right)^2} \right] \tag{3-96}$$

$$\ln \gamma_2 = x_1^2 \left[\tau_{12} \left(\frac{G_{12}}{G_{12} x_1 + x_2} \right)^2 + \frac{\tau_{21} G_{21}}{\left(x_1 + G_{21} x_2 \right)} \right] \tag{3-97}$$

The NRTL model has notable advantages over the Wilson equation. It predicts accurately both partially and completely miscible systems. Raal and Mühlbauer [1998] stated that this model provided good representation for strongly non-ideal mixtures and is readily generalized to multi-component systems. However, the inaccuracy of the NRTL in the range of very low concentration is evident. Vetere [2000] explains the behaviour and corrects the deficiency by introducing a volumetric molar ration term in the analytical form of the NRTL equation. The main disadvantage is associated with the necessity for fitting three parameters; its mathematical complexity poses problems in certain cases.

3.2.2.6 UNIQUAC liquid-phase model

Abrams and Prausnitz [1975] developed and proposed an equation that extends the quasi chemical lattice theory of Guggenheim. This new equation is based on the concept of local compositions and is known as the UNIversal QUAsi Chemical theory.

The UNIQUAC model treats the Gibbs excess energy as comprised of two parts, a combinatorial term and a residual term.

The excess Gibbs energy may be written as follows:

$$\frac{G^E}{RT} = \left(\frac{G^E}{RT} \right)_{combinatory} + \left(\frac{G^E}{RT} \right)_{residual} \tag{3-98}$$

where the combinatorial term accounts for molecular size and the residual for molecular interactions.

For a binary system,

$$\left(\frac{G^E}{RT}\right)_{combinatory} = x_1 \ln\frac{\Phi_1}{x_1} + x_2 \ln\frac{\Phi_2}{x_2} + \frac{z}{2}\left(x_1 q_1 \ln\frac{\theta_1}{\Phi_1} + x_2 q_2 \ln\frac{\theta_2}{\Phi_2}\right) \quad (3\text{-}99)$$

$$\left(\frac{G^E}{RT}\right)_{residual} = x_1 q'_1 \ln\left(\theta'_1 + \theta'_2 \tau_{21}\right) - x_2 q'_2 \ln\left(\theta'_2 + \theta'_1 \tau_{12}\right) \quad (3\text{-}100)$$

Where

$$\Phi_i = \frac{x_i r_i}{\sum_k r_k x_k} \quad (3\text{-}101)$$

$$\theta_i = \frac{x_i q_i}{\sum_k q_k x_k} \quad (3\text{-}102)$$

$$\tau_{ji} = \exp\left(-\frac{u_{ji} - u_{ii}}{RT}\right) \quad (3\text{-}103)$$

In these equations r_i and q_i are relative molecular volume and relative molecular surface area and τ_{12} and τ_{21} are the two adjustable parameters to account for binary interactions.

The corresponding expression for the activity coefficients is given by:

$$\ln\gamma_1 = \ln\left(\frac{\Phi_i}{x_i}\right) + \frac{z}{2} q_i \ln\left(\frac{\theta_i}{\Phi_i}\right) + l_i - \frac{\Phi_i}{x_i}\sum_j x_j l_j - q_i \ln\left(\sum_j \theta_j \tau_{ji}\right) + q_i - q_i \sum_j \frac{\theta_j \tau_{ij}}{\sum_k \theta_k \tau_{kj}} \quad (3\text{- }104)$$

Where,

$$l_i = \frac{z}{2}\left(r_i - q_i\right) - \left(r_i - 1\right) \quad (3\text{-}105)$$

In addition to the previous equation, z is the co-ordination number, usually set to ten, r, q and q' are structural size area and modified-area parameters respectively which are used in the determination of the parameters: l, Φ, θ, θ' and τ_{ij}.

The UNIQUAC equation is extremely useful in predicting multicomponent VLE in terms of binary parameters only. It describes liquid-liquid equilibrium well and builds in temperature

dependence. The UNIQUAC equation takes into consideration very large differences between sizes of molecules. Its main drawback is the greater mathematical complexity.

3.2.2.7 Group contribution liquid-phase model

Considering the possible number of compounds of interest in technological processes, it is unreasonable to expect experimental thermodynamic data for a significant fraction of this number. To partially remedy this problem, the excess Gibbs energy models are used in the correlation and prediction of experimental data. Through experimental data, activity coefficients are calculated to obtain binary interaction parameters to extend their applicability to mixtures.

A quantitative knowledge of interaction between groups of molecules from the reduction of experimental data can help to estimate the interaction between molecules and then estimate phase equilibria for systems for which no experimental data is available.

Theories of liquid-solution behavior based on well-defined thermodynamic assumptions have been attempted yielding predictive models with parameters to predict activity coefficients for other systems. The most notable of these are listed here.

1. The regular solution theory developed by Scatchard and Hildebrand [1962]. This model was developed from the theory of Van Laar; its relationships developed for the excess Gibbs energy are based on solubility parameters.

2. The analytical solution of groups (ASOG) model developed by Deer and Deal [1969]. This group-contribution model is based on the principle of independent action as proposed by Langmuir.

3. The UNIFAC method developed by Fredenslund et al. [1977] is based on the UNIQUAC equation. It depends on the idea that a liquid mixture may be considered a solution of the structural units from which the molecules are formed rather than a solution of the molecules themselves [Smith et al., 2005].

Every one of the group-contribution methods listed above has its limitation, advantage and disadvantage. For further details, the reader is referred to: Hildebrand and Scott [1964], Wilson and Deal [1962], Fredenslund et al. [1977], Kehiaian [1983] and Kojima [1997].

These and other related models are clearly discussed by Walas [1985], Sandler [1997], Ramjugernath [2000], Moodley [2002], Naidoo [2004] and Mühlbauer and Raal [1994].

3.2.3 The mixing rules

Mixing rules are necessary when equations of state for pure fluids are used to calculate various thermodynamic properties of fluid mixtures. There are basically two methods of applying an EoS to mixtures. Determination of the mixture's pseudo-critical properties, referred to as method A by Walas [1985] and of the EoS mixture parameters which are derived from those of the individual component, referred to as the method B by Walas [1985].

In method A, mixture-critical properties are determined by means of suitable mixing rules and thereafter calculation of the EoS a_m and b_m parameters is performed. The simplicity of these mixing rules is the mole-fraction-weighted sums of the corresponding property parameter for the component of the mixture. Several mixing rules on this method are available in Walas [1985].

In method B, the most commonly used pure-components a_i and b_i parameters are determined from pure component properties such as critical temperature, critical pressure, etc. [Raal and Mühlbauer, 1998]. Mixing rules are taken into account only to express the EoS a_m and b_m component as some function of composition and pure-component a_i and b_i parameters. The simplicity of the mixing rules is also the mole-fraction-weighted- sums of the corresponding EoS pure-component parameters for each of the components making up the mixture. More details concerning method B are given in Walas [1985].

The focus in this investigation will be on the method B since it is by far the most commonly used.

For the Van der Waals EoS, Lorentz and Berthelot proposed the following mixing rules [Raal and Mühlbauer, 1998]:

$$a_m = \sum_{i=1}^{n}\sum_{j=1}^{n} z_i z_j a_{ij} \tag{3-106}$$

$$b_m = \sum_{i=1}^{n}\sum_{j=1}^{n} z_i z_j b_{ij} \tag{3-107}$$

where z may express either the liquid or vapour phase composition of species i or j

For the R-K EOS, Redlich and Kwong proposed [Naidoo, 2004]:

$$a_m = \sum_{i=1}^{n}\sum_{j=1}^{n} z_i z_j a_{ij} \tag{3-108}$$

Where $a_{ij} = \left(a_i a_j\right)^{1/2}$

$$b_m = \sum_{i=1}^{n}\sum_{j=1}^{n} z_i z_j b_{ij} \tag{3-109}$$

For the SRK-CEOS, Soave introduced a binary interaction parameter k_{ij} in a_{ij}.

$$a_{ij} = \sqrt{a_i a_j}\left(1 - k_{ij}\right) \tag{3-110}$$

Peng and Robinson also considered the cross parameter a_{ij} as defined by Soave.

From (3-108) to (3-110), these equations are known as "the classical mixing rules" or "van der Waals one-fluid classical mixing rules". They have provided good representations of mixtures of hydrocarbons, hydrocarbons with inorganic gases, non-polar and slightly polar components but are not successfully applicable to mixtures of relatively moderate solution non-ideality [Naidoo, 2004].

Since the van der Waals mixing rules were proposed, there has been extensive progress made in research towards the development of new mixing rules. Several authors have proposed different approaches which have been quite successful [Raal and Mühlbauer, 1998]. Among them, the Huron-Vidal, the Wong-Sandler, the modified Huron-Vidal 1 (MHV1), the modified Huron-Vidal 2 (MHV2) and the PSRK mixing rules. The reader is referred to Coquelet [2003] for additional information. However, only the Wong-Sandler mixing rule will be fully described as it will be of service to this project.

The Wong-Sandler mixing rule (WSMR)

In 1992, Wong-Sandler developed a new mixing rule to extend the applicability of the van der Waals mixing rule to diverse systems. The Wong-Sandler mixing rule falls into the category of the density independent mixing rule which preserves the cubic nature of a cubic EoS. The new mixing rule requires activity coefficient models for the calculation of excess Helmholtz free energy since this provides correct low and high densities without being density dependent. It also provides the simplest method of extending the UNIFAC group contribution method or other low-pressure methods to high temperatures and pressures [Naidoo, 2004].

The mixing rule of Wong and Sandler [1992] states the mixture parameters as:

$$\frac{a_m}{RT} = Q\frac{D}{1-D} \tag{3-111}$$

$$b_m = \frac{Q}{1-D} \tag{3-112}$$

Where Q and D are defined as:

$$Q = \sum\sum z_i z_j \left(b - \frac{a}{RT}\right)_{ij} \tag{3-113}$$

With

$$\left(b - \frac{a}{RT}\right)_{ij} = \frac{1}{2}\left[b_i + b_j\right] - \frac{\sqrt{a_{ii}a_{jj}}}{RT}\left(1 - k_{ij}\right) \tag{3-114}$$

$$D = \frac{A^E_{EOS}\left(T, P = \infty, x_i\right)}{\Lambda RT} + \sum_{i=1}^{n} z_i \frac{a_i}{b_i RT} \tag{3-115}$$

and $A^E_{EOS}\left(T, P = \infty, x_i\right)$ is the excess Helmholtz free energy calculated at infinite pressure. The fugacity coefficients for the vapour and liquid phases calculated using the Soave (SRK) and the Peng-Robinson (PR) EoS are expressed as follows:

Soave (SRK) EoS:

$$\ln\hat{\phi}_i = -\ln\left[\frac{P\left(V - b_m\right)}{RT}\right] + \frac{1}{b_m}\left(\frac{\partial n b_m}{\partial n_i}\right)\left(\frac{PV}{RT} - 1\right) + \left(\frac{a_m}{b_m RT}\right) \left(\frac{1}{a_m}\left(\frac{1}{n}\frac{\partial n^2 a_m}{\partial n_i}\right) - \frac{1}{b_m}\frac{\partial n b_n}{\partial n_i}\right)\ln\left(\frac{V}{V + b_m}\right) \tag{3-116}$$

Peng-Robinson (PR) EoS:

$$\ln\hat{\phi}_i = -\ln\left[\frac{P\left(V - b_m\right)}{RT}\right] + \frac{1}{b_m}\left(\frac{\partial n b_m}{\partial n_i}\right)\left(\frac{PV}{RT} - 1\right) + \frac{1}{2\sqrt{2}}\left(\frac{a_m}{b_m RT}\right) \left[\frac{1}{a_m}\left(\frac{1}{n}\frac{\partial n^2 a_m}{\partial n_i}\right) - \frac{1}{b_m}\frac{\partial n b_n}{\partial n_i}\right]\ln\left[\frac{V + \left(1 - \sqrt{2}\right)b_m}{V + \left(1 + \sqrt{2}\right)b_m}\right] \tag{3-117}$$

The Wong and Sandler mixing rule has proven to be excellent in the correlation of VLE and LLE data. It accurately applies to both simple and complex systems consisting of polar and associating species. Combined with a cubic EoS, the Wong and Sandler mixing rule can be used for a wide range of highly non-ideal systems (including critical regions). Despite its capabilities to predict, correlate and model various numbers of systems, this mixing rule has failed for systems comprised of non polar systems with light gases.

For additional information, the reader is referred to Raal and Mühlbauer [1998] which presents an excellent review of the development of mixing rules.

3.2.5 Vapour-Liquid Equilibrium

Vapour-liquid equilibrium is a state or condition where a vapour phase is in equilibrium with its liquid phase. When two phases are brought into contact, an exchange of their different constituents takes place until the compositions of their respective phases becomes stable. The two phases are then said to be in equilibrium.

As mentioned earlier, Raal and Mühlbauer [1998] define equilibrium as there being no change in the properties of the material over time. Mathematically, this may be expressed by:

$$dG_i(T,P) = 0 \tag{3-118}$$

By definition,

$$dG_i = RTd\ln f_i \tag{3-119}$$

A further development of Equation (3-119) leads to Equation (3-120) which is a criterion for phases (liquid and vapour) at equilibrium in terms of fugacities.

$$f_i^l(T,P,x_i) = f_i^v(T,P,y_i) \tag{3-120}$$

The equation describing phases at equilibrium has been set and fugacities for each phase have to be calculated as well.

A set of VLE data is frequently represented in forms of plots called phase diagrams. The common plots are temperature versus vapour mole fraction y_i and liquid mole fraction x_i for isobaric condition and pressure versus vapour mole fraction y_i and liquid mole fraction x_i for isothermal condition. Other possible plots are vapour mole fraction y_i versus liquid mole fraction x_i for either the isothermal condition or the isobaric condition.

To date, analytical methods have been developed and proposed for the thermodynamic interpretation of binary HPVLE data. We distinguish the direct method, combined method and the modern direct method.

The combined method uses an equation of state and a liquid-phase model to describe the vapour non-idealities and the liquid non-idealities respectively.

In the direct method, an equation of state is used to describe both, the non-idealities of the liquid and vapour phases.

The modern direct method, which is a combination of the combined and the direct method, is used to overcome difficulties encountered in the combined and the direct method.

A comparison between the combined and the direct method with respect to modelling, prediction and correlation is available in Raal and Ramjugernath [1999].

3.2.5.1 The combined method

Initially, reduction of phase equilibrium data was undertaken using the combined method which was essentially a logical progression of the excellent low-pressure correlation techniques in use at the time. This method, also known as the $\gamma - \phi$ method, permits excellent representation of the liquid and vapour phases of complex systems in low to medium pressure range. The combined method uses an equation of state and a liquid-phase model to respectively describe the vapour non-idealities and the liquid non-idealities. Hence at equilibrium we have:

$$\hat{f}_i^v = y_i \hat{\phi}_i^v P = \hat{f}_i^l = x_i \gamma_i f_i^{OL}(T, P) \tag{3-121}$$

The fugacity coefficient (ϕ_i) and the activity coefficient (γ_i) are calculated using an equation of state and the Gibbs- Duhem equation (relating the activity coefficient to the molar excess Gibbs free energy) respectively. Equations (3-122) and (3-123) illustrate this.

$$\ln \hat{\phi}_i^v = \left(\frac{1}{RT}\right) \int_V^\infty \left[\left(\frac{dP}{dn_i} \right)_{T,V,n_j} - \frac{RT}{V} \right] dV - \ln\left[\frac{PV}{RT}\right] \tag{3-122}$$

$$\sum x_i d \ln \gamma_i = \sum x_i d\left(\frac{\overline{G}_i^E}{RT}\right) = \left(-\frac{\Delta H}{RT^2}\right) dT + \left(\frac{\Delta V}{RT}\right) dP \tag{3-123}$$

The purpose of γ_i the activity coefficient is to relate the liquid fugacity $\hat{f}_i^l$ at mole fraction *x*, *T* and *P* to some other condition where its value is accurately known. This other condition is the standard $\left(f_i^{OL}\right)$ state and represents the known and defined thermodynamic condition of a component at which its activity coefficient equals 1. The combine method works well except at conditions below the critical region. It has a correlative ability that depends on the excess Gibbs free energy model chosen for the liquid phase and the EoS that describe the vapour phase. However the $\gamma-\phi$ method has its limitations to some extent. Among these, its extrapolation to a wider range of temperatures and pressures is not possible since model parameters obtained at one temperature are not always applicable to others. Further, the use of two different models for the vapour and liquid phases produces bad results in the critical region.

3.2.5.2 The direct method

The direct method also known as the $\phi-\phi$ method was developed to overcome the difficulties of describing supercritical components and therefore the high-pressure critical region in the combined method.

The direct method uses fugacity coefficients to describe the liquid and vapour phase non-idealities of a mixture at the equilibrium state.

The result in the equilibrium condition is described by:

$$\hat{f}_i^v = y_i\hat{\phi}_i^v = \hat{f}_i^l = x_i\hat{\phi}_i^l \tag{3-124}$$

The vapour-phase fugacity coefficient ($\hat{\phi}_i^v$) is calculated from Eq. (3-122). Similarly the liquid-phase fugacity coefficient is calculated from (3-125).

$$\ln\hat{\phi}_i^l = \frac{1}{RT}\int_v^\infty\left[\left(\frac{\partial P}{\partial n_i}\right)_{T,V,n_j} - \frac{RT}{V}\right]dV - \ln\left[\frac{PV}{RT}\right] \quad (j \neq i) \tag{3-125}$$

To calculate the fugacity coefficient from an EoS through Equation (3-125), parameters *a* and *b* (from an EoS) are necessary to account for the molecular interaction energy and the molecular size. When equations of state are used for highly non-ideal mixtures and the liquid phase in the direct method, the mixing rules for those parameters are necessary [Chen et al., 1996]. Accordingly, researchers have proposed “mixing rules” to facilitate the determination of these parameters. The $\phi-\phi$ approach works well up to the critical region and its accuracy

depends on the EoS chosen and the number of adjustable parameters. The mixing rules play also a significant role in the accuracy. However, the method rates from poor to fair in the modelling of highly polar and structurally complex systems. The direct method is predictive when the UNIFAC contribution model is used to determine the excess Gibbs free energy. It also has the correlative ability that depends on the complexity of the EoS, mixing rules and the adjustable parameters.

In the last few years, several attempts have been made to use the direct method to model VLE data for refrigerant systems. It is the case of Silva-Olivier and Galacia-Luna [2002], Rivollet et al. [2004] and Hakim et al. [2008]. These authors used different EoS with different mixing rules incorporating the NRTL model. The results obtained were found consistent with the experimental data. In this regard, the direct method was chosen as the analytical method. This will be of service to this project.

3.2.5.3 The modern direct method

This method is a combination of the combined and the direct method. It was developed to firstly overcome numerous problems associated with the use of separate models to describe the vapour and liquid phases in the combined method and lastly the difficulties in defining standard states especially for supercritical components.

The new approach is based on the incorporation of activity coefficients into the vapour and liquid phase fugacity coefficients. This is achieved by using novel mixing rules which combine EoS and excess Gibbs or excess Helmholtz free energies.

Traditional EoS are used to correlate as well as predict (in certain cases) VLE behavior over wide ranges of temperature and pressure for complex systems that previously could only be described by activity coefficient models.

3.2.6 Analytical methods for HPVLE

As mentioned earlier, three methods have been developed for the calculation of HPVLE data; the combined, the direct and the modern direct method. For each method different approaches are used.

Three approaches are of great use in the direct and combined methods: the dew point, the bubble point and the flash calculations. When the system temperature and the liquid composition x are given, the approach is known as the bubble point pressure calculation. Otherwise, it is known as the dew point pressure calculation which means temperature and vapour composition y are fixed.

At fixed pressure, these approaches are either known as the bubble point temperature or the dew point temperature depending on whether the liquid or the vapour composition is given.

In the flash calculation mode, temperatures and pressures are known and the phase compositions are calculated using thermodynamic models.

Particular attention was drawn to the flash calculations for the direct method. This will be of service to this project since only isothermal measurement will be undertaken.

Different steps considered for the calculation as well as regression of isothermal VLE data using the direct method (flash calculation) are schematically shown in Figure 3.2.

An excellent review on analytical methods as well as its correspondent approaches for the HPVLE data calculation can be found in Naidoo [2004], Raal and Mühlbauer [1994] and Prausnitz and Chueh [1968].

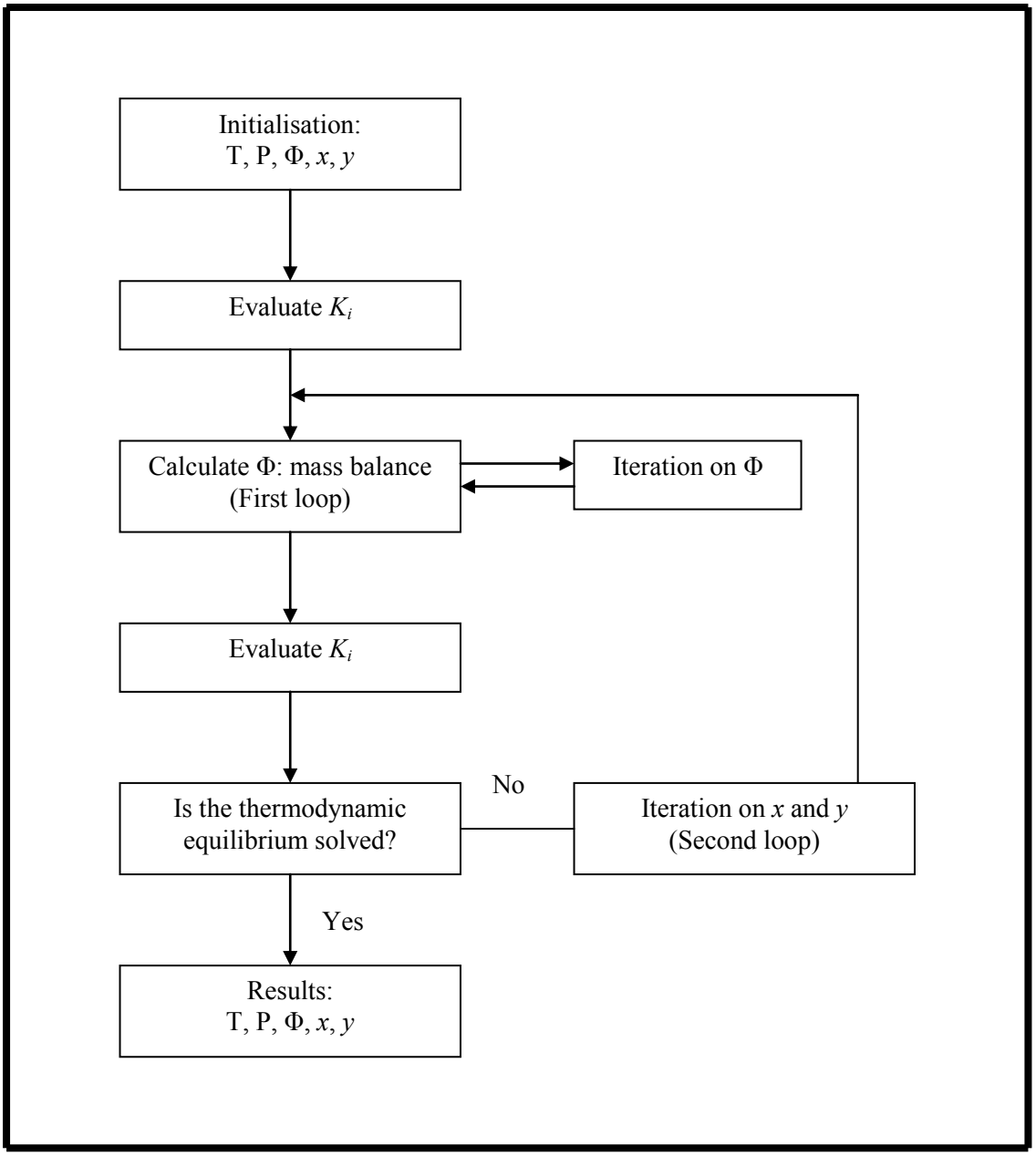

Figure 3-2: Block diagram for a T-flash calculation [Coquelet, 2003]

3.2.7 Choosing thermodynamic models

There is no universal combination of thermodynamic models to correlate phase behaviour. However, choosing thermodynamic models that correlate well phase behaviour depends on the properties of the system of interest. One should carefully analyze components making up the system, the type of molecules and the type of intermolecular forces.

In this research project, attention is drawn to refrigerant systems and most particularly to the mixture of hydrocarbon and fluorochemical systems. In the account for hydrocarbons, saturated alkanes are considered. This type of molecules is nonpolar. Perfluorocarbons and

fluoropolymers are considered for fluorochemical compounds; these are mostly polar molecules. However, the intermolecular forces between compounds of interest are van der Waals forces; therefore the interactions between molecules are weak.

Numerous models have been proposed to provide reasonably accurate predictions/correlation of phase behaviour for various systems. Some of these models are presented at the beginning of the chapter. Their capabilities and limitations are also discussed.

Several attempts have been made to use such models to correlate VLE data for refrigerant systems. Among these, Valtz et al. [2002] measured the binary system consisting of propane + 1,1,1,2,3,3,3 –heptafluoropropane (227ea) at temperatures from 293.16 K to 353.18 K and pressures up to 3.4 MPa. The data measured data were correlated with the Soave-Redlich-Kwong EoS and several mixing rules involving the NRTL model. In each case, the measured data were found consistent with the models but the best results were obtained with the Wong-Sandler mixing rules. Coquelet et al. [2003] also measured VLE data for the azeotropic difluoromethane + propane system at temperatures from 294.83 to 343.26 K and pressures up to 5.4 MPa. The measured data were correlated with the Soave-Redlich-Kwong EoS and MHV1 mixing rules involving the NRTL model. The models chosen correlated well the data except the data measured at 343.26 K (location of two critical points) where the Peng-Robinson EoS and the Wong-Sandler mixing rules were used and yielded good results. The Wong-Sandler mixing rules are flexible and work well in the critical region. Later on, Ramjugernath et al. [2009] measured isothermal VLE data for the hexafluoroethane (116) + propane system at temperatures from (263 to 323) K. The full set of isothermal VLE data was correlated with the Peng-Robinson EoS, incorporating the Mathias-Copeman alpha function, with the Wong-Sandler mixing rule utilizing the NRTL activity coefficient model. The experimental results were found consistent with the modelled data.

Others VLE data measurements were performed for systems involving hydrocarbon and fluorochemical compounds at various temperatures and pressures. A combination of the Peng Robinson EoS using the Mathias-Copeman alpha function and the Wong Sandler mixing rules involving the NRTL model was used as the thermodynamic models. The results obtained were in excellent agreement with the modelled data. These VLE data are available in Coquelet [2003]. Since several authors have proven this combination to be successful for modelling systems involving hydrocarbon and fluorochemical compounds, this will also be used in this project.

3.3 Thermodynamic Consistency tests

The inaccuracies that are frequently encountered in the measuring experimental phase equilibrium properties such as VLE data have led researchers to come up with methods to ensure the quality of such data. The thermodynamic relationship that is most often used for thermodynamic consistency test is the Gibbs-Duhem equation. Thereby, it serves as the basis of all thermodynamic consistency tests.

The Gibbs-Duhem equation inter-relates the activity coefficients, the partial Gibbs free energy, or the fugacity coefficients of every single component in a given mixture. It is expressed:

$$\sum_i x_i d\ln\gamma_i = \sum_i x_i d\left(\frac{\overline{G}_i^{\,E}}{RT}\right) = \left(-\frac{\Delta H}{RT^2}\right)dT + \left(-\frac{\Delta V}{RT}\right)dP \qquad (3\text{-}126)$$

A complete binary VLE data set is judged to be thermodynamically consistent when it satisfies both globally and locally the Gibbs-Duhem equation. But this is not a sufficient condition since it is not guaranteed that the data are correct. However, if it does not satisfy the Gibbs-Duhem equation, it is certain that they are incorrect [Chueh et al., 1965].

The computation of phase equilibrium data at low pressure is commonly performed either in an integral area test discussed in Raal and Mühlbauer [1998], in a differential test [Van Ness et al., 1973], or an infinite dilution test [Kojima et al., 1990].

Thermodynamic analysis in HPVLE is much more difficult and less certain than in LPVLE, this is because:

In HPVLE there is a strong pressure dependence of the mixture molar volume at saturation.

An EoS is used to model the vapour phase in order to account for vapour non-idealities.

In most high-pressure equilibria, the more volatile component is often supercritical, therefore the standard state definition must be considered.

Different thermodynamic consistency tests are obtained by different manipulations of the Gibbs-Duhem equation. They are:

1. The Chueh et al. [1965] test, which is an extension of the integral test for LPVLE to HPVLE, requires an EoS to model the vapour phase fugacity.

2. The Mühlbauer and Raal [1991] test is a modified "Chueh et al [1965] test" that uses only P-T-y data and the liquid-phase molar volumes are not needed. However, an EoS is used to calculate the vapour-phase molar volumes and fugacity coefficients.

3. The Bertucoo et al. [1997] test is an extension method from moderate pressure to high pressure for binary isothermal data, where the direct method is used. The SRK EoS with the Huron-Vidal mixing rules has been applied to this data reduction procedure

4. The Van Ness et al. (1973) point test is an improvement to the area test. This test requires thermodynamic models to calculate the vapour mole fraction. Both the direct and combined are used.

The consistency test used in this work is that of Van Ness et al. [1973] this test has been used by several researchers and has been deemed adequate for systems similar to the ones being investigated.

The Van Ness et al. (1973) point test

Van Ness et al. [1973] developed the point test primarily based on the Gibbs-Duhem equation. This test requires thermodynamic models to calculate the vapour phase mole fraction from the experimental data.

The point test establishes a comparison between the calculated and the measured vapour mole fraction. This comparison generates residual Δy_1 which grants some insight into the thermodynamic consistency for the experimental VLE data.

According to Danner and Gess [1990], a complete binary VLE data set is said to be thermodynamically consistent when the average absolute deviation between the calculated and the measured vapour mole fraction is less than 0.01.

CHAPTER

FOUR

EXPERIMENTAL APPARATUS

One of the primary objectives of this research is to construct and commission a new static analytical apparatus capable of accurate HPVLE data measurement in cryogenic conditions. Accordingly, this chapter will be focused on the description of the new static analytical apparatus.

High-pressure vapour-liquid equibrium data measurement is a difficult and time consuming task as measurements are often taken manually. An obvious solution would be affordable automation which would permit efficient operation of the apparatus and increase accuracy of one's results.

The use of the new static analytical apparatus might enable one to rapidly determine accurate and precise HPVLE data consisting of: pressure, temperature, liquid, and vapour composition.

The principal features required of the new apparatus are:

1. A constant-volume and visual equilibrium cell capable of VLE measurement by dew and bubble point method
2. A method of agitating the equilibrium cell content
3. A withdrawal and sampling method of the liquid and vapour phases
4. An environment that maintains isothermal conditions in the equilibrium cell
5. A degassing method for the cell contents
6. Devices for pressure and temperature measurement
7. A method of analyzing the liquid and vapour phases

A schematic diagram illustrating the essential features and layout of the new static analytical experimental apparatus is shown in Figure 4.1.

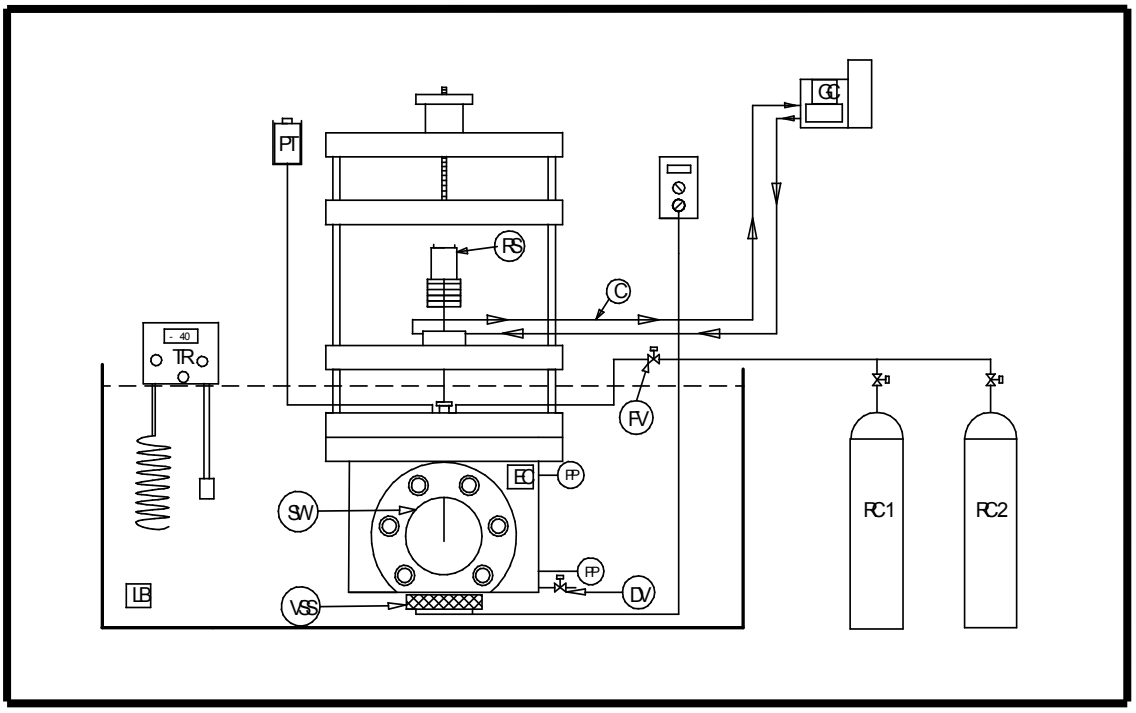

Figure 4-1: Scheme of the static analytic apparatus

DV: drain valve, EC: Equilibrium Cell, FV: Feeding Valve, GC: gas chromatography, LB: Liquid Bath, PP: Platinum Probe, PT: Pressure Transducer, RC1, 2: Component 1 and 2, RS: ROLSI sampler, SW: sapphire window, TR: Heater circulator, VSS: Stirrer Assembly.

4.1. Experimental equipment description

4.1.1. Equilibrium cell

The main feature of the experimental apparatus is the equilibrium cell which was constructed from a 316 stainless steel consisting of a cylindrical cavity with two sapphire windows. It has an internal diameter of 30 mm and a length of 85 mm which results in an effective internal volume of approximately 60 cm^3. This is illustrated in Figure 4.2. See also Photograph 4.1 and 4.2.

The equilibrium cell with sapphire windows was designed to facilitate observation of the liquid level, viewing of the phases in equilibrium, and to observe the adjustment of the capillary of the mobile ROLSI ^{TM} sampler into either the liquid or vapour phase during sampling. It allows the user to determine whether or not the supercritical state of the system has been reached, and to observe the formation of additional phases that might occur within certain temperatures and pressures ranges.

Synthetic sapphire windows with 33 mm of diameter and 14 mm of thickness were installed and presented a viewing diameter of 22 mm on both the front and back side of the equilibrium cell. To avoid any friction between metal and glass, the windows were encased in a gasket material which was tightly press fitted into the body of the equilibrium cell. Vital 'O' rings were used as sealing method between the gasket material and the sapphire windows. They were also used between the sapphire and the body of the equilibrium cell. Each window was placed at its respective position and bolted on to the cell by means of 5 mild steel bolts of 8 mm.

The equilibrium cell was fitted with a cap through which the mobile ROLSI ^{TM} pneumatic capillary passed. A 316 stainless steel flange blind 110 mm in diameter and 10 mm thick was used as a support for the ROLSI ^{TM} sampler. The displacement of the ROLSI ^{TM} pneumatic capillary within the cell was achieved from a differential screw adjuster fitted with M12 threads. This was assisted by two 316 stainless steel tie-rods 10 mm in diameter and 210 mm in length attached to the equilibrium cell by means of three flange blinds of similar dimensions as the one described previously. The two other tie-rods 10 mm in diameter and 160 mm in length were used to support the middle flange blinds.

Two holes 3 mm in diameter were drilled in the top of the equilibrium cell body into the cylindrical cavity (cell). One served as a line to the pressure transducer, the other was used as a line to the filling/evacuating valve. Another 5 mm-diameter hole was drilled in the equilibrium cell body at its lower left hand side. This served as a drain valve. It was used when the normal drainage of the cell was not effective and substances remained at the bottom of the equilibrium cell.

The mobile ROLSI ^{TM} sampler used for sampling phases in equilibrium has a passage through which the sampling lines to and from to the gas chromatograph pass. Two lengths of fine bore-1/8" stainless steel tubing with an approximate length of 700 mm were used as sampling lines.

The bottom of the equilibrium cell body was machined to be as thin as possible (10 mm). This facilitates communication between the stirring bar inside the cell and the magnetic stirrer at the bottom of the body of the cell. Therefore, it enhances rapid attainment of equilibrium between phases.

The design and choice of the material of the cell were undertaken according to the operating conditions of the project (from low temperatures up to 100 $^{\circ}$C and pressure up to 10 MPa). A 316 stainless steel type was used for the entire body of the cell due to its magnetic properties and inertness to organic materials. All fittings and valves were SWAGELOK throughout the entire apparatus.

To perform accurate measurement of temperature inside the equilibrium cell, two Pt-100 sensors were inserted into the body of the cell, one located at the top and the other at the bottom of the cell. A pressure transducer was used for pressure measurement and was mounted in a heated block slightly above the cell. Its connection to the equilibrium cell was possible via heated capillary tubing.

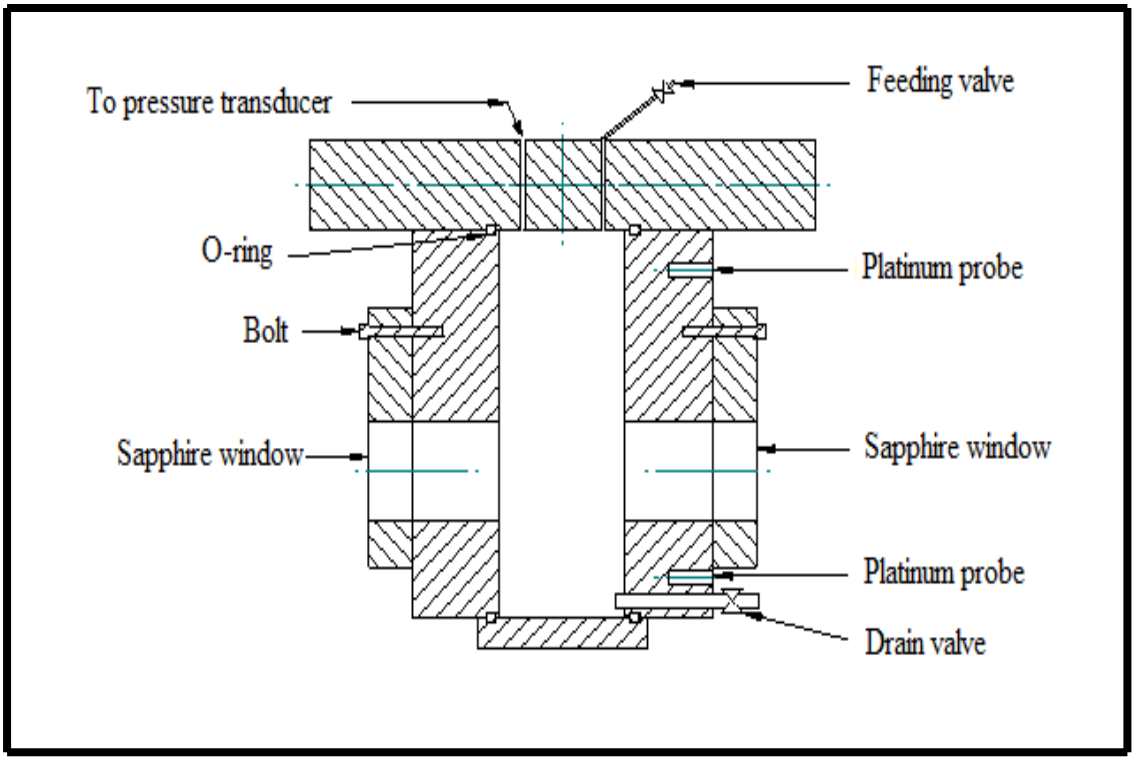

Figure 4.2: **Equilibrium cell**

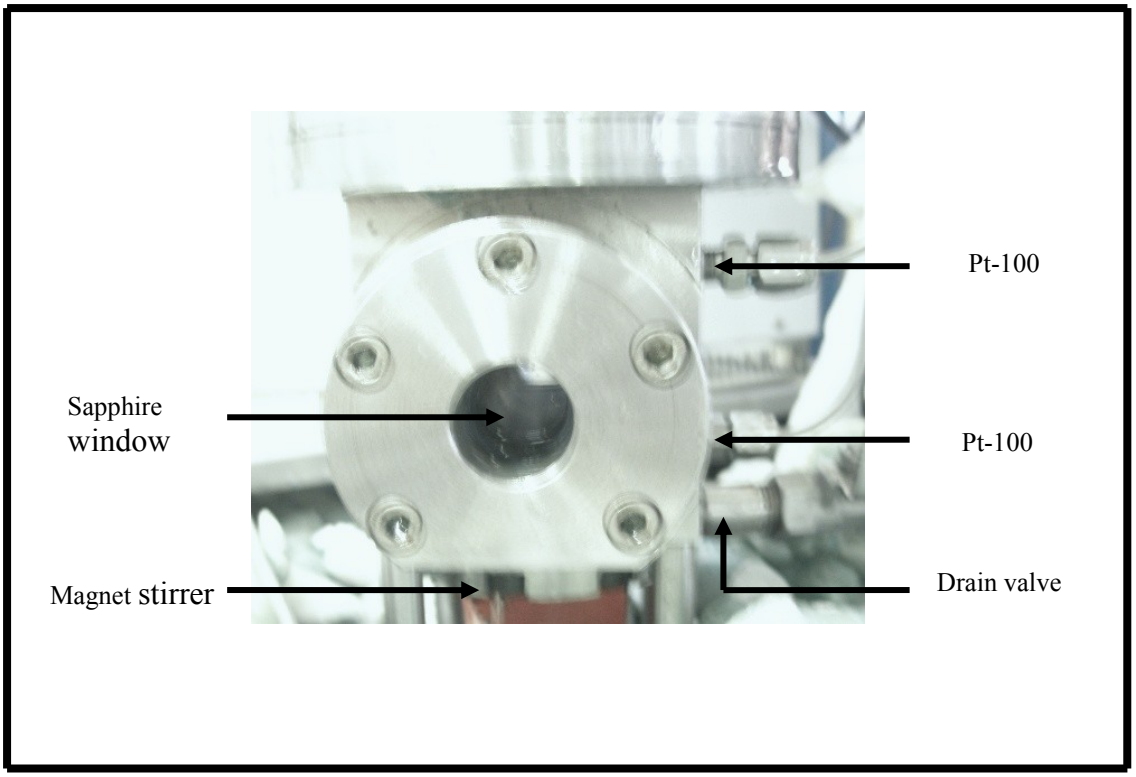

Photograph 4.1: Overview of the equilibrium cell

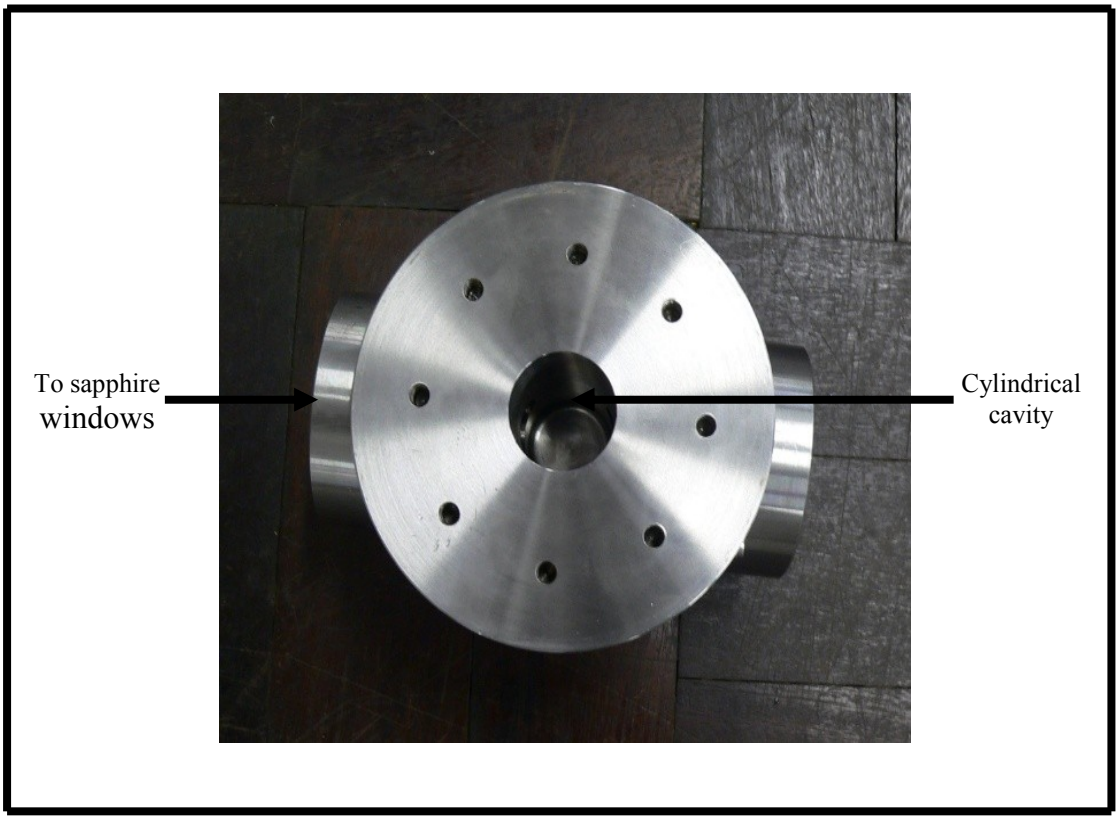

Photograph 4.2: Upper view of the equilibrium cell

4.1.2 Equipment for the agitation of the equilibrium cell contents

A stirring mechanism was incorporated into the final design of the static experimental apparatus for the agitation of the equilibrium cell contents. This was imperative as it helped to achieve efficient intensive mixing as well as the rapid attainment of equilibrium. Therefore, the long time required for phases to reach equilibrium in a static apparatus was reduced.

The stirring mechanism consisted of a Heidolph Model RZR 2021 mechanical stirrer provided by LABOTEC which was outside the main assembly (see Photograph 4.3) and a magnetic stirrer which was placed at the bottom of the equilibrium cell body. The Heidolph Model RZR 2021 mechanical stirrer has the highest torque of its class and two gear speeds which range from 40 to 400 rpm and 200 to 2000 rpm. It was also designed for continuous operation.

The two stirrers were linked by means of two sprockets and a roller chain which transmitted motion from to the other. Two sprockets wheels of 25 teeth and 9 mm-pitch were used. They were incorporated to the main assembly in such a way that one was directly coupled with the shaft from the mechanical stirrer and the other was placed at the bottom of the equilibrium cell body. To ensure proper mixing, a stirring bar 12 mm in length was placed inside the equilibrium cell. Rotation of this was later induced by magnetic coupling by means of an externally located rotating magnetic drive. High speed stirring which resulted in an intense and deep vortex was vital as it helped a rapid mass transfer between phases therefore, shortening the equilibration time.

A space of 20 mm was kept between the bottom of the equilibrium cell body and the magnetic stirrer which was based upon one of the sprocket wheels. This helped preventing any friction between metals and rendering unnecessary the use of any material such as Teflon to avoid metal to metal friction.

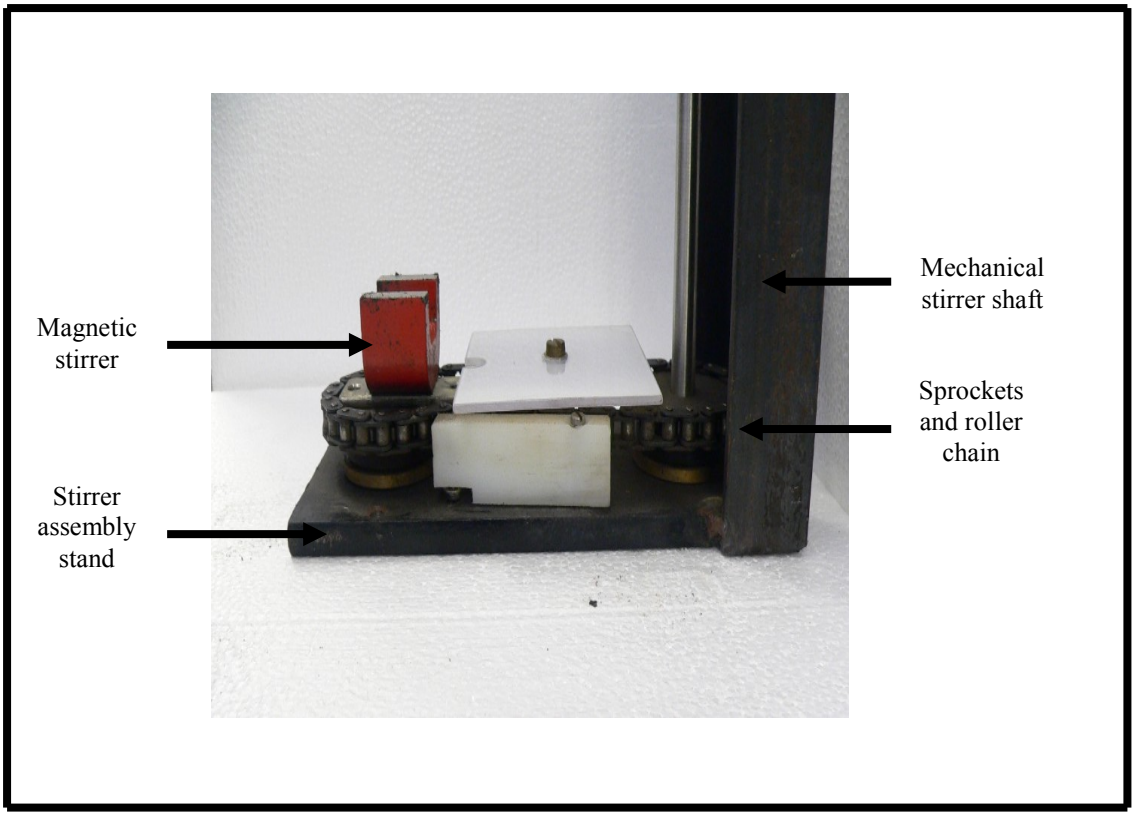

Photograph 4.3: Stirrer assembly

4.1.3 Sampling method for the liquid and vapour phases

Accurate liquid and vapour sampling is among the most difficult challenges to overcome in HPVLE measurement using a static apparatus. A small representative sample of liquid and vapour must be removed from a high-pressure space without disturbing the equilibrium condition [Raal and Mühlbauer, 1998].

Owing to numerous difficulties previously experienced in the liquid and vapour phases sampling, the TEP (Thermodynamique des Equilibres des Phases) laboratory of Mines Paristech developed a novel technique called "Rapid Online Sampler Injector (ROLSI ^{TM})" to overcome the sampling problems in the HPVLE data measurement techniques.

The ROLSI ^{TM} was specially developed for sampling of high-pressure fluids and the analysis of samples by gas chromatography. It is directly connected to a reactor or to a pressure online. However, it allows the in situ removal of repeatable and representative samples from the medium to be analyzed without any contamination or disturbance of it. Its incorporated heating system allows the instant vaporization of a liquid sample or maintaining a gaseous sample removed at high temperature in a gaseous state. Its maintenance proves to be easy and

inexpensive. Hence, the ROLSI ™ was the obvious choice for a method of sampling the liquid and vapour phases for this project. Photograph 4.4 clearly displays the ROLSI ™ sampler.

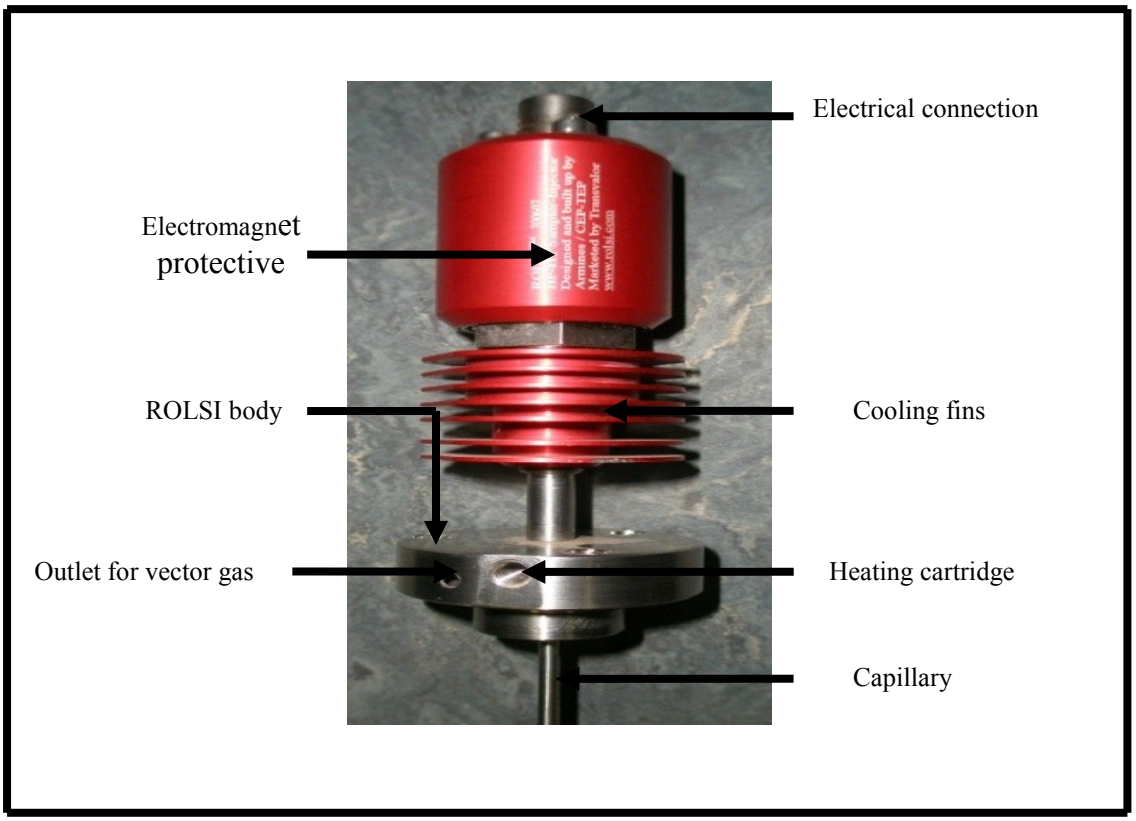

Photograph 4.4: **General view of a ROLSI ™ sampler**

Despite its advantages, the ROLSI™ sampler is limited to some extent. It is the case for sampling of low-pressure fluids. To overcome this, the new apparatus uses the ROLSI™ sampler online with a 6-port gas chromatograph valves. A clear explanation to this is provided in the next paragraph. However, it is very important to set the 6-port valve to facilitate the analysis of phases in equilibrium through the gas chromatograph. There are two modes of operation of the gas chromatograph sampling: the flushing and the sampling modes.

In the flushing mode, the sampling line coming from the ROLSI ™ sampler is closed off and the helium gas that is sent to the gas chromatograph injector splits into reference and carrier lines. The carrier split is sent to the 6-port valve; and the exit helium from the 6-port valve goes to the gas chromatograph injector. The six ports of the gas chromatograph valve are connected to one another so that port 1 communicates with port 2; the other ports connect with one another in a loop. Port 3 communicates with port 4, port 5 with port 6 and port 3 with port 6 via the ROLSI ™ sampler. The set up of the four ports (3, 4, 5 and 6) is connected to a vacuum via ports 4 and 5. This helps in creating a vacuum inside the loop. The vacuum created is also an advantage in performing sampling for low-pressure fluids using the

ROLSI ™ sampler. During a flushing process, port 1 serves as helium inlet and port 2 a helium outlet to the gas chromatograph injector.

In the sampling mode, the sampling line coming from the ROLSI ™ sampler to the gas chromatograph is open to allow the carrier gas to carry sample to the gas chromatograph. During this process, the six ports of the gas chromatograph valve are connected as follows. Port 2 communicates with port 3, port 3 communicates with port 6 via the ROLSI ™ sampler and port 6 with port 1. These ports, altogether, make a loop. The remaining ports, 3 and 4, communicate with each other and are connected to a vacuum. Similarly as in the flushing process, ports 2 and 1 serve respectively as the helium inlet and helium outlet to injector.

The flushing and sampling modes of the gas chromatograph sampling are schematically illustrated in Figure 4.3.

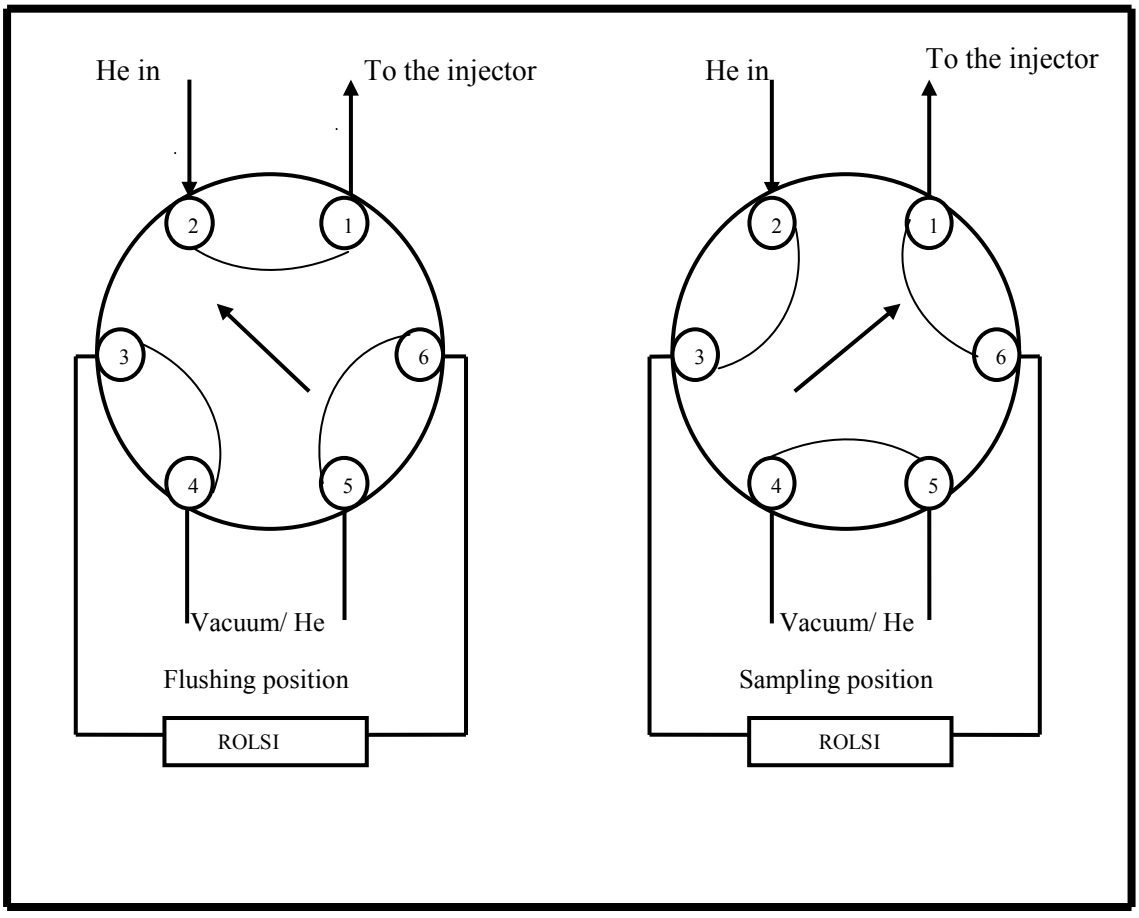

Figure 4.3: Schematic diagrams showing the 6-port GC valve

4.1.4 Liquid bath

In order to perform accurate measurement of temperature and to check for thermal gradient, the equilibrium cell was immersed in a thermo-regulated liquid bath provided by FMH electronics. It has a length of 40.5 cm, a width of 30 cm and a height of 23 cm which result in an internal volume of roughly 27.9 liters. Polystyrene material and aluminum foil were used to cover the top of the bath to minimize cell temperature fluctuations to within a value less than 273.16 K between the top and the bottom temperature probes.

The liquid bath was designed to maintain an isothermal equilibrium cell environment devoid of any thermal gradients for the measurement of true VLE data. Pure ethanol was used as liquid bath and the working temperature ranged from 223 up to 263 K.

The following important characteristics were incorporated in the design of the apparatus through the liquid bath to ensure a stable and uniform temperature profile.

- Temperature control
- Liquid agitation
- A refrigeration unit

An immersion circulator (Grant optima GR150 supplied by Polychem Supplies) is a high performance programmable digital thermostat with a simple user interface. This was placed in the liquid bath and allowed fast set-up of multiple parameters through a powerful menu system. It provides control for temperature-controlled applications over the range of -50 to 50ºC. The temperature range depends firmly on the coolant fluid used. Pure methanol (99.9%) is recommended for cryogenic conditions. The unit includes a powerful heater for fast heat-up, and an integral pump for circulating temperature controlled fluid around external apparatus as well.

To make the liquid circulation in the bath efficient, another unit was used as an add-on to the immersion circulator: a pump circulator. The latter was supplied by Labfix. It is a type of pump used to circulate liquid, gases or slurries in a closed circuit. Circulator pumps as used in hydronic systems are usually electrically powered. When used in laboratories, they are often small and rated at a fraction of a horsepower.

For measurement below ambient temperatures, an immersion cooler supplied by Polyscience was placed into the bath. This later provides convenient cooling and reduces the need for dry ice or liquid nitrogen in Dewar flasks. A readout accuracy of ± 0.1˚C and set points ranging from 253.15 K made this unit more suitable for our operating conditions.

4.2 Temperature and pressure measurements

The most conveniently measured independent variables in the study of phase equilibrium in a fluid system are temperature and pressure. Being one of the great challenges encountered during HPVLE experimentation, special attention needs to be taken while measuring pressure and temperature for phases in equilibrium. Benedict [1977] and Nicholas and White [1982] have numerous reviews on this subject.

4.2.1 Temperature measurement

Many physical processes and properties are dependent on temperature and its measurement is crucial in industry and science in applications ranging from process control to the improvement of internal combustion.

Temperature is the most measured process variable in industrial automation.

In this work, we have opted for resistance thermometer detectors (RTDs) as our temperature measurement devices. RTDs are temperature sensors that exploit predictable change in electrical resistance of some materials with changing temperature. Resistance is measured by applying a constant current and measuring the voltage change across the resistor. By far the most common RTDs used in industry have a nominal resistance of 100 ohms at 0 °C, and are called Pt-100 sensors.

Because of its applicability across a wide temperature range (523.15 to 1123.15 K) and relatively uniform characteristics in that range, platinum is the most common material from which resistance thermometers are constructed.

Temperature measurement throughout the entire apparatus was carried out by the means of Pt-100Ω resistance thermometers that were supplied by WIKA. Its accuracy and class were 0.1 K and A respectively. For accurate and precise temperature measurement within the equilibrium cell, two Pt-100 sensors were inserted into wells drilled into the end plates of the equilibrium cell body: one at the top and the other at the bottom corresponding to the vapour and liquid phases respectively. Other Pt-100 sensors were also used to measure temperatures at different locations within the apparatus. The temperatures of the sampling lines, the pressure transducer line, the pressure transducer block, the body of the ROLSI sampler and the six-port GC valve heat block were measured. These temperatures were important in that they helped to avoid either the partial condensation of the vapour phase or the partial vaporization of the liquid phase during experimental runs as well as during the sampling sessions.

Intermittent calibration was undertaken for the two Pt-100 sensors used to measure the equilibrium cell temperature and resulted in an uncertainty of ± 0.09 K (refer to chapter five for the calibration procedure). Other Pt-100 sensors were not calibrated because their errors were not considered to have great significant influence on the results.

An Agilent 34970A data acquisition switch unit was connected online with a personal computer to perform temperature data acquisition.

Temperature control system

To accurately control process temperature throughout the entire experimental system, ACS-13A digital indicating controller devices supplied by Shinko were used. This type of controller accepts data from a temperature sensor such as a thermocouple or RTD as input. It compares the actual temperature to the desired control temperature, or set point, and provides output to a control element. This helps preventing any form of condensation or Vapourisation of samples travelling from the equilibrium cell to the GC via transfer lines. This could negatively affect the reliability of information from the phases being sampled. Several points such as the pressure transducer block, the pressure transducer line, sampling lines, the body of the ROLSI^{TM} sampler and the six-port valve were heated and their temperatures monitored. Variac transformers with ratings from 120 V to 600 VAC single and three phase and fractional to 700 Amps were used to assist the heating process. Heater cartridges were used to assist heating the pressure transducer block and the six-port GC valve block, Nichrome wires were used for the sampling lines.

4.2.2 Pressure measurement

The equilibrium cell pressure was measured with a P-10 pressure transducer (certified accurate to within 0.1%) supplied by WIKA. This type of pressure transducer provides the readings in gauge pressure (where the reference is atmospheric pressure). The P-10 pressure transmitter has a pressure range from 0 to 10 MPa.

During the pressure measurement process, the pressure acts directly on the membrane in the transducer, deforms it and changes the electrical resistance in the transmitter. The measuring principle of the transmitter is based upon the Wheatstone bridge set up [Hambley, 2005].

To determine any deviation and to correct for errors, the P-10 pressure transducer was periodically calibrated against a standard pressure transducer which resulted in an uncertainty of ± 0.0016 MPa (refer to chapter five for the calibration procedure).

The pressure transducer is highly sensitive to temperature and therefore, it was mounted in a block above the cell and connected to the cell by a short length of fine- bore (1/8") stainless steel tubing. The whole assembly was thermoregulated to avoid condensation and ensure the isothermal conditions.

4.3 Composition measurement

In any chemical or bioprocessing industry, the separation and/ or analysis of a product from a complex mixture is a necessary and important step in the production line. Today, there exists a wide variety of methods in which industries can accomplish these goals.

To analyze vapour and liquid phases during HPVLE experimentation, two methods are routinely used: chromatography, which is an external analysis, and, spectroscopy, an in situ analysis.

Chromatography is a very important analytical tool that relies on differences in partitioning behaviour between a flowing mobile phase and a stationary phase to separate the components in a mixture. There are several types of chromatography depending on the type of sample involved.

A gas chromatograph is a chemical analysis instrument for separating components based on their volatilities. The heart of the separation process is the column. The column is coated with a stationary phase which greatly influences the separation of the compounds. There are three types of columns: packed, capillary and new development columns.

Detectors are used in a gas chromatograph to monitor the outlet stream from the column. It registers and evaluates continuously the time and quantity of the components as they come out. There are two types of detectors; a thermal conductivity detector (TCD) and a flame ionization detector (FID). The principle of the TCD is based upon the measurement of thermal conductivity of the gas flowing around it whereas in the FID, the effluent from the column passes through a hydrogen-air flame which breaks down organic molecules and produces ions. Ions are then collected on a biased electrode and produce an electrical signal.

In this project, the analysis of phases in equilibrium was carried out using a Shimadzu model GC-17A chromatograph configured with both the flame ionization detector (FID) and the thermal conductivity detector (TCD) connected to a data acquisition system fitted with GC solution analysis software (version 2.30.00). Good separation of the components was achieved using a Poropak Q packed column.

Periodic GC calibrations were undertaken for all the components investigated in this project. The GC calibration procedures are outlined respectively in Chapter five and Appendix A.

4.4. Auxiliary equipment

To exclude undesirable compounds from the equilibrium cell, a degassing process was undertaken. This was accomplished by the use of a standard vacuum pump. The vacuum inlet pipe from the cell to the vacuum pump passed via an empty Erlenmeyer to prevent the passage of anything that could damage the pump. The degassing process also involved subjecting the associated filling lines to the cell at low pressure using a vacuum pump.

A compression device described by Mühlbauer [1990] was used for components that are subcritical at room temperature. Components exhibiting this property present difficulties while filling the equilibrium cell. The amount that can be added to the equilibrium cell is limited. The compression device was used to force subcritical components into the cell until the desired equilibrium cell pressure was obtained. The reader is referred to Chapter five for the experimental procedure regarding the compression device.

4.5. Data logging

A 34970A data acquisition switch unit supplied by Agilent Technologies was connected to a personal computer via an RS232 interface for displaying and recording temperature and pressure measurements.

The Agilent 34970A data acquisition unit is a numerical multi-meter with 6 ½ digits or 22-bit of resolution. It has a built-in signal conditioning which measures thermocouples, RTDs and thermistors, ac/dc volts and current, resistance, frequency and period. Scanning of up to 250 channels per second made this type of data acquisition unit ideal in terms of speed and accuracy.

Agilent BenchLink Data Logger 3 software supplied with the 34970A data acquisition provided a Microsoft Windows ® interface for test configuration and real time data display and analysis. Figures 4.5 and 4.6 clearly show the two interfaces.

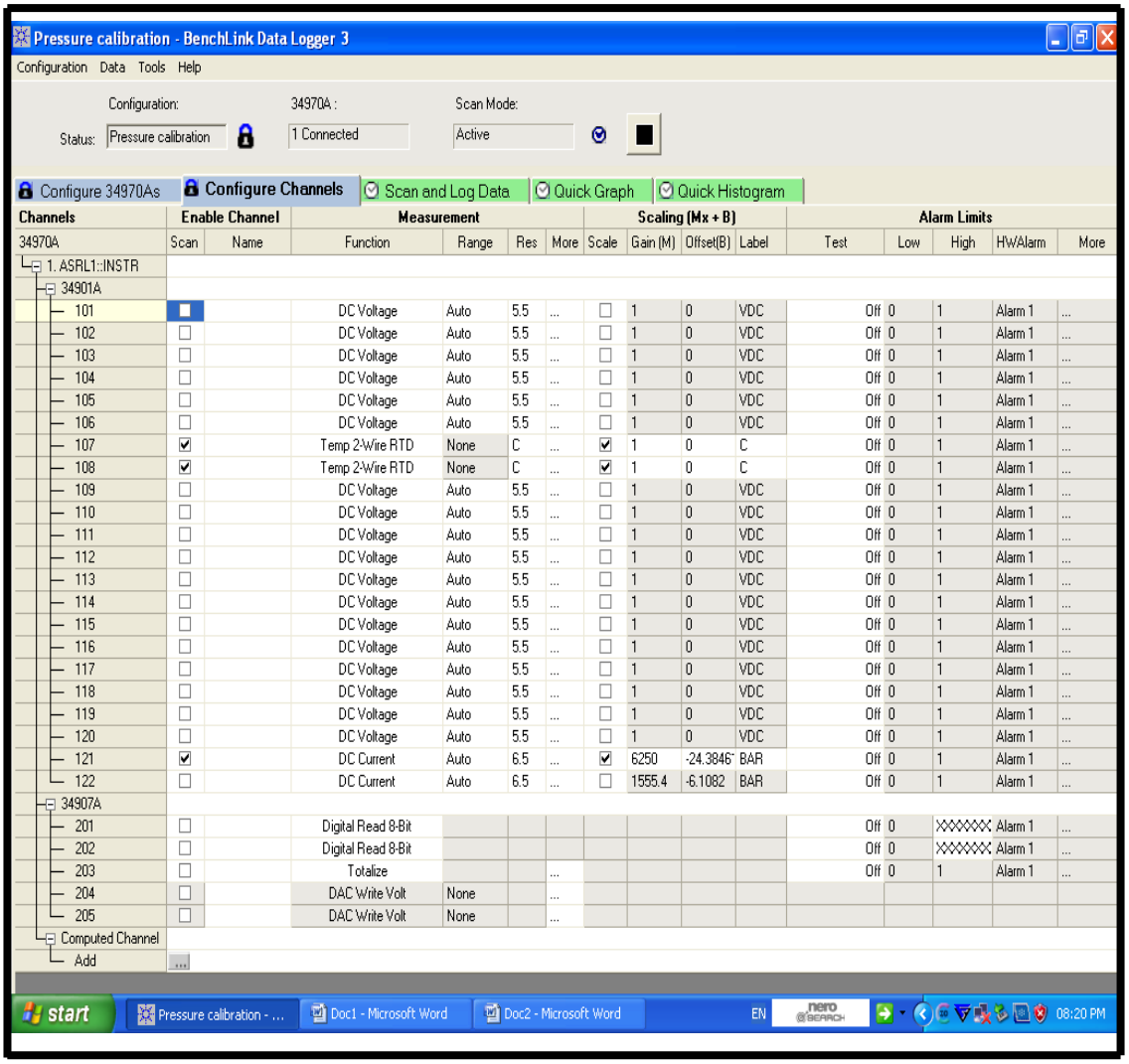

Figure 4.4: BenchLink Data Logger 3 test configuration interface

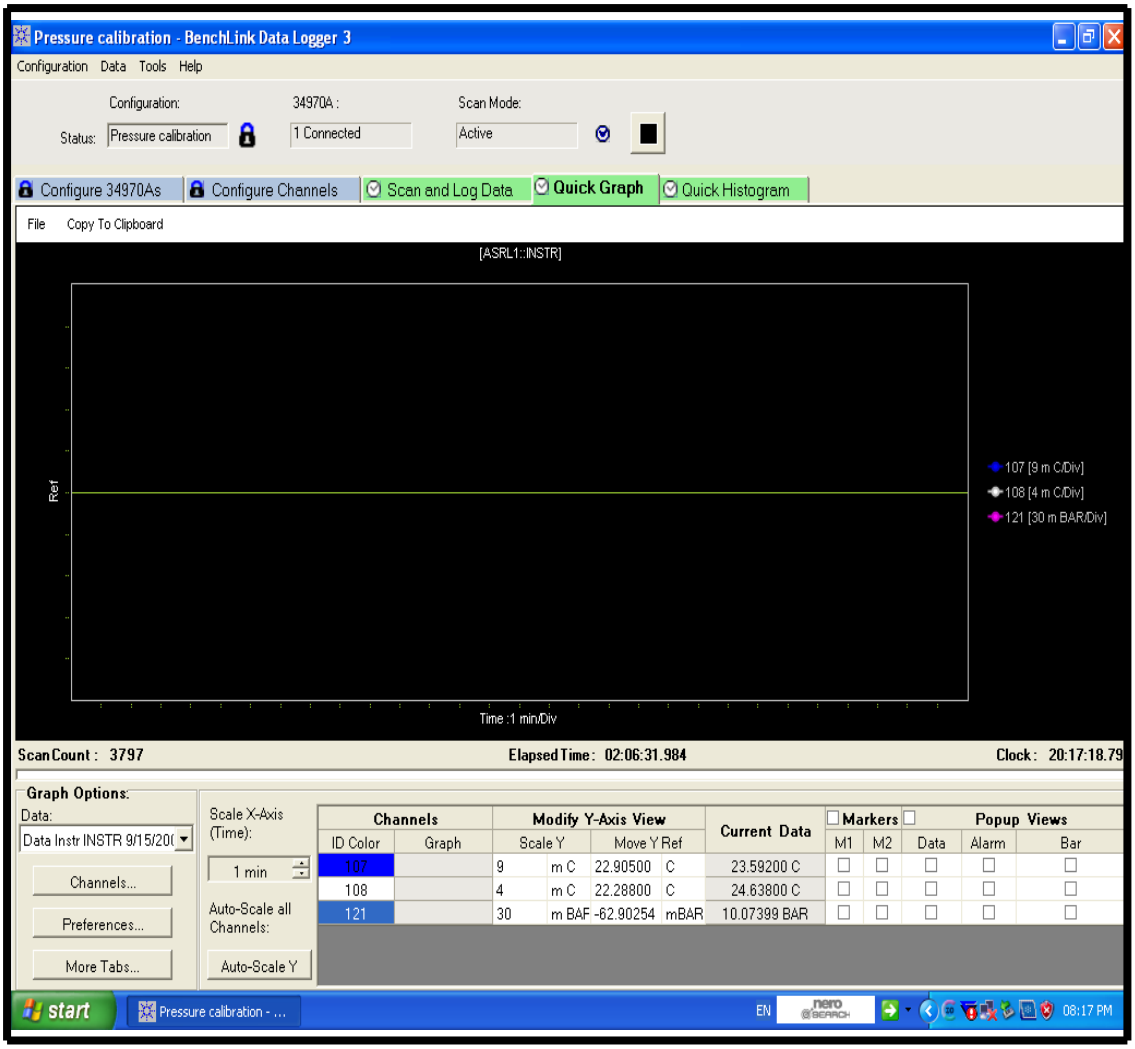

Figure 4.5: BenchLink Data Logger3 real time data display interface

During calibration procedures as well as experimental runs, Pt-100 sensors and pressure transducer used for the equilibrium cell temperature and pressure respectively were connected to different channels of a slot. The configuration chosen depended upon the characteristics of each device. Intensity and pressure range were considered for the pressure transducer while resistance and temperature range were considered for Pt-100 sensors.

4.6. Safety features

High pressure equipment is inherently dangerous and a lack of adequate knowledge of its design, construction and working procedure may result in disaster.

To maximize performance and ensure safety for both the experimenter and the equipment, Ramjugernath [2000] devoted an entire section to safety. The following is an important list of safety aspects that were considered during the design of the new HPVLE apparatus.

1. The design calculations of the entire apparatus were undertaken with a +100% over design safety factor.
2. Pressure relief valves were placed at different locations such as pressure transducer line and the sampling line to the gas chromatograph. These were set in accordance with the pressure range for the pressure measurement instrument. The pressure relief valve placed before the pressure transducer helped to prevent an over pressure that could damage it. Similarly, the pressure relief valve placed on the sampling line to the gas chromatograph helped regulating the sample pressure. Over pressure could damage the gas chromatograph.

3. A durable and transparent plastic sheet was placed on the liquid bath stand through which the experimenter could see the inside of the equilibrium cell. This protected the experimenter from a direct eye-contact with the viewing windows since over pressure could cause an explosion.

4. Aluminum foil was used to wrap all the heated elements throughout the entire apparatus. This firstly helped to contain the heat and ensure isothermal conditions and secondly it prevented the experimenter from burns.

5. An exhaust fan was placed on top of the experimental apparatus and was switched on at all time the experimental equipment was running. This assisted in removing any toxic substances that could have a negative effect on the laboratory environment. For the same purpose, all vent lines were connected to the fume cupboard.

CHAPTER

FIVE

EXPERIMENTAL PROCEDURE

Achieving accurate VLE data requires an understanding of some factors that contribute to the accuracy achieved during the experimental procedure. These factors consist of the preparation of the experimental apparatus and the starting procedure of an experimental run.

The guidelines and outline of factors named above which are also discussed below are derived from the one proposed by Coquelet [2003].

5.1. Preparation of the experimental apparatus

5.1.1. Equipment Calibration

This section focuses on the verification of the measuring instrument against an accurate standard one to determine any deviation and correction for errors. Measuring instruments for temperature, pressure and composition are taken into account.

5.1.1.1. Temperature and pressure sensor calibration

The only way to be confident in a temperature measuring instrument is to have it calibrated.

The two Pt-100 sensors allocated to the cell, at different levels, were initially calibrated against a calibrated standard 100Ω platinum resistance using a processor calibrator CPH6000 supplied by WIKA. The standard probe is certified accurate to within ± 0.03 K. The three sensors (two Pt-100s and the standard calibrated Pt-100) were placed close to one another and immersed in a liquid bath. Vigorous stirring of the liquid in the bath was essential to ensure uniform temperature during the calibration procedure. The calibration range of the two Pt-100s extended from 243.15 to 323.15 K.

Pressure and temperature data acquisition were performed via a personal computer connected online with an Agilent 34970A switch/unit.

To ascertain the accuracy and reproducibility of the results obtained, all measurements were repeated three to four times and only the results that correlated to within 0.1% were used to obtain an average temperature value.

Pressure measurement was carried out by means of a pressure transducer. Prior to being connected to the equilibrium cell; the transducer was calibrated against a CPT 6000 standard pressure transducer using a HD250 test pump supplied by WIKA. The standard transducer is certified accurate to within 0.025 %. Having the two pressure transmitters connected to the pump, the same pressure was applied to both sensors when the pump was in operation. The comparison between the two measured values helps one to verify the accuracy of the pressure transmitter under calibration. The pressure calibration range extended from 0.3 to 6.1 MPa. The reason for this range is that the HD250 test pump used during the pressure calibration process could only go up to 6.5 MPa and the range (0.3 to 6.1) MPa corresponds well to the pressure range foreseen for VLE data measurements in this project.

In order to ascertain the accuracy and reproducibility of the calibration of the pressure transmitter, the calibration procedure was repeated three to four times and only results that correlated to within 0.1% were considered to obtain the average pressure value.

The type of pressure transmitter used in this project gives the reading in gauge (where the atmospheric pressure is taken as reference). A digital barometer was used to measure the atmospheric pressure during the calibration procedure.

5.1.1.2. Gas Chromatograph detector calibration

In this study, the analysis of the equilibrium phase compositions was carried out using a Shimadzu gas chromatograph model GC-17A configured with both the flame ionization detector (FID) and the thermal conductivity detector (TCD). The GC was connected to a data acquisition system. The TCD was used as a detector and a Poropak Q was chosen as the analytical column.

The gas chromatograph detector was calibrated for different systems investigated prior to any analysis.

Various methods are available for calibration of the GC detector. However, only two methods are considered to achieve accurate results. The internal standardization method and direct injection method. The reader is referred to Tranchant [1969], Grab [1995] and Raal and Mühlbauer [1998] for additional details.

The direct injection method, which is slightly less accurate than the internal standardization method, was used in this study for several reasons. Firstly, the binary system under investigation consisted of components that were in their gaseous state at room temperature hence, standard solutions containing a mixture of both components could not be prepared.

Secondly, the equilibrium samples to be analyzed were supplied directly from the equilibrium cell via a ROLSI ™ sampler to the gas chromatograph, which in return precluded the addition of a standard of known quantity to the sample before analysis.

The main concern when using the direct injection method is the reliability of the method and repeatability of the injection of a known volume of each pure component into the GC. During this process, a plot of peak area versus number of moles is generated. This may be stated as:

$$A_i = C_i . n_i + D_i \tag{5.1}$$

Or

$$A_i = C_{1,i} . n_i^{\,2} + C_{2,i} . n_i + D_i \tag{5.2}$$

where the response factor C_i is the proportionality constant between the number of moles n_i passing the detector and the peak area A_i , D_i is a constant at the origin.

The constant at the origin D_i is not taken into account in the calculation of number of moles issued from the ROLSI ™ sampler. This is explained by the injection's default due to the construction of the syringe.

GC calibrations of the TCD for propane (R290), hexafluoroethane (R116), octafluoroethane (R218), ethane (R123) and hexafluoropropylene oxide (HFPO) were undertaken in this study. The GC operating conditions and column details are presented in Table 5.1 and Table 5.2, respectively. The results obtained are graphically presented in chapter six. The GC calibration procedure is extensively outlined in Appendix A.

Table 5-1: Operating conditions for the GC with the Poropak Q column

Operating conditions	**R116 + propane**	**R218 + ethane**	**HFPO + propane**
TCD detector temperature (◦C)	200	200	200
Injector temperature (◦C)	150	150	150
carrier gas pressure (kPa)	150	160	120
Column temperature	150	80	120
carrier gas flowrate (cc/min)	30	30	30

Table 5-2 Poropak Q column details

Column	Poropak Q
Supplier	LANGET
Material	SS
Column length (m)	3.0
OD (mm)	3.2
ID (mm)	2.0
Film thickness (μm)	165
Max. Temperature (◦C)	250

5.1.2 Purity of chemicals

All chemicals used in this study were found to be within the purity range needed and no further purification was undertaken.

Propane

A 45 kg bottle of instrument grade propane was supplied by Afrox with a certified purity of 99.5%. The bottle pressure was roughly 0.95 MPa. Impurities consisted mainly of propylene, isobutane, butane and methane at quantities less than 1 ppm.

Hexafluoroethane

Hexafluoroethane (R116) was purchased from Messer Grieshem with a certified purity of 99.99 % in a 12 kg cylinder. The bottle pressure was roughly 3.37 MPa. The major impurities indicated were methane, carbon dioxide, water and $N_2 + O_2$, all of which present at less than 1 ppm.

Octafluoropropane

High purity octafluoropropane was supplied by Air Products with a certified purity of 99.99 % in a 5 kg cylinder. The cylinder pressure was approximately 0.88 MPa. The major impurities consisted of organic impurities, moisture, carbon monoxide, carbon dioxide, nitrogen /oxygen, all of which were present at less than 10 ppm.

Ethane

Instrument grade ethane was purchased from Air Products South Africa (Pty) Ltd with a certified purity of 99 % in a 14.5 kg cylinder. The cylinder pressure was approximately

4.19 MPa. The major impurities indicated were: oxygen, water, propylene, isobutene and *n*-butane, all of which were present at less than 1 ppm.

Hexafluoropropylene oxide (HFPO)

A 12.5 kg bottle of hexafluoropropylene oxide was supplied by NECSA with a certified purity of 99.99 %. Further information such as impurities of the product was not supplied.

5.1.3 Preparation of the equilibrium cell

The reader is referred to Figure 5.1 (an illustration of the layout of the experimental apparatus). For clarification the following sections are relevant to the experimental measurement techniques. The most vital experimental variables for accurate and precise vapour-liquid equilibrium data measurement are the system equilibrium pressure and temperature as well as the composition. Along with the experimental variables, tests for leaks in the experimental apparatus are added.

Preparation of the entire experimental apparatus and particularly the equilibrium cell meant firstly detection of leaks. The equilibrium cell was pressurized and if any leak was found by a decrease in the pressure reading then a Snoop® leak detector was used on all fittings and seals to locate the leak.

The equilibrium cell and all the lines that convey samples to the gas chromatograph were pressurized with the aid of propane to a value approximately equal to the maximum operating pressure of the equipment and left over-night. The pressure reading was checked the next day for any decrease in pressure reading. The experimental apparatus was deemed ready for use only if the pressure drop due to a drop in temperature or a leak rate through fittings was within a specified tolerance.

To remove any trace impurities, sampling lines that conveyed samples to the gas chromatograph were heated to 423.15 K, a temperature of 100 K higher than the highest operating temperature (323.15 K). Once the desired temperature was reached, the transfer lines were flushed successively with the carrier gas. The GC traces of the sample were sufficient to confirm whether any impurities remained in the lines.

Before commencing with the measurements, all valves were closed and the GC valve turned to the flushing position. Valves V1, V3 and V6 were thereafter opened and the equilibrium cell was flushed several times with the heavier component of the system under investigation and vented via valve V9. This helped to remove any impurities that remained in the cell. Thereafter, with the aid of a mechanical jack, the cell was immersed in a temperature regulated

liquid bath filled with ultra pure ethanol/ glycol-ethylene solution or specified medium for isothermal measurement.

Similarly, the gas chromatograph (GC) was set to the required operating conditions for sample analysis. The entire apparatus comprising the equilibrium cell and its associated lines was thereafter evacuated to a relatively low pressure using a standard vacuum pump. Valves V1, V2, V3, V4 and V8 were then opened. This ensured the absence of impurities that could affect the results.

5.1.3.1 Start-up procedure

The general protocol of measurement of accurate isothermal binary vapour liquid equilibrium data can be summarized as follows. The equilibrium cell is initially loaded with the least volatile component (generally, this is the component with the lowest vapour pressure) from its cylinder. The desired bath temperature is set, stirrers switched on and adjusted to ensure vigorous stirring and one waits for equilibrium to be reached.

Thermal equilibrium is confirmed when the fluctuations in the measured temperature between the two probes (inserted at two different locations of the cell corresponding to the vapour and liquid phases) are less than 0.1 K within their temperature uncertainty. After recording the vapour pressure at the equilibrium temperature, the more volatile component is introduced stepwise, leading to successive equilibrium mixtures with overall increases in the content of the light component. After each introduction of the new light component, vigorous stirring is undertaken until an equilibrium state is attained. Mechanical equilibrium is assumed to be reached when there is no fluctuation in the measured pressure. This takes approximately 15 to 20 minutes for systems comprised of refrigerants.

At the equilibrium state, five to six samples of both phases (vapour and liquid) are withdrawn and sampled by means of the ROLSI ^{TM} sampler and analyzed by a gas chromatograph.

This experimental procedure was followed for the binary systems: Propane + hexafluoroethane, octafluoropropane + ethane and hexafluoropropylene oxide + propane.

5.1.3.1.1 Propane (1) + hexafluoroethane (2) binary system

Initially all valves were closed, except valves V1, V2, V3, V4 and V6. The equilibrium cell with its associated lines was evacuated to 0.05 MPa for at least half an hour and all valves were shut off afterwards. Valves V1, V3 and V6 were then opened and a rough volume of 5cm^3 of propane (the less volatile component) was loaded into the equilibrium cell from its cylinder. The system temperature was set on the immersion circulator temperature controller,

the chilling unit switched on and the liquid bath was allowed to cool. Meanwhile, the stirrer was switched on and valves V1, V2 and V9 were once again opened, so the cell contents could vent to the atmosphere. This helped the degassing process as well as in positioning the liquid-level within the equilibrium cell.

For the vapour pressure measurements of pure propane, the desired bath temperature was regulated in a stepwise manner. We waited for the equilibrium to be reached and recorded pressures at each temperature. Vapour pressure measurements for propane were recorded for temperatures ranging from 243.15 to 303.15 K.

After recording the vapour pressure for propane, the liquid bath was set to a selected temperature (263.15 K) for an isothermal run. Thereafter, hexafluoroethane (the more volatile component) was introduced stepwise, leading to successive equilibrium mixtures of increasing over all R116 content. After each addition of R116, equilibrium was assumed when the system pressure remained unchanged to within ± 1.0 kPa for at least ten minutes with vigorous stirring.

At each equilibrium condition, five to six samples of the vapour and liquid phase were withdrawn and sampled by means of the ROLSI^{TM} sampler and then analyzed using the gas chromatograph to check for reproducibility of the peak areas.

5.1.3.1.2 Octafluoropropane (1) + ethane (2) binary system

The general experimental protocol for vapour liquid equilibrium data consisting of a binary system as previously discussed was applied to this present system as well. Since the vapour pressure of ethane at room temperature is roughly 4.19 MPa, the amount of gas able to be added to the cell is limited. Thus, a compression device [Mühlbauer, 1990] is required for pressures higher than 4.19 MPa.

The compression device allowed the less volatile component (ethane) to be forced into the equilibrium cell until a desired higher pressure was observed. On the experimental apparatus, Valves V2, V3, V4 and V8 were initially left open for a period of half an hour and the compression device with its associated filling lines was evacuated to a relatively low pressure using a standard vacuum pump. This technique prevented impurities contaminating the lines. Valves V6, V3 and V4 were thereafter opened and ethane was loaded into the compression chamber for a period of approximately 10 minutes after which valves V6, V3 and V4 were closed. On the other side of the compression device, Valve V5 was opened and nitrogen was loaded into a compressed air chamber of the compression device at a relatively high pressure to displace the built-in piston. This allowed an increase in pressure of the contents in the

compression chamber. A pressure gauge was connected to the compression chamber for displaying pressure. For higher pressures, the compression chamber was heated proportionally using heater cartridges.

For the Octafluoropropane (1) + ethane (2) system, the experimental protocol was continued as follows. At room temperature, the equilibrium cell and its associated filling lines were firstly evacuated to 0.1 Pa and then filled with the Octafluoropropane (the less volatile component) in a procedure similar to that described for the propane/hexafluoroethane binary system. The venting of the equilibrium cell prevented the presence of anything other than residual air.

For the pure component vapour pressure measurements of octafluoropropane, the equilibrium cell was immersed in a temperature regulated liquid bath and selected temperatures ranging from 264.05 to 308.04 K were set. During this process, the total system pressure was recorded at each thermal equilibrium condition.

Thereafter, isothermal vapour liquid equilibrium measurements were undertaken at selected temperatures (264.05, 271.15, 278.15, 303.04 and 308.04 K). Ethane, the lighter component, was introduced to make up new mixture compositions for the new or preceding measurements. For pressures higher than 4.19 MPa, the compression device was used. At each addition of ethane, mechanical equilibrium was assumed when the total pressure system remained constant for a least period of ten minutes under efficient stirring.

At each equilibrium condition, the stirrer speed was reduced to half its original speed and thereafter, five to six samples of both the vapour and liquid phase were withdrawn using a pneumatic sampler and analyzed using a gas chromatograph.

5.1.3.1.3 HFPO (1) + propane (2) binary system

The experimental protocol followed was as in section 5.1.3.1.1 and 5.1.3.1.2.

The compression device was also used here for pressures higher than the vapour pressure for HFPO at room temperature.

Having measured the vapour pressure of HFPO within the temperature range of 253.30 and 302.84 K, the next step consisted of the VLE data measurement for the binary system. Propane (the heavier component) was loaded first and then HFPO (the more volatile component) was added stepwise, leading to successive equilibrium mixture of increasing over all HFPO content.

Isothermal vapour-liquid equilibrium data were measured for three isotherms, 283.05, 303.05 and 323.05 K and pressures ranging from 0.437 to 2.000 MPa.

5.2 Vapour and Liquid Sampling Procedure

At the equilibrium state, the stirrer speed was reduced to half its initial speed. This helped to prevent either vapour bubbles or liquid droplets being entrained in the ROLSI capillary while sampling one phase or the other.

In the meantime, the sampling lines or transfer lines were heated by means of Nichrome wire and maintained at a temperature not higher than 423.15 K. This was set to prevent condensation of samples that could occur while being processed to the GC. Variacs were utilized as power supply to the Nichrome winding. The 6-port GC valve was also heated and maintained at 443.15 K, a temperature of 20 K higher than the temperature of the sampling lines. The 6-port valve was housed in a block wherein heater cartridges were inserted to assist in the heating process. This also prevented condensation of samples.

The body of the ROLSI ^{TM} sampler incorporates heating systems which allowed the samples to heat up and be maintained a temperature of 403.15, less than the temperature of the sampling lines. This helped not only to prevent either condensation or vaporization of samples but also the instant vaporization of a liquid sample or the maintaining of a vapour sample removed at high temperature in a gaseous state.

Having followed different steps clearly presented above, one could turn the 6-port GC valve from the flushing to the sampling position, position the ROLSI ^{TM} capillary in the vapour phase part of the equilibrium cell and commence the sampling.

The samples were firstly withdrawn from the vapour phase and then the liquid phase using the ROLSI ^{TM} sampler and sent to the GC via the 6-port GC valve for composition analysis.

The ROLSI ^{TM} sampler was connected to an online set up which had two timing sets: the time between sample taking and the sample removal time. The first time was set to monitor the time between sample withdrawals and therefore to avoid having a stack of different sample area peaks on the GC. The second time was set in function of the sample size to be withdrawn from the equilibrium cell.

The ROLSI ^{TM} sampler capillary was flushed with the phase to be analyzed between successive samplings. At least five samples were withdrawn, to ensure repeatability of the samples.

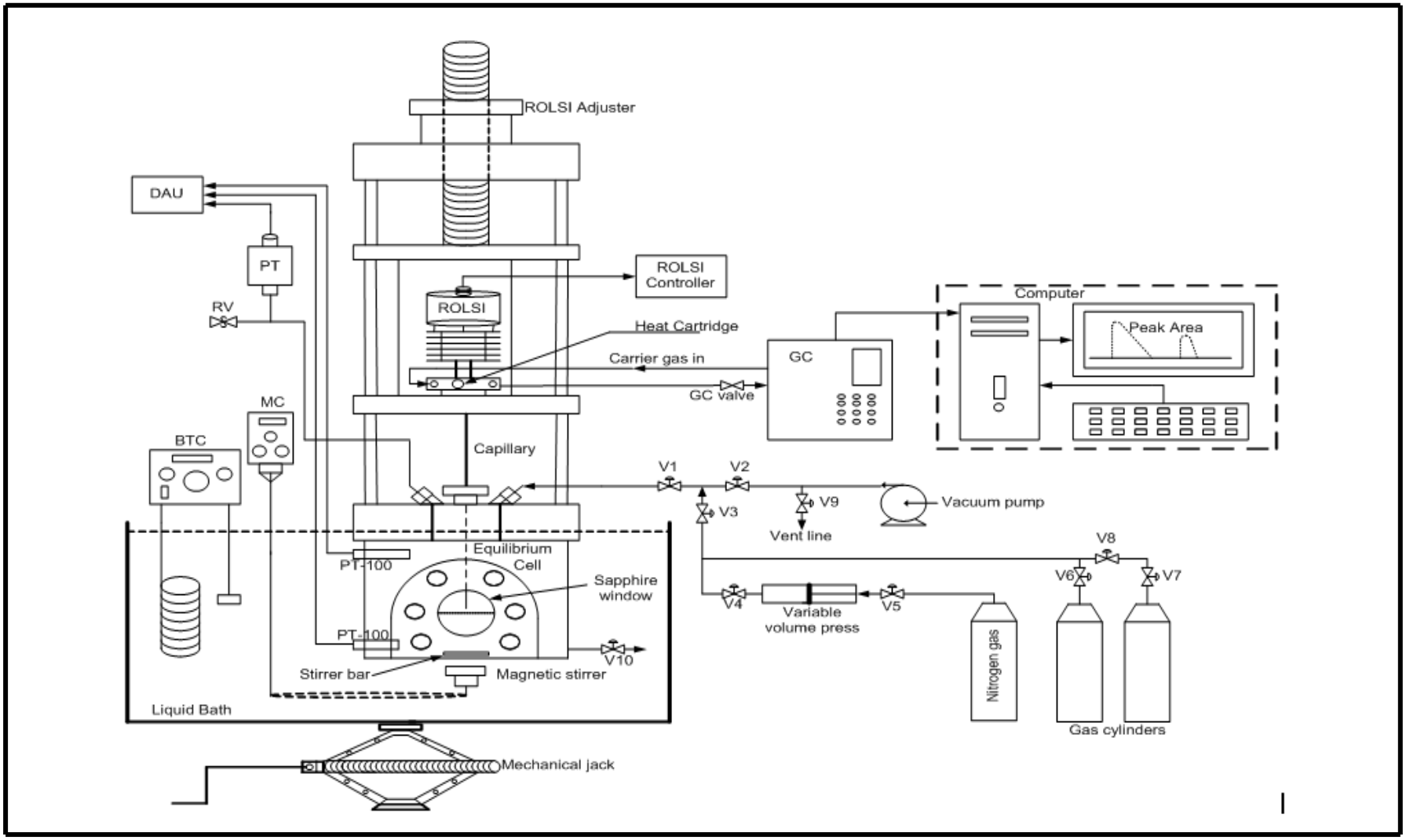

Figure 5.1: Layout of the experimental procedure for HPVLE data measurements

CHAPTER

SIX

RESULTS AND DISCUSSION

A new experimental apparatus was constructed and commissioned for accurate and precise HPVLE data measurement at temperatures ranging from low temperatures up to 373 K and absolute pressures from 0 to 10 MPa.

The belief that the HPVLE apparatus was well designed and constructed is justified when the experimenter is able to produce high quality data of satisfactory accuracy, comparable to those from reliable published sources.

Prior to any measurement, the temperature and pressure measurement devices were calibrated against standard devices. GC calibrations were also undertaken for components making up the binary systems under investigation.

The new HPVLE apparatus was tested by measuring vapour pressures of propane between 253.20 and 302.84 K. Further tests of the apparatus involved isothermal VLE data measurement for the binary system consisting of hexafluoroethane (R116) (1) + propane (2) at 263.15 K and pressures ranging from 0.328 up to 1.180 MPa. This system was chosen since it lies within range of the systems of interest for this project, namely binary systems containing fluorochemical components and hydrocarbons. Furthermore, Ramjugernath et al. [2009] successfully measured VLE data for this system at various temperatures using a similar apparatus.

Thereafter, new isothermal VLE data were measured for two binary systems:

- Octafluoropropane (1) + ethane (2) at five temperatures ranging from 264.05 to 308.04 K and pressures ranging from 0.298 up to 4.600 MPa.
- Propane (1) + hexafluoropropylene oxide (HFPO) (2) at 283.05, 303.05 and 323.05 K and pressures up to 2.000 MPa.

This chapter is devoted to the presentation of the results obtained for the equipment test, vapour pressures as well as VLE data. In addition VLE results for the new systems are included.

Modelling of the measured data was then performed and the results as well as a discussion of those results are presented. THERMOPACK in-house software developed by the TEP

laboratory of the ENSMP (Ecole National Superieur des Mines de Paris) was used to fit and correlate data.

6.1 Temperature and pressure calibration

6.1.1 Temperature calibration

The two Pt-100s used to measure the equilibrium cell temperature were calibrated following the procedure extensively outlined in section 5.5 of chapter five. The temperature range extended from 243.15 to 323.15 K.

A linear regression was performed to correct the temperatures measured by the two Pt-100 probes and the actual temperatures measured by the standard probe. The correlation is expressed in Equation (6-1) with parameters from Table 6.1. Figure 6.1 shows the uncertainties in the temperature measurement for both Pt-100s. The uncertainty in the temperature measurement is estimated to be within ± 0.09 K. The accuracy of the temperature calibration was difficult to control at low than at high temperatures. This explains the scattering of data points on Figure 6.1.

$$T_{Calculated}\left(^{\circ}C\right) = A * T_{read} + B \tag{6-1}$$

Table 6.1: Calibration curve parameters for the top and bottom Pt-100s

		Parameters	
Pt-100s	**Temperature (K)**	**A**	**B**
Top	243.15 to 323.15	0.9986	-0.5794
Bottom	243.15 to 323.15	0.9982	-0.7502

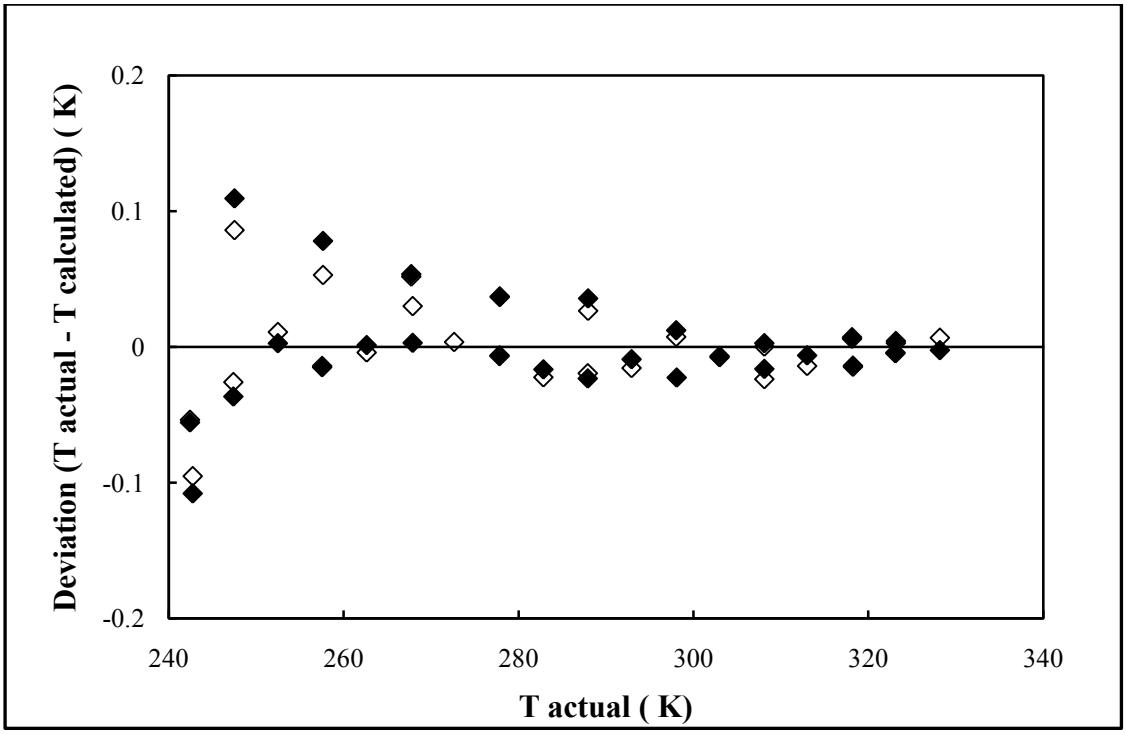

Figure 6.1: Deviation in the temperature measurement for the top (◊) and bottom (♦) Pt-100s

6.1.2 Pressure calibration

A calibration procedure was undertaken for the P-10 pressure transducer used for the equilibrium cell pressure measurement. The pressure calibration ranged from 0.3 to 6.1 MPa. A linear relation, as shown in equation (6-2) with parameters from Table 6.2, was performed to correlate the pressures measured by the P-10 transducer and the pressures measured by the standard pressure transducer.

The uncertainty in the pressure measurements is estimated to be within ± 0.0016 MPa for the full scale reading of the P-10 pressure transducer. Its graphical presentation is shown in Figure 6.2.

$$P_{calculated}(MPa) = A * P_{read} + B \tag{6-2}$$

Table 6.2: Calibration parameters for pressure transducer

		Parameters	
Pressure transducer	**Pressure range (MPa)**	**A**	**B**
P-10	0.3 to 6.1	1.0008	0.0648

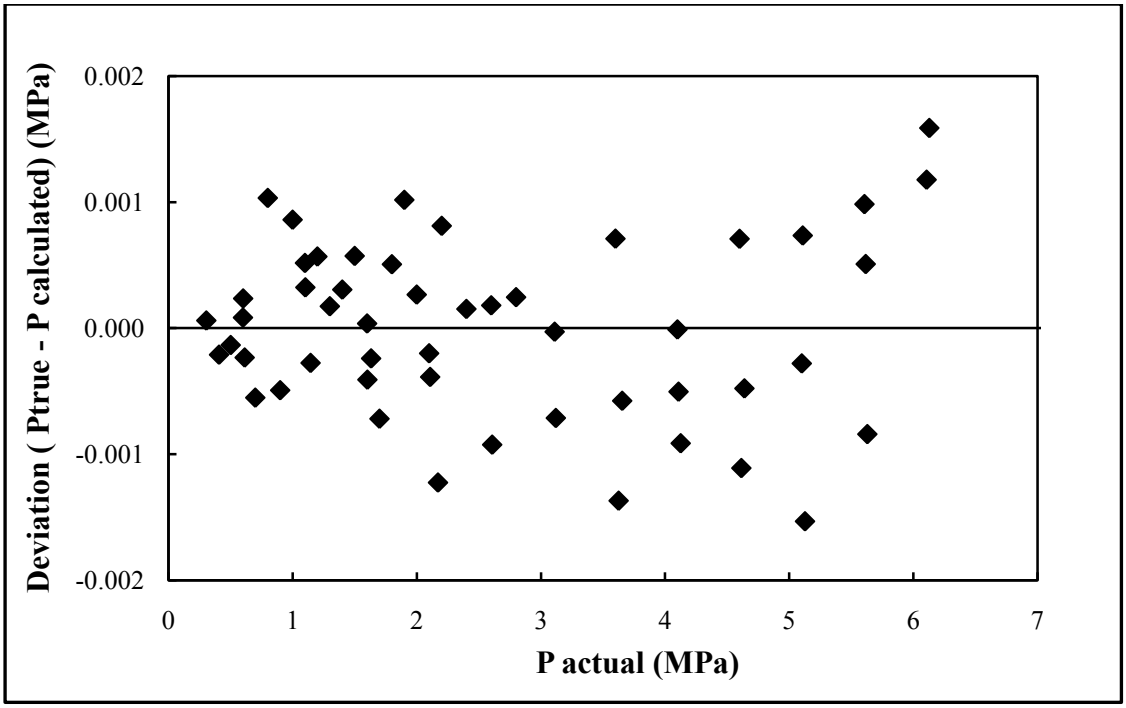

Figure 6.2: Deviation in the pressure measurement for the P-10 pressure transducer

6.2 Pure components vapour pressure measurement

The static method allows measurement of vapour pressures over a wide range of temperatures. The pure component vapour pressures for the investigated components namely propane, octafluoropropane, hexafluoropropylene oxide (HFPO) and ethane were measured at various temperatures. The measured data were fitted to the Peng-Robinson EoS incorporating the Mathias-Copeman alpha correlation in Tables 6.3, 6.5, 6.7 and 6.9. A discussion is presented as well.

Table 6.3: Experimental and correlated vapour pressure for propane

T / K	P exp (MPa)	ΔP (MPa)
253.30	0.239	-0.001
258.07	0.287	0.000
263.05	0.346	0.003
266.06	0.382	0.002
270.05	0.434	0.001
273.07	0.475	-0.001
277.96	0.550	-0.002
283.03	0.636	-0.002
287.95	0.729	-0.002
292.90	0.833	0.001
293.04	0.832	-0.003
297.86	0.946	0.003
302.84	1.069	0.004

Table 6.4: Mathias-Copeman coefficients for propane adjusted on the measured pure component vapour pressure

Coefficients	Propane
C_1	0.795
C_2	-3.106
C_3	11.944

Table 6.5: Experimental and correlated vapour pressure for octafluoropropane

T / K	Pexp (MPa)	Δ P (MPa)
253.30	0.194	0.000
258.11	0.238	0.002
263.23	0.287	-0.001
264.05	0.297	-0.001
268.17	0.343	-0.001
271.05	0.383	0.001
278.15	0.483	0.002
282.74	0.553	-0.002
292.81	0.743	-0.001
308.04	1.124	0.005
312.78	1.256	-0.001
322.96	1.604	-0.005

Table 6.6: Mathias-Copeman coefficients for octafluoropropane adjusted on the measured pure component vapour pressure

Coefficients	Octafluoropropane
C_1	1.026
C_2	-3.098
C_3	14.725

Table 6.7: Experimental and correlated vapour pressure for HFPO

T (K)	Pexp (MPa)	ΔP (MPa)
283.03	0.432	-0.003
283.01	0.437	0.003
293.04	0.590	-0.001
303.01	0.787	0.001
313.10	1.030	0.001
323.07	1.324	-0.002

Table 6.8: Mathias-Copeman coefficients for HFPO adjusted on the measured pure component vapour pressure

Coefficients	HFPO
C_1	1.235
C_2	-4.860
C_3	18.702

Table 6.9: Experimental and correlated vapour pressure for ethane

T/K	Pexp (MPa)	ΔP (MPa)
263.96	1.891	0.001
270.96	2.254	-0.003
277.92	2.665	0.000
283.02	3.000	0.004
292.89	3.731	0.003
302.86	4.606	-0.018

Table 6.10: Mathias-Copeman coefficients for ethane adjusted on the measured pure component vapour pressure

Coefficients	Ethane
C_1	0.638
C_2	-3.609
C_3	26.880

The experimental pure component vapour pressure data for propane, octafluoropropane, HFPO and ethane were fitted to the Peng-Robinson EoS incorporating the Mathias-Copeman alpha function. The ΔP values in Tables 6.3, 6.5, 6.7 and 6.9 indicate a good fit of the experimental data by the model. The Mathias-Copeman coefficients (C_1, C_2, C_3) for propane, octafluoropropane, HFPO and ethane presented respectively in Tables 6.4, 6.6, 6.8 and 6.10 were all adjusted on the experimental data.

6.3 Binary vapour-liquid equilibrium data

Isothermal vapour liquid equilibrium measurements were undertaken for the binary systems comprising of: R116 (1) + propane (2), ethane (1) + octafluoropropane (2) and HFPO (1) + propane (2).

The experimental VLE data were modelled using the THERMOPAK software. The data were modelled via the direct method using the Peng-Robinson EoS with the Mathias- Copeman alpha correlation and the Wong-Sandler mixing rule incorporating the NRTL activity coefficient model. This combination has proven to be successful and widely used in the regression for systems involving fluorochemical as well as hydrocarbon components. [Ramjugernath et al., 2009], [Madani et al., 2008], [Coquelet et al., 2009] and [Theveneau et al., 2006] have used and reported this combination in their work.

In fact, the NRTL activity coefficient model contains three adjustable parameters, α_{ji}, τ_{ji} and τ_{ij}. For binary systems comprising of fluorochemical and hydrocarbon components, it is recommended to set the non randomness parameter α_{ji} equal to 0.3. The Wong-Sandler mixing rule uses an additional interaction binary parameter, *kij*. The parameters τ_{ji}, τ_{ij} and *kij* were adjusted directly onto the experimental VLE data through a modified simplex algorithm using the flash calculation objective function, which is defined as follows.

$$F = \frac{100}{N}\left[\sum_{1}^{N}\left(\frac{x_{\exp} - x_{cal}}{x_{\exp}}\right)^2 + \sum_{1}^{N}\left(\frac{y_{\exp} - y_{cal}}{y_{\exp}}\right)^2\right] \qquad (6\text{-}3)$$

where N is the number of data points; x_{exp} and x_{cal} are the experimental and calculated liquid mole fractions and y_{exp} and y_{cal}, the experimental and calculated vapour mole fractions, respectively.

The uncertainties in the measurement of mole fractions were also investigated and are defined by:

$$\frac{\Delta z_1}{z_1} = (1 - z_1)\sum \frac{\Delta n_i}{n_i} \tag{6-4}$$

Where $\frac{\Delta z_1}{z_1}$ is the uncertainty in the measurement for mole fractions, with $z_1 = x_1$ or y_1; $\frac{\Delta n_i}{n_i}$ is the uncertainty in the determination of mole fraction for components i.

The uncertainty in the measurement regarding relative volatility is defined by:

$$\frac{\Delta \alpha_{12}}{\alpha_{12}} = 2\sum \frac{\Delta n_i}{n_i} \tag{6-5}$$

where $\frac{\Delta \alpha_{12}}{\alpha_{12}}$ is the uncertainty in the measurement regarding the relative volatility. The rest is defined as in equation (6-4).

Deviations from experimental and calculated liquid and vapour mole fractions were determined from AAD and BIASU calculations:

$$AAD(\%) = (100/N)\sum \left| (U_{cal} - U_{\exp})/U_{\exp} \right| \tag{6-6}$$

$$BIASU(\%) = (100/N)\sum \left((U_{\exp} - U_{cal})/U_{\exp} \right). \tag{6-7}$$

Where N is the number of data points and $U = x_1$ *or* y_1.

6.3.1 R116 (1) + propane (2) binary system

Isothermal VLE data measurements were undertaken for the binary system consisting of R116 (1) + propane (2) at 263.15 K and pressures ranging from 0.328 to 1.180 MPa. The measured data were compared with those reported by Ramjugernath et al. [2009]. This system was chosen since its investigation is part of the ongoing investigation of thermophysical properties of fluorochemical systems, which is related to the second objective of this project.

The gas chromatograph calibration plots for pure R116 and propane are presented in Figures 6.3 and 6.5. Their relative differences in the number of moles are presented in Figures 6.4 and 6.6. The isothermal VLE data measured are presented in Table 6.11 and graphically compared with the modelled data in Figure 6.7. Furthermore a plot of relative volatility versus the liquid molar fraction x_1 for both the experimental and the modelled data is shown in figure 6.8.

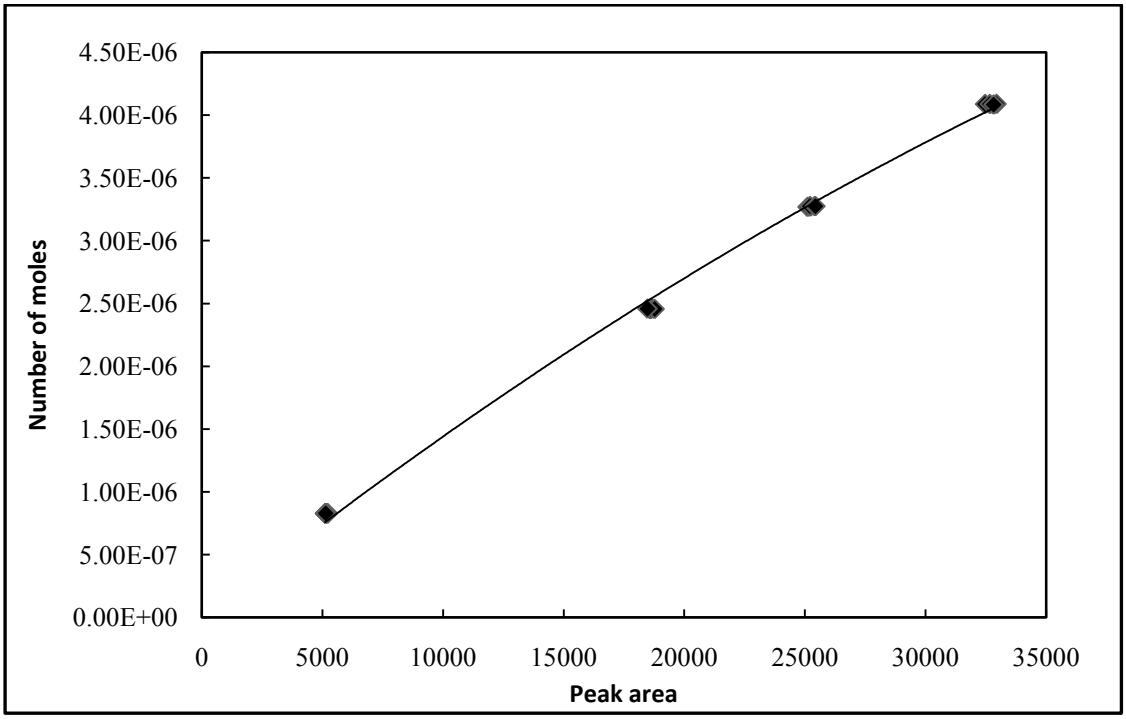

Figure 6.3: GC calibration plot for pure R116

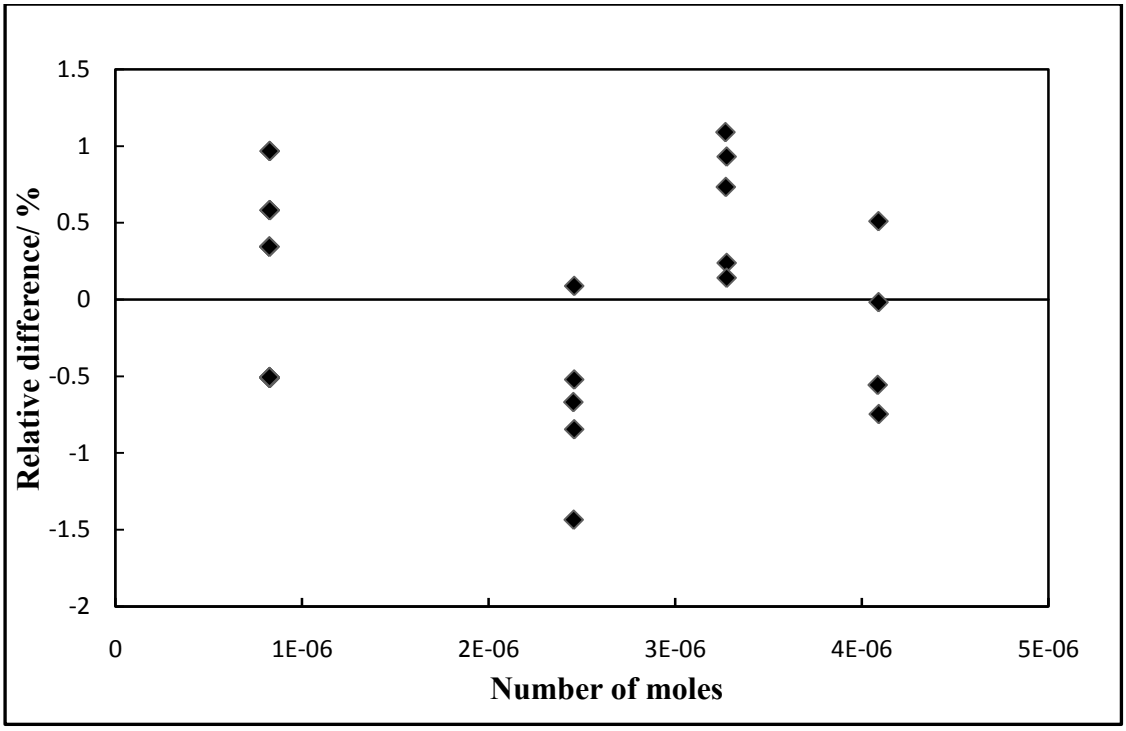

Figure 6.4: Relative difference for R116 on the number of moles

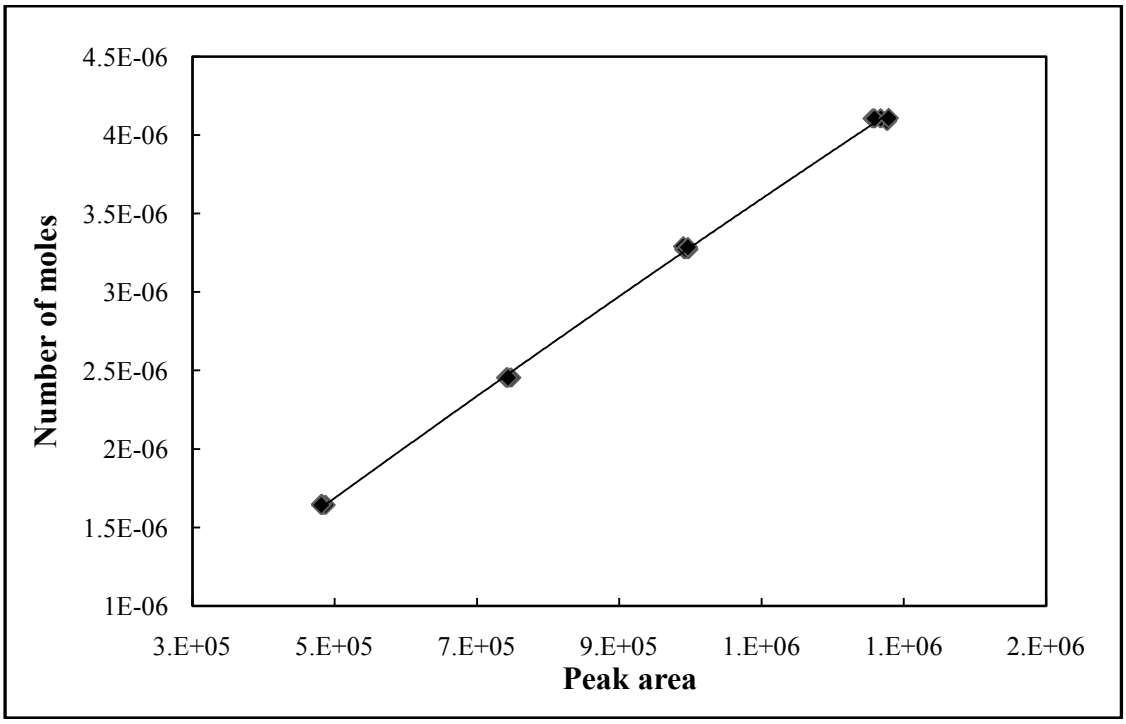

Figure 6.5: GC calibration plot for pure propane

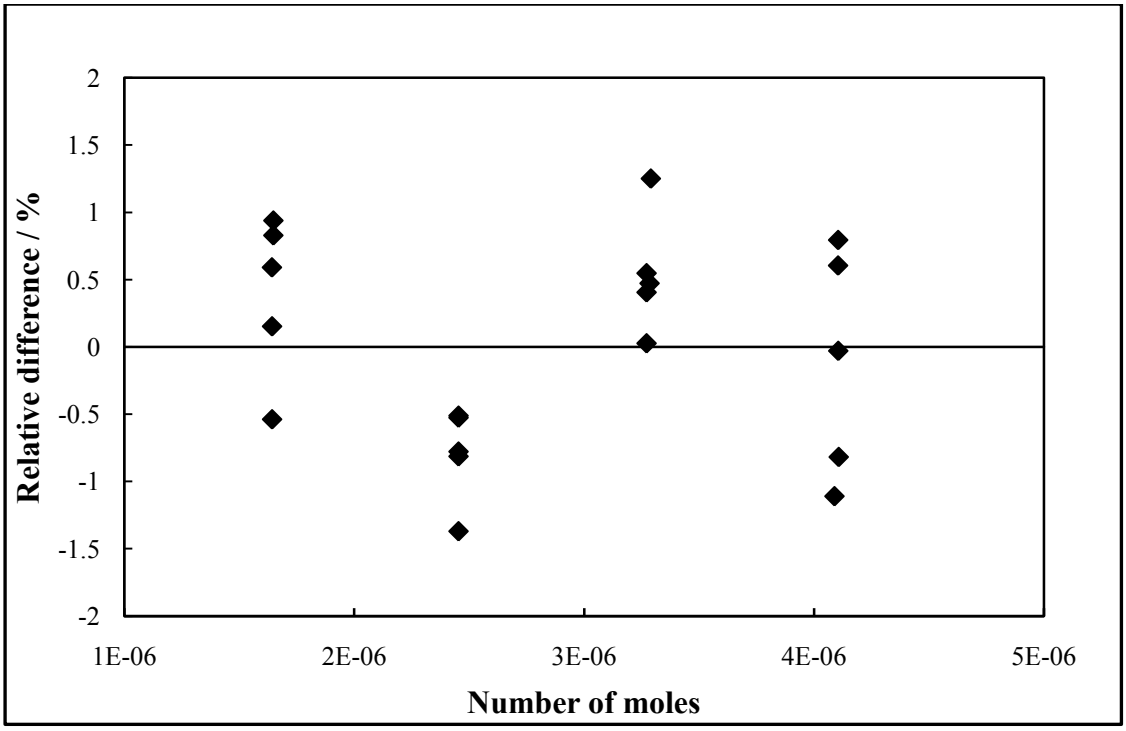

Figure 6.6: Relative difference for propane on the number of moles

The maximum uncertainty in the determination of the mole fraction is estimated to be within ± 2.5% for both pure propane and pure R116.

Table 6.11: P-x-y VLE data for the R116 (1) + propane (2) at 263.15 K

P (MPa)	x_1	y_1
0.328	0.000	0.000
0.477	0.023	0.267
0.653	0.060	0.450
0.860	0.131	0.575
1.044	0.271	0.659
1.180	0.435	0.718

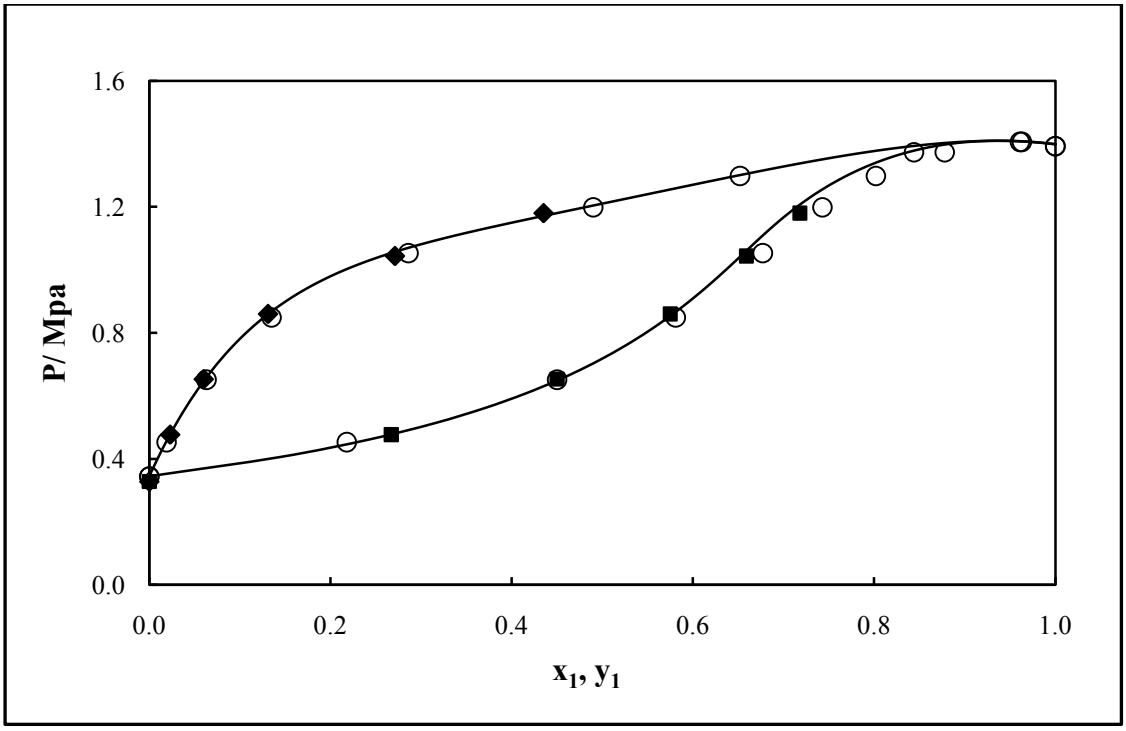

Figure 6.7: Plot of the P-x-y data for the system R116 (1) + propane (2) at 263.15 K. experimental data (♦), PRMCWS + NRTL model (—), [Ramjugernath et al., 2000] (○).

Table 6.12: Regressed Model parameters with the (PRMCWS+NRTL) model for the R116 (1) + propane (2) system at 263.15 K

Parameters	Model parameters
τ_{12} (J * mol^{-1})	3890
τ_{21} (J * mol^{-1})	3540
k_{12}	-0.02

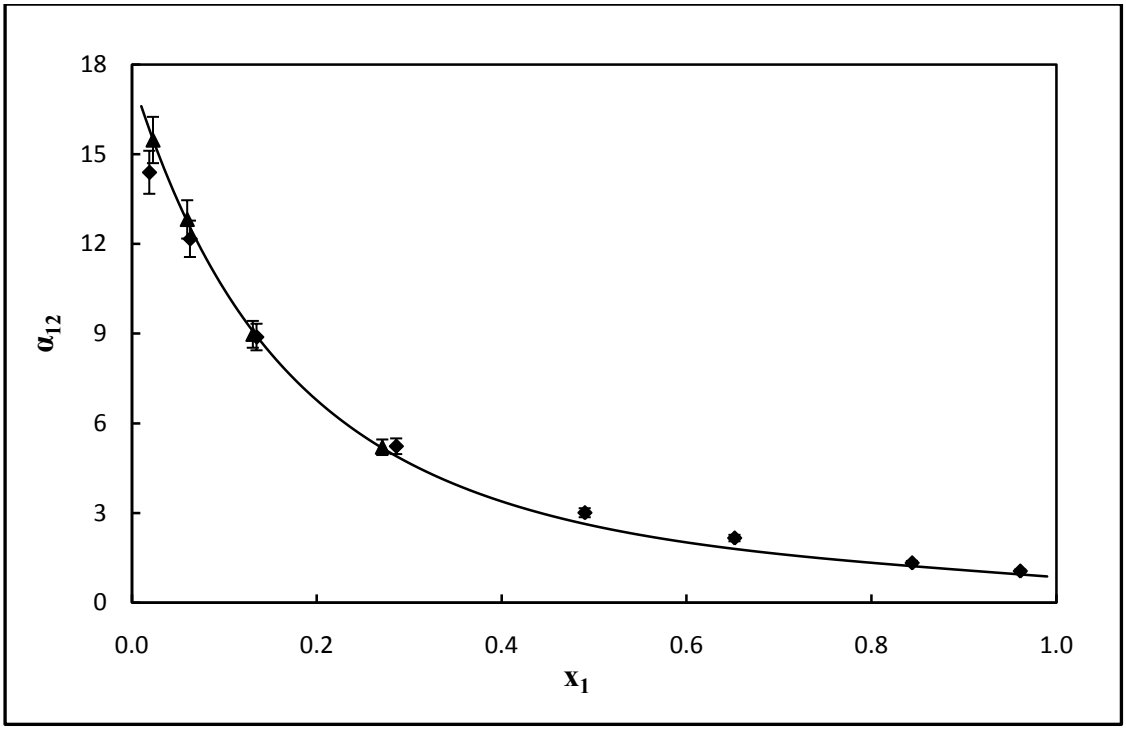

Figure 6.8: Plot of the relative volatility versus the liquid molar fraction for the system R116 (1) + propane (2) at 263.15 K. [Ramjugernath et al., 2000] data (♦) and experimental data (▲). Error bars are shown at 5 %.

The measured data were correlated with the Peng-Robinson EoS using the Mathias-Copeman alpha function and the Wong Sandler mixing rules involving the NRTL model. The adjusted parameters are listed in Table 6.12. The measured data are in a very good agreement with the data given in literature, as shown in Figure 6.7.

This system also helped to ascertain that the thermodynamic models used gives a best fit of the experimental VLE data.

A further comparison was also undertaken utilizing the relative volatility versus the liquid molar fraction for both the measured data and that of Ramjugernath et al. [2000] data. Having the error bars set at 5%, the measured data show once again a good coherence with the data measured by Ramjugernath et al. [2000], except at low concentrations where a disparity is noticed. This is clearly shown in Figure 6.8.

The results obtained confirm that the new apparatus is deemed to generate accurate HPVLE data measurements.

6.3.2 Octafluoropropane (1) + ethane (2) binary system

The binary system consisting of octafluoropropane (1) + ethane (2) was investigated. Its VLE data was measured at 264.05, 271.05, 278.05, 303.04 and 308.04 K and pressures ranging from 0.298 to 4.600 MPa. The critical properties of octafluoropropane and ethane are presented in Appendix B.

The gas chromatograph calibration plots for pure ethane and pure octafluoropropane are presented in Figures 6.9 and 6.11. Their relative differences on the number of moles are presented in Figures 6.10 and 6.12. The VLE data measured are presented and graphically compared with the model in Table 6.13 and Figure 6.12 respectively. The relative volatility versus the liquid molar fraction x_1 for both the measured and the modelled data are graphically compared in Figure 6.14.

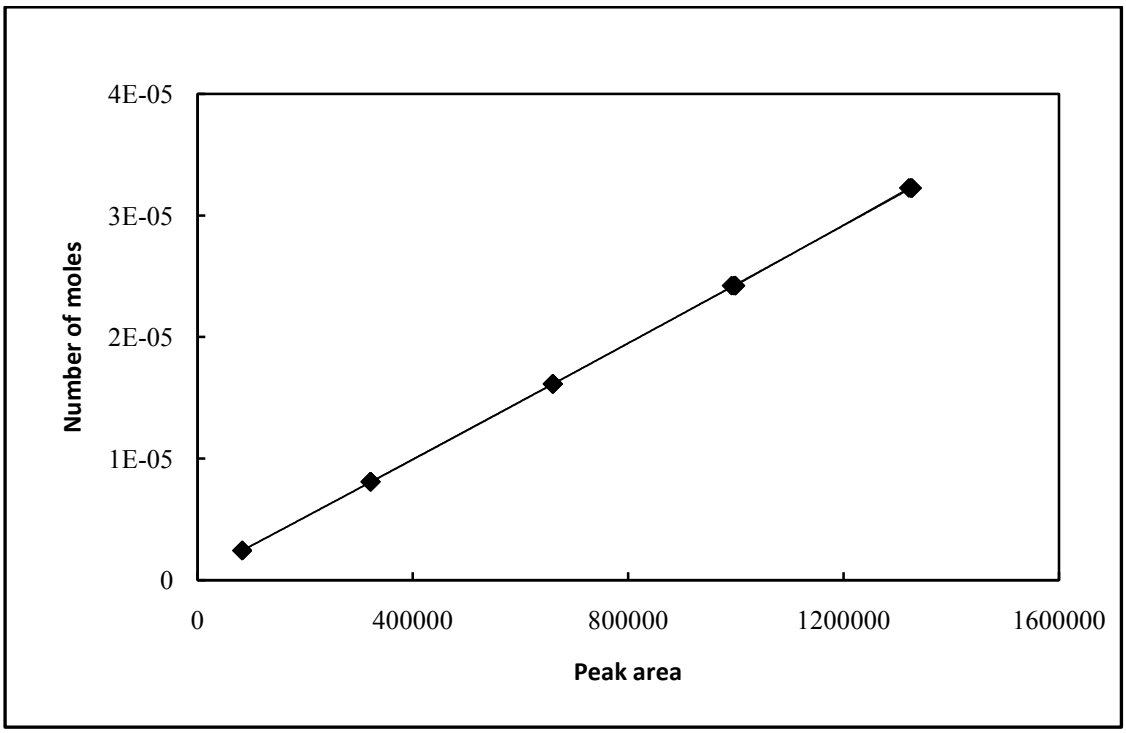

Figure 6.9: GC calibration plot for pure ethane

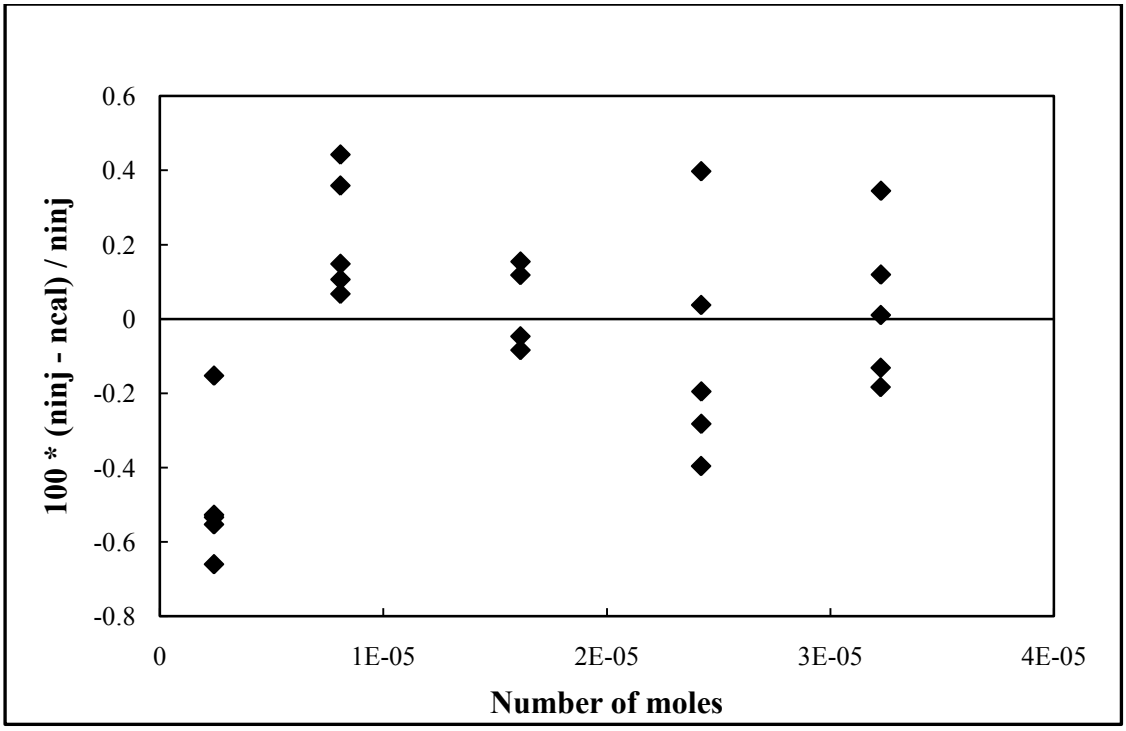

Figure 6.10: Relative difference for ethane on the number of moles

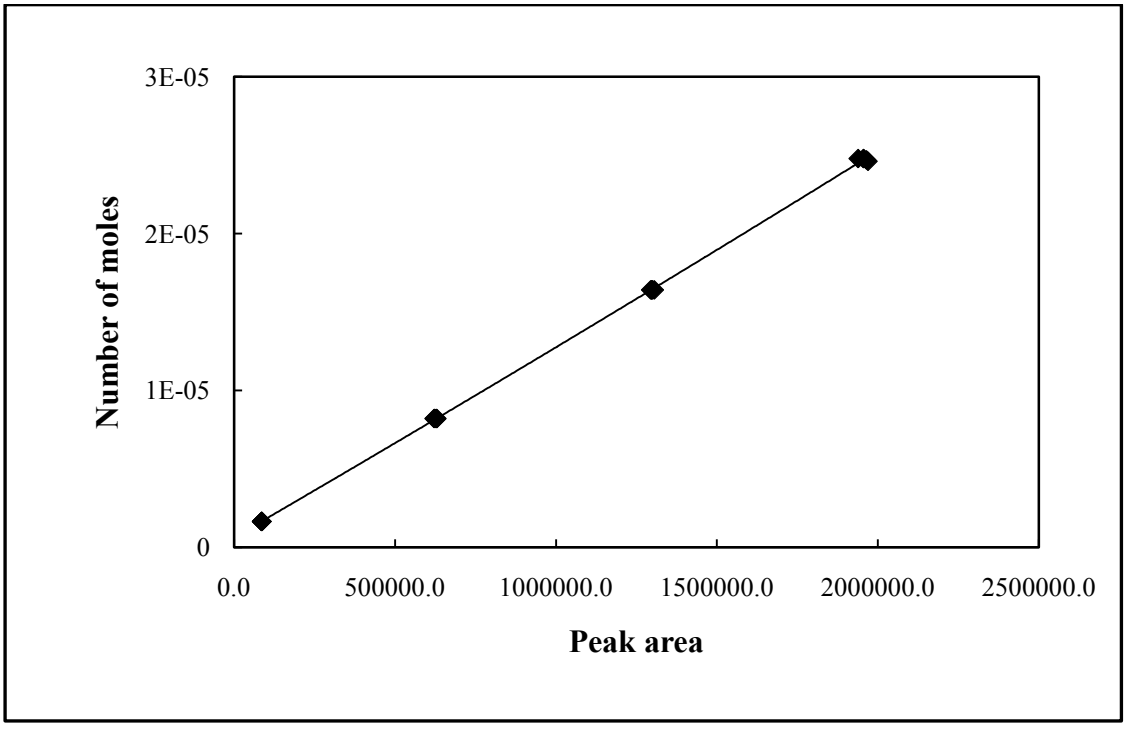

Figure 6.11: GC calibration plot for pure octafluoropropane

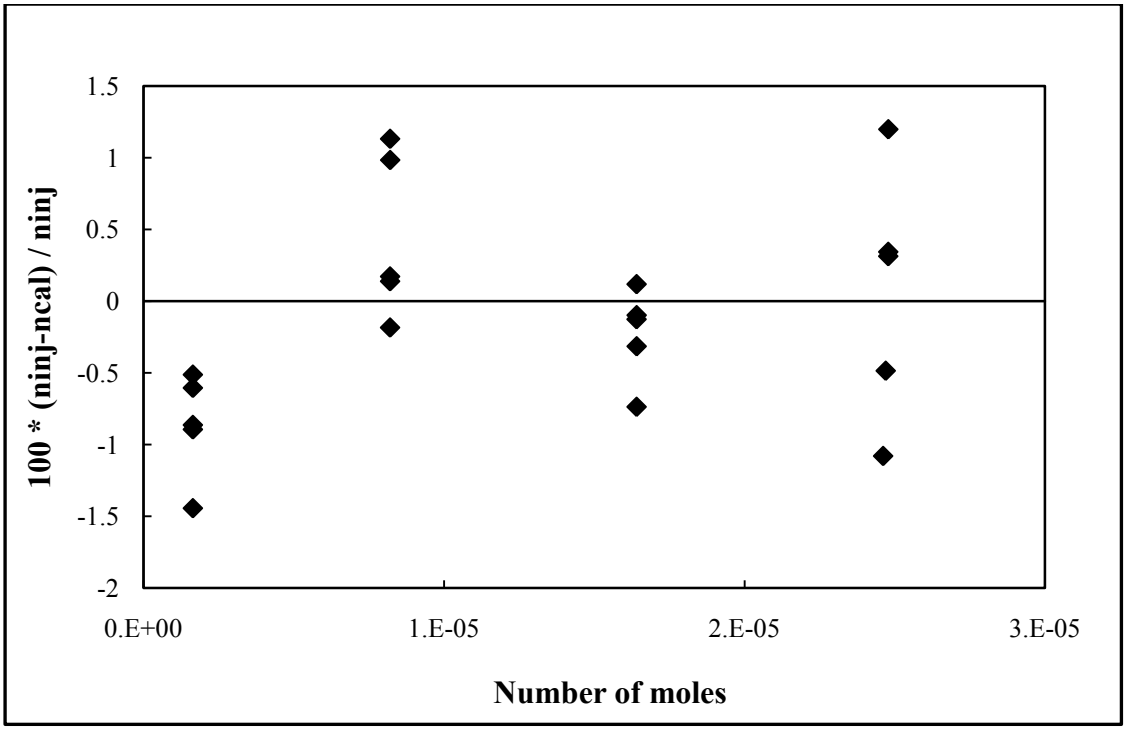

Figure 6.12: Relative difference for octafluoropropane on the number of moles

The maximum uncertainty in the determination of mole fractions is estimated to be within ± 2.1 % for both pure ethane and pure octafluoropropane.

Table 6.13: P-x-y data for the octafluoropropane (1) + ethane (2) system

Pressure (MPa)	x_1	y_1	Pressure (MPa)	x_1	y_1
	T = 264.05 K			**T = 271.05 K**	
0.298	0.000	0.000	0.383	0.000	0.000
0.473	0.064	0.386	0.569	0.069	0.350
0.713	0.158	0.599	0.791	0.141	0.537
0.938	0.251	0.722	1.069	0.246	0.662
1.117	0.357	0.776	1.256	0.331	0.720
1.266	0.445	0.815	1.461	0.437	0.770
1.402	0.542	0.843	1.693	0.569	0.824
1.550	0.661	0.873	2.112	0.866	0.929
1.693	0.781	0.901	2.275	1.000	1.000
1.862	1.000	1.000			
	T = 278.05 K			**T = 303.04 K**	
0.483	0.000	0.000	0.995	0.000	0.000
0.772	0.086	0.389	1.656	0.144	0.369
0.930	0.138	0.499	1.981	0.222	0.495
1.231	0.238	0.623	2.255	0.291	0.557
1.451	0.319	0.689	2.556	0.373	0.616
1.675	0.418	0.738	2.973	0.486	0.677
1.865	0.519	0.784	3.295	0.580	0.721
2.068	0.622	0.825	3.690	0.688	0.771
2.331	0.766	0.878	4.149	0.838	0.842
2.498	0.867	0.922	4.334	0.878	0.884
2.700	1.000	1.000	4.467	0.920	0.924
			4.600	1.000	1.000
	T = 308.04 K				
1.124	0.000	0.000			
1.534	0.081	0.233			
1.859	0.153	0.357			
2.221	0.236	0.459			
2.630	0.332	0.551			
3.029	0.432	0.620			
3.416	0.526	0.664			
3.685	0.601	0.695			

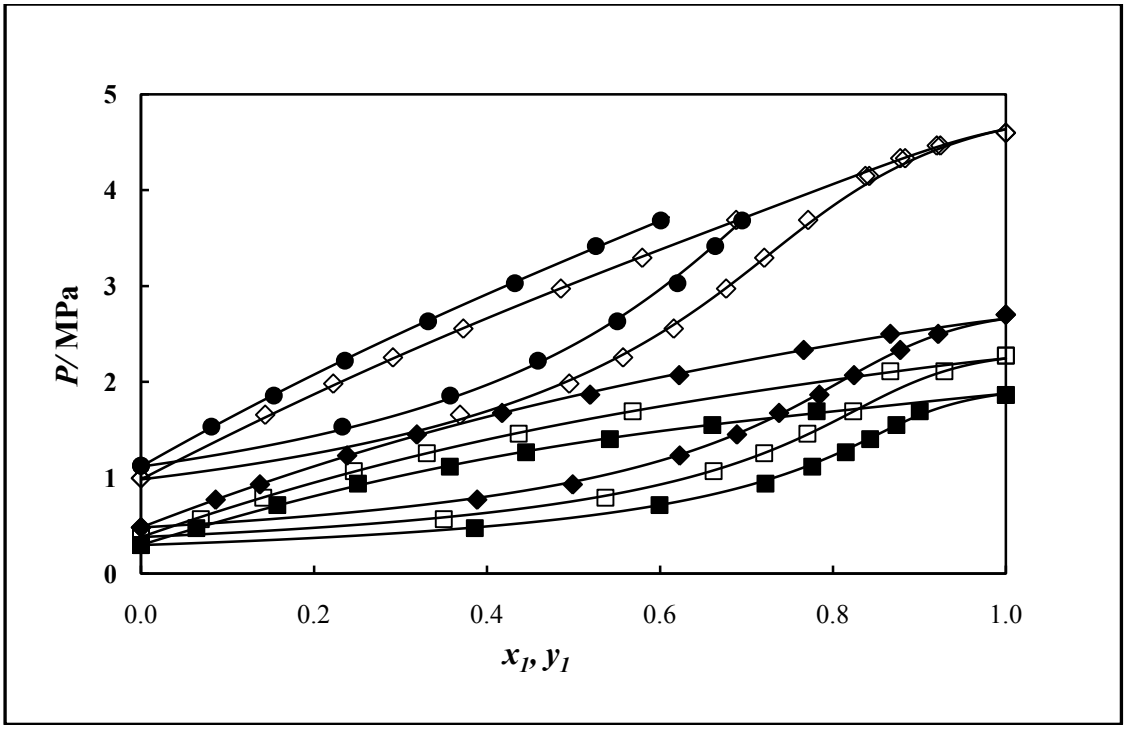

Figure 6.13: Plot of the P-x-y data for the octafluoropropane (1) + ethane (2) system; ◊, 264.05 K; ■, 271.05 K; ♦, 278.05 K; □, 303.04 K; ●, 308.04 K; —, PRMCWS+NRTL model

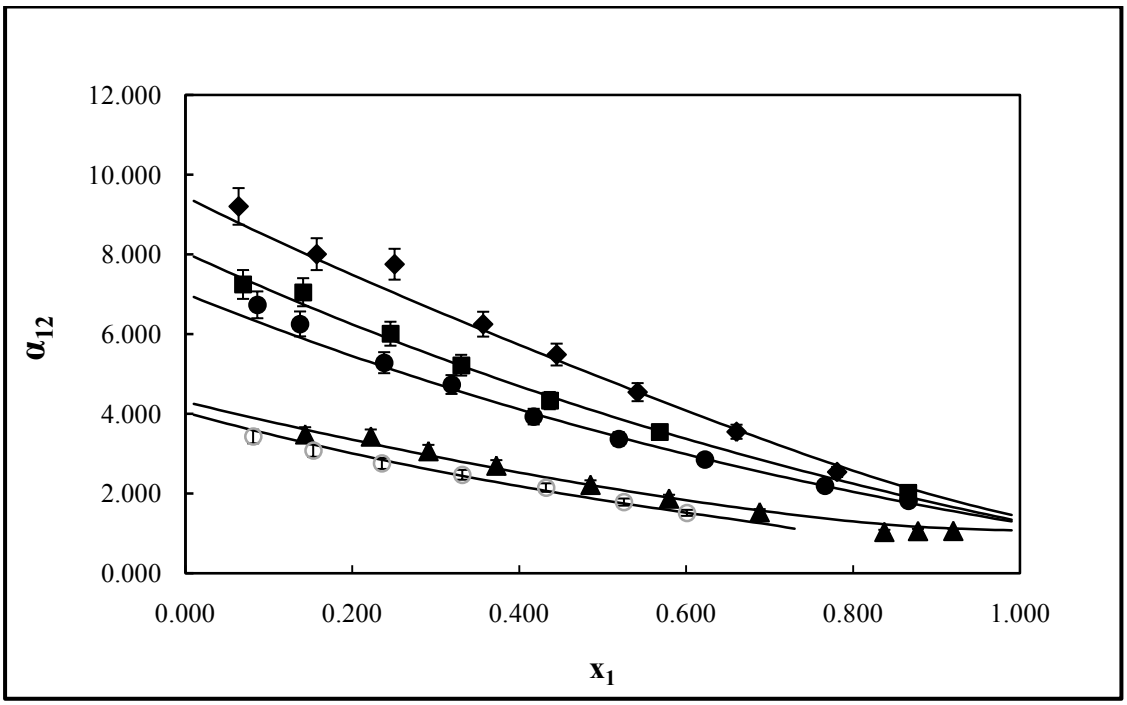

Figure 6.14: Plot of the relative volatility versus x_1 for the octafluoropropane (1) + ethane (2) system; ♦, 264.05 K; ■, 271.05 K; ●, 278.05 K; ▲, 303.04 K; ○, 308.04 K and —, modelled data. Error bars are shown at 4.5 %.

Taking into account the relative deviations in the number of moles due to calibrations, the measured data are presented with a resulting uncertainty of less than 2% for both the vapour and the liquid mole fraction.

The isotherms measured near the critical region of ethane exhibited a different behaviour from the others. The VLE data at 303.04 K, a temperature close to the critical temperature of ethane (305.32 K), revealed very close compositions of the vapour and liquid phase in a high concentration range of ethane. At 308.05 K (a temperature above the critical temperature of ethane) the phase envelope presents a critical behaviour. Experimentally, the supercritical state was observed, showing a disappearance of the vapour and liquid phases that is similar to a plasma growing hazy appearance inside the entire cell.

The calculation of the relative volatility was undertaken for the measured as well as the modelled data. Figure 6.14 shows a plot of the relative volatility versus the liquid molar fraction. The error bars on the measured data are set to 5%. Both the measured and the modelled data show an excellent agreement as can be seen from Figure 6.14.

The regressed parameters are presented in Table 6.14. Their correlations with temperatures are shown in Figure 6.15 for τ_{ji} and τ_{ij} and in Figure 6.16 for kij.

The regressed parameters seem to be independent of temperature except at low temperature (264.05 K). This behaviour carries on even above the critical temperature of ethane. At 264.05 K, a different behaviour is noticed in the trend-line. The explanation could be a failure of the thermodynamic models to regress the VLE data at low temperatures. A discontinuity in the trend (above the critical temperature of ethane) is also expected. Further measurement at low temperatures and above the critical temperature of ethane will confirm these hypotheses.

Table 6.14: Model parameters regressed with the PRMCWS+NRTL model for the octafluoropropane (1) + ethane (2) system

	Temperature (K)				
Parameters	264.04	271.04	278.05	303.05	308.05
τ_{12} **(J * mol^{-1})**	2284	4074	3914.3	3890	3766
τ_{21} **(J * mol^{-1})**	187.7	-149.0	-155.9	-361.1	-71.4
k_{12}	0.4	0.3	0.3	0.3	0.3

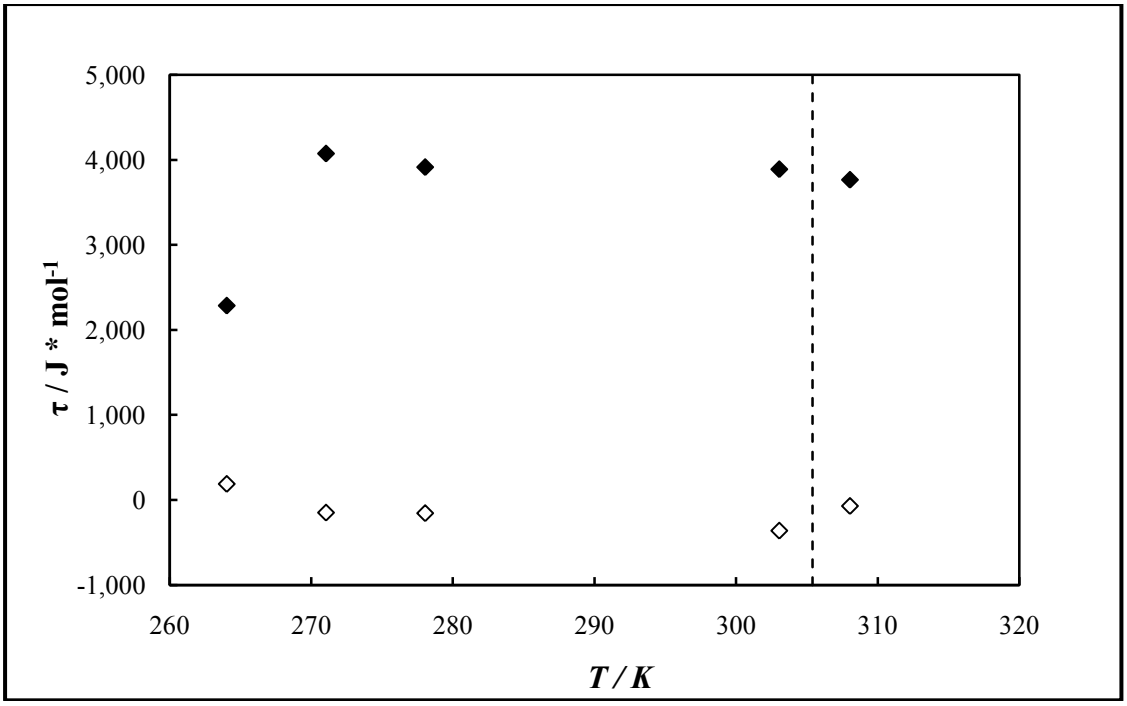

Figure 6.15: Plot of the NRTL model parameters versus the temperature for the five isotherms measured (♦, τ_{12}; ◊, τ_{21}; - - -, critical temperature of ethane) for the octafluoropropane (1) + ethane (2) system

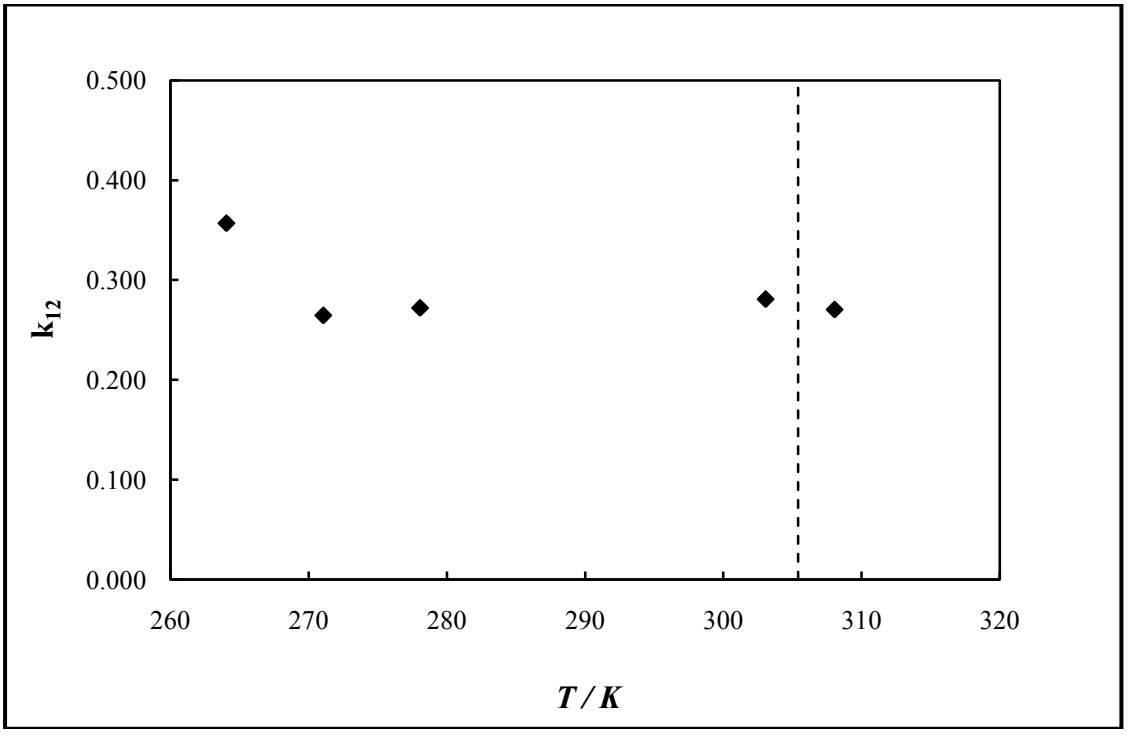

Figure 6.16: Plot of the Wong Sandler binary interaction parameter (k_{12}) versus temperature for the five isotherms measured (- - -, critical temperature of ethane) for the octafluoropropane (1) + ethane (2) system

The relative deviation, BIASU and the AAD obtained are presented in Table 6.15. The results obtained for both the BIASU and the AAD lie within ± 2.5 %.

Table 6.15: Relative deviation, BIASU and the AAD obtained by comparing measured VLE data with the modelled (PRMCWS+NRTL) data

T / K	Bias *x* %	AAD *x* %	Bias *y* %	AAD *y* %
264.05	-0.42	1.57	0.62	0.98
271.05	1.43	0.48	1.15	1.30
278.05	-0.10	0.97	0.73	0.93
303.04	-0.34	1.08	-0.29	1.22
308.04	0.05	1.05	-0.95	1.76

6.3.3 HFPO (1) + propane (2) binary system

This system has previously never been measured. Measurements were performed for three isotherms exhibiting azeotropic behaviour. The critical properties of both HFPO and propane are presented in Appendix B.

The GC calibrations plots for pure HFPO and propane as well as their relative differences on the number of moles are presented in Figures 6.17, 6.18, 6.19 and 6.20, respectively. The P-x-y data at 283.05, 303.05 and 323.05 K are presented in Table 6.16. Figure 6.21 compares the new experimental data with the correlated data. And at last, a graphical comparison of the relative volatility for both the experimental and the modeled data is presented in Figure 6.22.

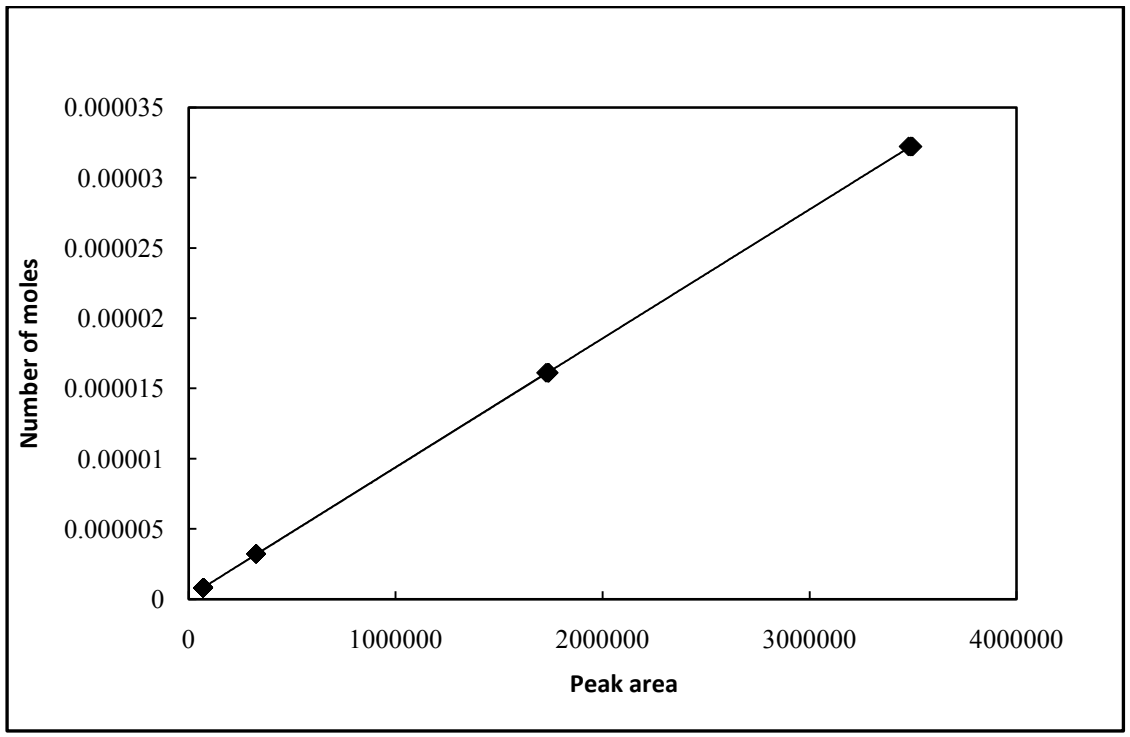

Figure 6.17: GC calibration plot for pure HFPO

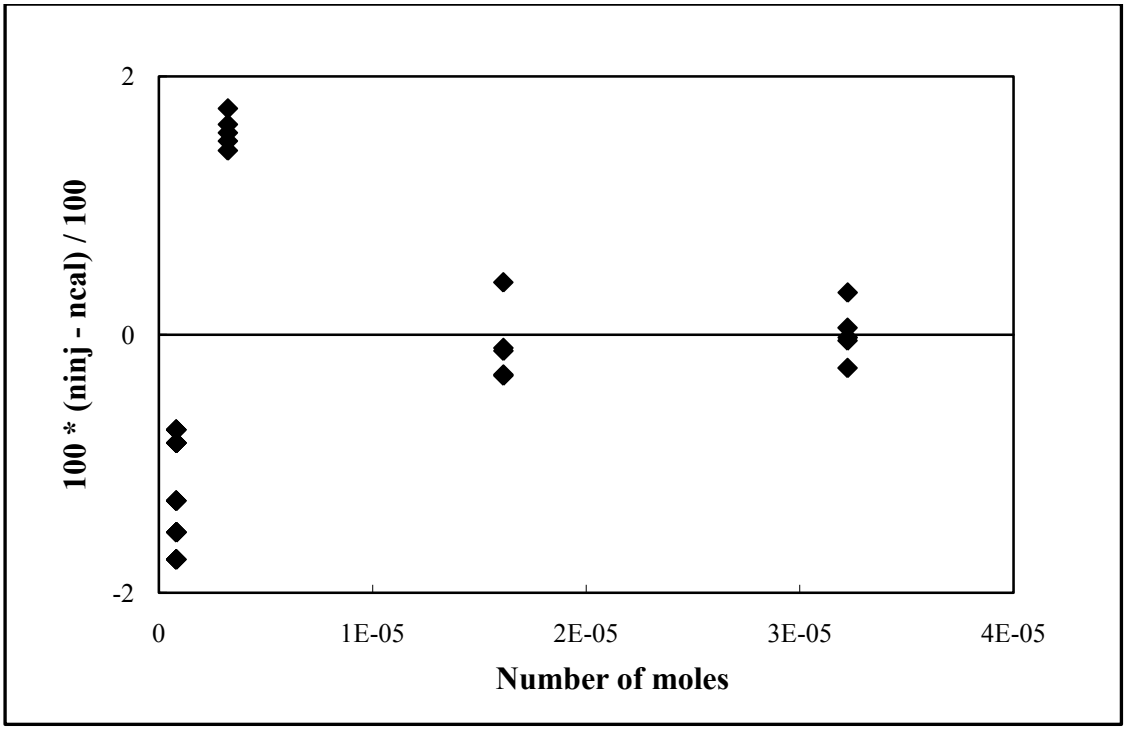

Figure 6.18: Relative difference for HFPO on the number of moles

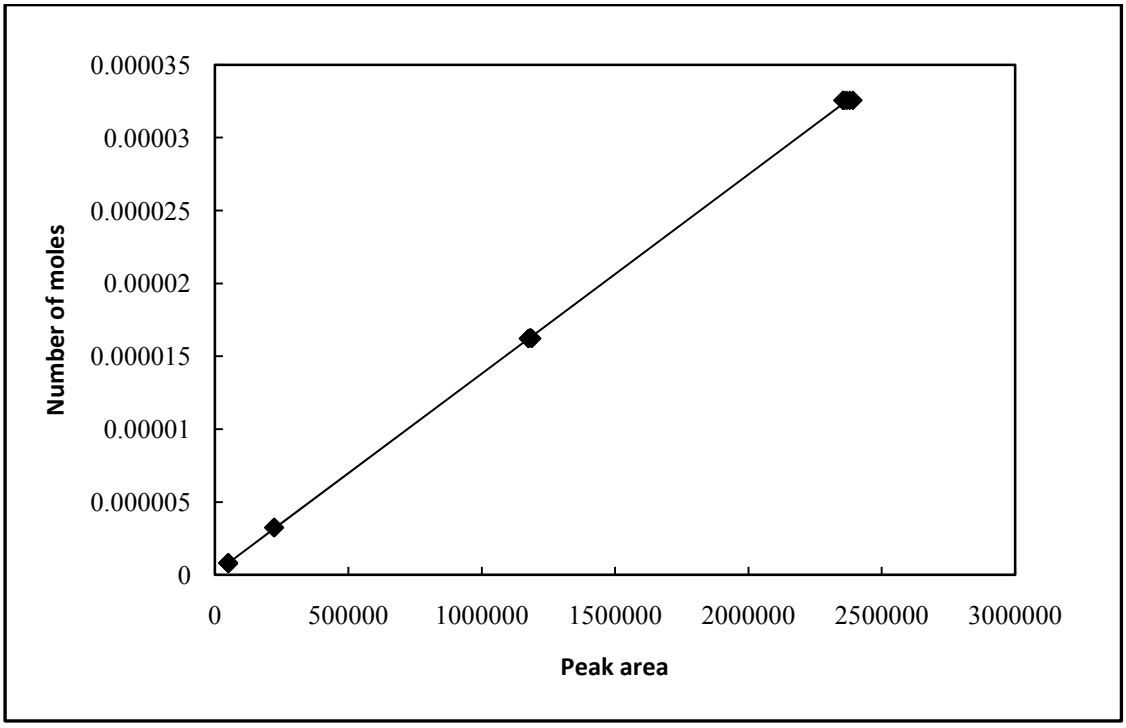

Figure 6.19: GC calibration plot for pure propane

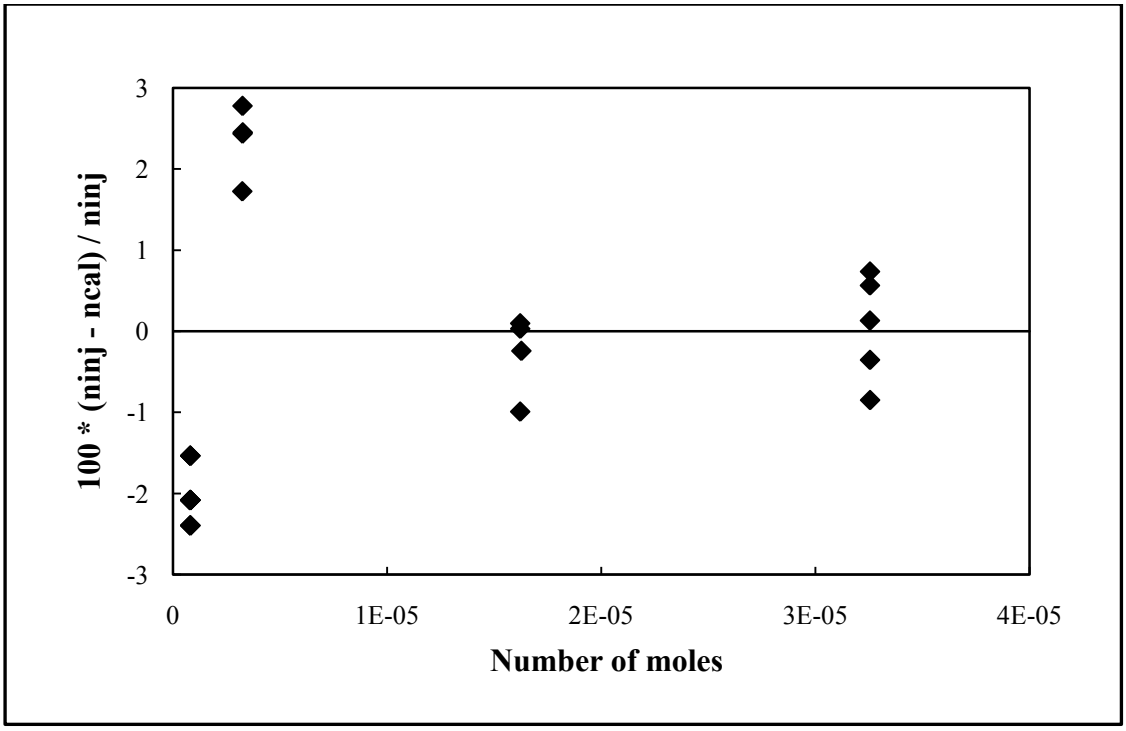

Figure 6.20: Relative difference for propane on the number of moles

The maximum uncertainty in the determination of mole fractions is estimated to be within ± 4.2 % for both pure propane and pure HFPO.

Table 6.16: P-x-y data for the HFPO (1) + propane (2) system

Pressure (MPa)	x_1	y_1
	T = 283.05 K	
0.437	0.000	0.000
0.528	0.074	0.223
0.600	0.166	0.361
0.643	0.235	0.433
0.691	0.343	0.514
0.723	0.434	0.566
0.736	0.477	0.591
0.742	0.502	0.600
0.748	0.540	0.618
0.748	0.696	0.692
0.685	0.950	0.897
0.629	1.000	1.000
	T = 303.05 K	
0.787	0.000	0.000
0.915	0.081	0.185
1.009	0.164	0.303
1.072	0.222	0.369
1.157	0.333	0.464
1.225	0.476	0.558
1.260	0.646	0.657
1.256	0.778	0.743
1.233	0.853	0.799
1.159	0.953	0.914
1.070	1.000	1.000
	T = 323.05 K	
1.324	0.000	0.000
1.511	0.091	0.154
1.684	0.193	0.284
1.790	0.277	0.368
1.885	0.374	0.447
1.959	0.488	0.524
1.987	0.556	0.577
2.000	0.622	0.629
1.956	0.827	0.796
1.909	0.887	0.841
1.817	0.956	0.928
1.703	1.000	1.000

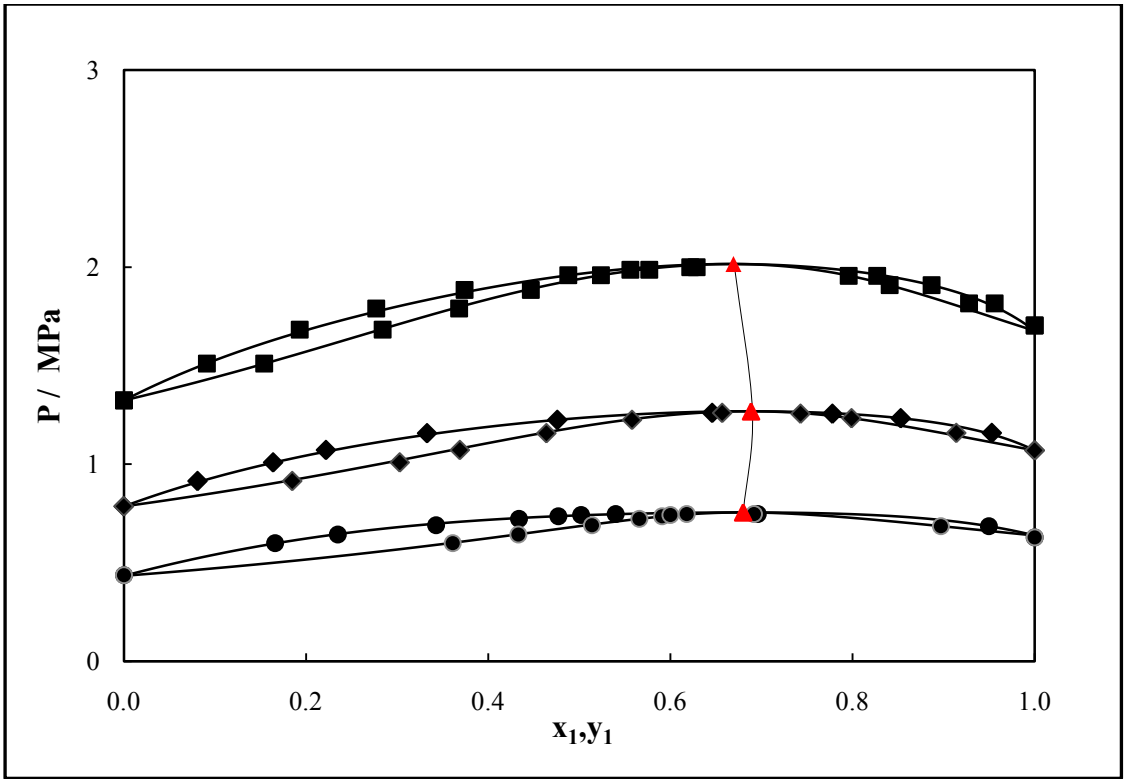

Figure 6.21: Plot of the P-x-y data for the HFPO (1) + propane (2) system; ●, 283.05 K; ♦, 303.05 K; ■, 323.05 K; —, —▲—▲— , azeotropic line, (—) model

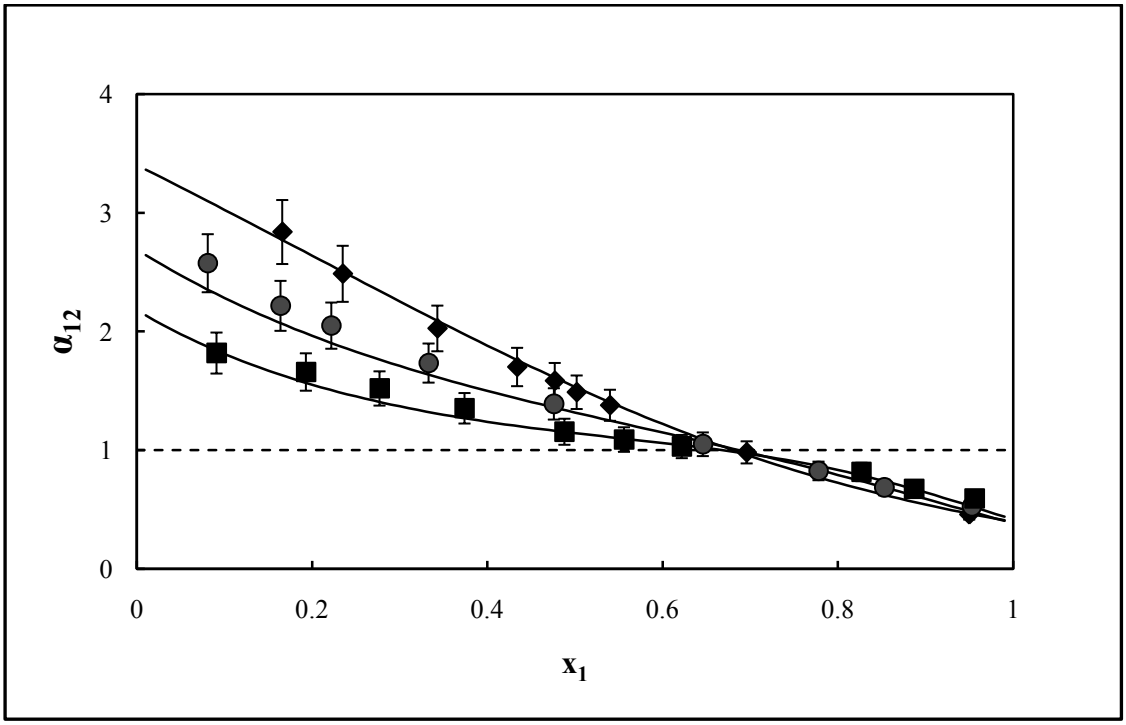

Figure 6.22: Plot of the relative volatility versus x_1 for the system HFPO (1) + propane (2); ♦, 283.05 K; ●, 303.05 K; ■, 323.05 K; ▲ and —, modeled data. Error bars are shown at 9.5 %.

Taking into account the relative deviation in the number of moles due to calibrations, the measured data are presented with a resulting uncertainty of less than 2% for both the vapour and the liquid mole fraction.

This system revealed an azeotrope for each isotherm studied. The azeotropic composition has been calculated to be about 0.68, 0.68 and 0.66 at 283.05, 303.05 and 323.05 K, respectively. The azeotrope composition did not vary at temperatures ranging from 283.05 to 303.05 K, however a slight difference could be noticed at 323.05 K. From the results obtained, one could say that: the azeotropic composition tends to be richer in propane as the temperature increases.

The relative volatility for both the measured and the modelled data were calculated and presented in Figure 6.22 as a relative volatility versus the liquid molar fraction plot. This does not only indicate the ease or difficulty of using the distillation to separate the more volatile component from the heavier one in a mixture but it also shows the coherence between the measured and the modelled data. However, the data measured were compared with the modelled data and found to be coherent except at low concentrations for isotherms measured at 283.05 and 303.05 K where a slightly deviation was noticed.

The model parameters regressed with the PRMCWS + NRTL model are presented in Table 6.17. Graphical presentations of the NRTL model parameter and the Wong-Sandler binary interaction parameter versus temperature are shown in Figures 6.23 and 6.24, respectively.
The results obtained show the behaviour of the regressed parameters below the critical temperature of propane, the light component.

Table 6.17: Model parameters regressed with the PRMCWS+NRTL model for the HFPO (1) + propane (2) system

	Temperature / K		
Parameter	283.05	303.05	323.05
τ_{12} (J * mol^{-1})	3128	5763	6953
τ_{21} (J * mol^{-1})	46.7	1648.6	2597.9
k_{12}	0.3	-0.1	-0.2

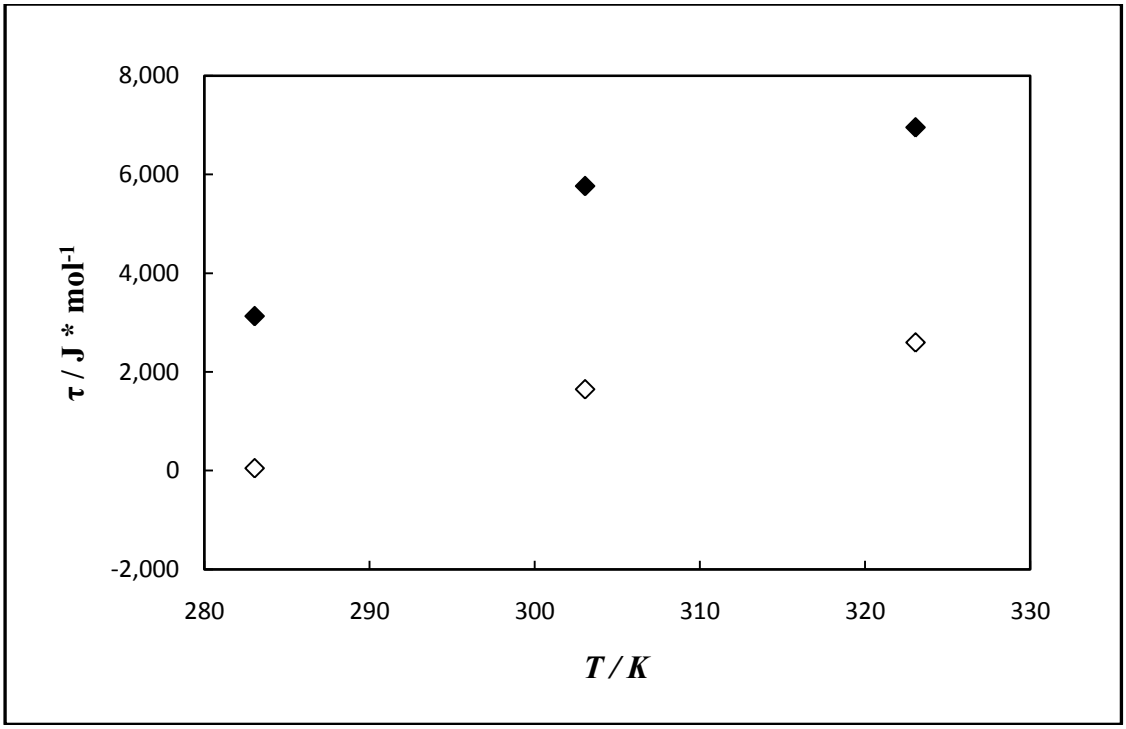

Figure 6.23: Plot of the NRTL model parameters versus the temperature for the three isotherms measured (♦, τ_{12}; ◊, τ_{21}) for the HFPO (1) + propane (2) system

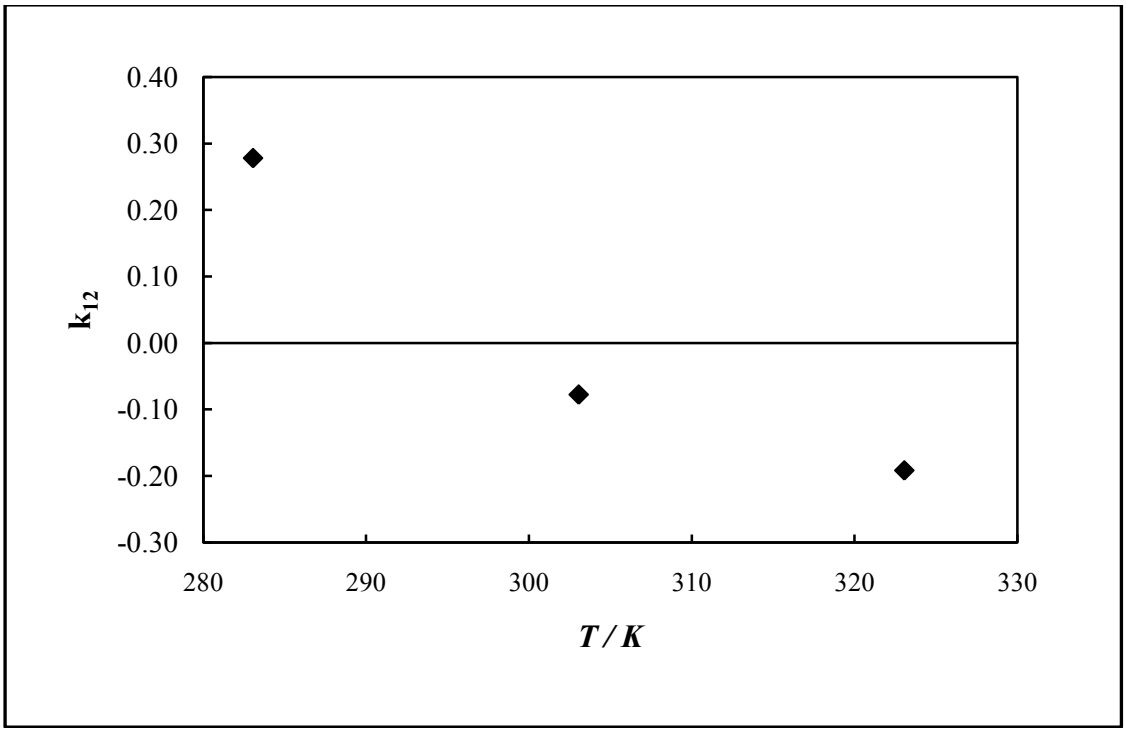

Figure 6.24: Plot of the Wong Sandler binary interaction parameter (k_{12}) versus temperature for the three isotherms measured for the HFPO (1) + propane (2) system

The relative deviation, BIASU and the AAD between the experimental and the modelled data is presented in Table 6.18. The results obtained show a deviation of 2.04 % as the highest, for both the BIASU and AAD.

Table 6.18: Relative deviation of AAD and BIASU obtained by comparing experimental VLE data with the modelled (PRMCWS+NRTL) data

T / K	Bias *x* %	AAD *x* %	Bias *y* %	AAD *y* %
283.05	0.63	2.03	0.63	0.77
303.05	-1.29	2.04	1.49	1.77
323.05	--0.78	2.02	0.87	0.90

6. 4 Thermodynamic consistency testing

Different thermodynamic consistency tests are obtained by different manipulations of the Gibbs-Duhem equation. These tests serve as a confirmation for thermodynamic consistency of the experimental data. Several tests are described in section 3.5 of chapter three

The point test of Van Ness et al. (1973) was utilized for the ethane (1) + octafluoropropane (2) and the HFPO (1) + propane (2) binary systems for all isotherms measured.

6.4.1 Octafluoropropane (1) + ethane (2) system

The point test establishes a comparison between the measured and the calculated vapour mole fraction of the light component. The test requires the average of the absolute deviation of the vapour mole fraction to be 0.01 for the experimental VLE data to be thermodynamically consistent.

Isothermal VLE data measurements for the binary system involving ethane (1) + octafluoropropane (2) were performed at five temperatures (264.05, 271.05, 278.05, 303.04, and 308.04 K) and the measured data were regressed following the modelling procedure described in section 6.3.2. A comparison of the measured vapour mole fraction with the calculated ones was undertaken and yielded an average absolute deviation of less than 0.01 for all isotherms measured. The measured data is therefore considered to be thermodynamically consistent.

The results obtained for each isotherm are presented in Table 6.19. A graphical representation is also shown in Figure 6.25.

Table 6.19: Point test results for the average absolute deviation of the vapour mole fraction of ethane for the ethane + octafluoropropane system

Temperatures / K	Average $\lvert\Delta y_1\rvert$
264.05	0.006
271.05	0.006
278.05	0.005
303.04	0.007
308.04	0.006

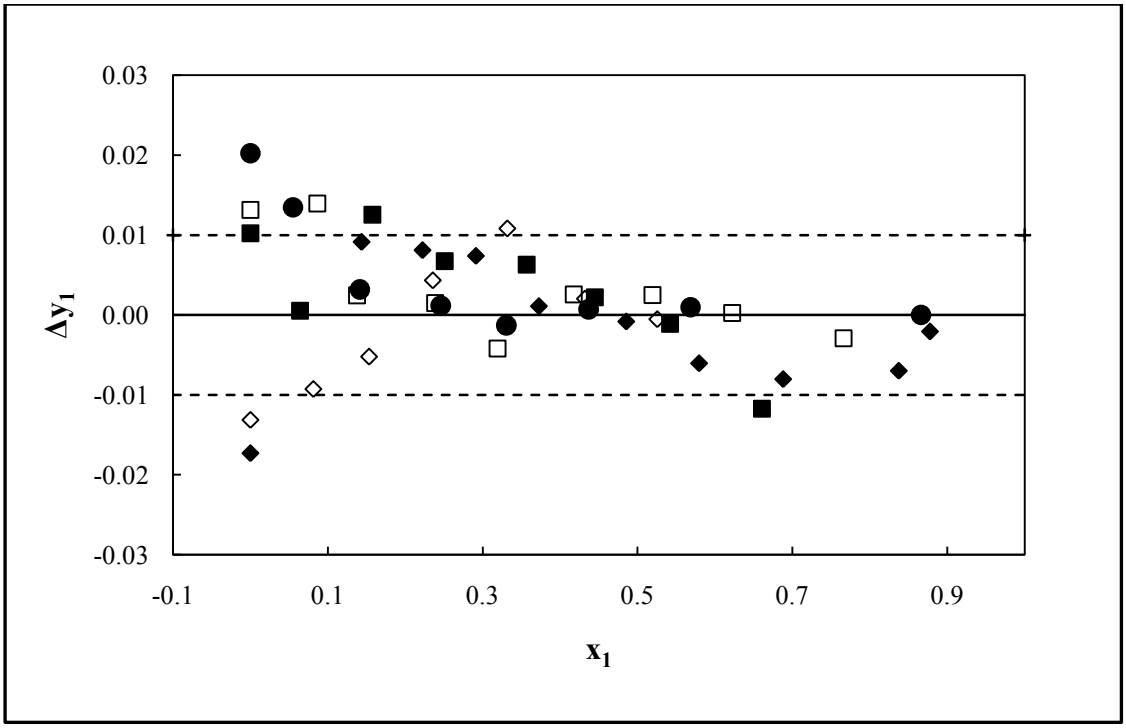

Figure 6.25: Plot Δy_1 versus x_1 for five isotherms (■, 264.05 K; ●, 271.05 K; □, 278.05 K, ♦, 303. 05 K; ◊, 308.04 K; - - - , boundary lines for the point test) for the ethane + octafluoropropane system

6.4.2 HFPO (1) + propane (2) binary system

The point test was once again employed to check the thermodynamic consistency of the experimental VLE data for the system consisting of HFPO (1) + propane (2). Measurements were performed for three isotherms; 283.05, 303.05 and 323.05 K.

An average absolute deviation between the measured and the calculated vapour mole fraction of HFPO was undertaken. This yielded values less than 0.01 for all isotherms measured. The experimental VLE data are thus considered to be thermodynamically consistent according to the point test.

The results obtained are listed in Table 6.20 and are presented in Figure 6.26.

Table 6.20: Point test results for the average absolute deviation of the vapour mole fraction for the HFPO + propane system

Temperatures / K	Average $\|\Delta y_1\|$
283.05	0.004
303.05	0.008
323.05	0.005

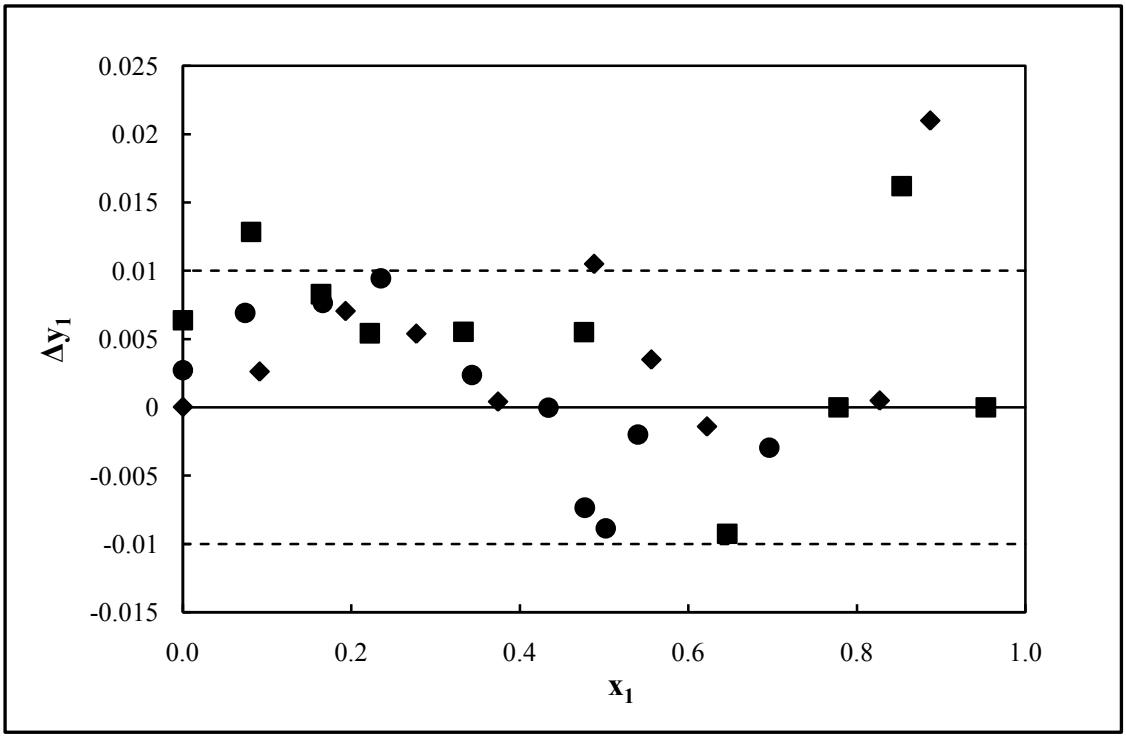

Figure 6.26: Plot Δy_1 versus x_1 for three isotherms (●, 283.05 K; ■, 303.05 K; ♦, 323. 05 K; - - - , boundary lines for the point test) for the HFPO + propane system

CHAPTER

SEVEN

CONCLUSIONS

The primary objectives of this project were to construct and commission a new static analytical apparatus capable of measuring high-pressure vapour-liquid equilibrium data in a range of temperatures for multicomponent systems involving fluorochemicals components.

Its operating conditions ranged from low temperatures to 373.15 K and absolute pressures ranging from 0 up to 10 MPa.

The new apparatus incorporates the ROLSI ^{TM}; a novel technique for online sampling of phases in thermodynamic equilibrium. A GC equipped with both the FID and TCD detector was used for sample analysis.

Isothermal VLE data measurements were performed for three binary systems involving R116 (1) + propane (2), ethane (1) + octafluoropropane (2) and HFPO (1) + propane at various temperatures and high pressures.

VLE data measurements for the R116 (1) + propane (2) binary system were performed at 263.15 K in order to verify the reliability of the equipment. The measured data were compared to the ones of Ramjugernath [2000]. Excellent agreement was found attesting to the proper functioning of the apparatus and the experimental procedure. The new experimental apparatus was therefore deemed to provide sufficiently accurate HPVLE data.

VLE data for the Ethane (1) + octafluoropropane (2) binary system were measured for five isotherms. Measurements at 264.05, 271.05 and 278.05 K presented similar behaviour unlike the behaviour measured at 303.04 K (temperature near the critical temperature of ethane). Very close compositions for both the vapour and the liquid phase were, however, noticed in a high concentration range of ethane. At 308.04 K (the supercritical region of ethane), critical behaviour was noticed. The measured data constitute a novel set of VLE data.

Three isotherms were measured for the HFPO (1) + propane (2) binary system at 283.05, 303.05 and 323.05 K. The data had not been measured previously and therefore constituted new sets of VLE data.

The HFPO (1) + propane (2) binary system revealed a homogeneous azeotrope for each isotherm measured. The azeotropes' compositions were revealed respectively at 0.68, 0.68 and

0.66 at 283.05, 303.05 and 323.05 K. It has been found that the azeotropic composition decreases with an increase in temperature.

Separation for components involving this binary system is feasible using two distillation columns, operating at two different pressures and temperatures.

The measured VLE data for systems investigated and enumerated above were regressed using thermodynamic models. The direct method using the Peng-Robinson equation of state with the Mathias-Copeman alpha function and the Wong-Sandler mixing rules utilizing the NRTL activity coefficient model was employed. The model parameters were adjusted onto the experimental data through a modified simplex algorithm using the flash calculation objective function. Deviations from experimental and calculated liquid and vapour mole fractions were determined from AAD and BIASU and found to be within 2.04 % for systems newly measured.

The thermodynamic models chosen correlated well the data except the data measured at low temperature for the octafluoropropane + ethane system. The model parameters seemed to be independent of temperature when temperature is greater than 271 K, but that is not the case for the lower temperature, 264.05 K.

Finally, the measured data were subjected to the thermodynamic consistency test. The point test indicated that all the binary systems measured for this project were deemed to be thermodynamically consistent.

CHAPTER

EIGHT

RECOMMENDATIONS

Modifications to the new static-analytical apparatus to improve measurements of VLE data near the critical region are suggested. Other recommendations include further measurements to fully describe the behaviour of systems investigated in this research study.

8.1. Positioning of the ROLSI^{TM} capillary

Measurements of VLE data near the critical region has been quasi-impossible using the new static analytical apparatus. This is explained by the difficulty to accurately position the ROLSI capillary in either the vapour or liquid phase present in the equilibrium cell. A solution could be the use of a ROLSI sampler with two capillaries (one for the vapour phase and the other for the liquid phase) or a transparent liquid bath.

8.2 Future work

In terms of fully describing the phase behaviour, there was not enough time to measure VLE data for systems of interest at various temperatures and pressures. The VLE data measurements for the Ethane (1) + octafluoropropane (2) and the HFPO (1) + propane (2) systems were only performed at conditions below the critical region of their light components. Further VLE data measurements (above the critical region) of theses will help describing their behaviour.

REFERENCES

Abbott, M M and Prausnitz, J M, (1987), "Generalized Van der Waals Theory: A Classical Perspective", *Fluid Phase Equilibria*, Vol. 37(1), pp. 29-62.

Ashcroft, S J, Shearn, R B and Williams, G J J, (1983), "A visual Equilibrium Cell for Multiphase Systems at Pressures up to 690 Bar", *Chem. Eng. Res. Dev*., Vol. 61, pp. 51-55.

Bertucoo, A M Barolo and Erlvassore, N, (1997), "Thermodynamic Consistency of Vapour-Liquid Equilibrium Data at High-Pressure*", AIChE J*., Vol. 43(2), pp. 547-554.

Besserer, G J and Robinson, D B, (1971), "A High Pressure Autocollimating refractometer for Determining Coexisting Liquid and Vapour phase Densities," *Can. J. Chem. Eng*., Vol. 49, pp. 651-656.

Bradshaw, S M, (1985), "A Static Equilibrium Cell for High-Pressure and Temperature Vapour-Liquid Equilibrium Measurements", MSc. Eng. Dissertation, school of chemical Engineering, University of Natal, Durban, South Africa.

Bouchot, C and Richon, D, (1998), "Direct Pressure-Volume-Temperature and Vapour-Liquid Equilibrium Measurements with a Single Equipment Using a Vibrating Tube Densimeter up to 393 K and 40 MPa: Description of the Original apparatus and New Data", *Ind. Eng. Chem. Res*., Vol. 37, pp. 3295-3304.

Christiansen, L J and Fredenslund, A, (1975) "Thermodynamic Consistency Using Orthogonal Collocation of Computation of Equilibrium Vapour Compositions at High-Pressures", *Fluid Phase equilibria*, Vol. 71, pp. 63-83.

Chueh, P L, Muirbrook, N K and Prausnitz, J M, (1965), "Part 2. Thermodynamic Analysis", *AIChE J*., Vol. 11(6), pp. 1097-1102.

Coquelet, C, (2003), "Etude des Fluides Frigorigènes. Mesures et Modélisations", Thèse de doctorat, Ecole des Mines de Paris, France.

Deiters, U K and Schneider G M, (1986), "High-Pressure Phase Equilibria: Experimental Methods", *Fluid Phase Equilibria*, Vol. 29, pp. 145-160.

Dohrn, R, Bünz A P, Devlieghere, F and Thelen, D, (1983), "Experimental Measurements of Phase Equilibria for Ternary and Quaternary Systems of Glucose, Water, CO2 and Ethanol with a Novel Apparatus", *Fluid Phase Equilibria*, Vol. 83, pp. 149-158.

Dorau, W, Kremer, H W and Knapp, H, (1983), "An Apparatus for the Investigation of Low temperature, High-Pressure, Vapour-Liquid and Vapour-Liquid-Liquid Equilibria", *Fluid Phase Equilibria*, Vol. 11, pp. 83-89.

Francisco, J S and Maricq, M M, (1996), "Making Sure That Hydrofluorocarbons Are Ozone Friendly", *Acc. Chem. Res*., 29(8), pp. 391-397.

Fredenslund, Aa, Mollerup, J and Christiansen, L J, (1973), "An Apparatus for Accurate Determinations of Vapour-Liquid Equilibrium Properties and Gas PVT Properties", *Cryogenics*, Vol. 13 (1), pp. 1086-1099.

Freitag, N P and Robinson, D B, (1986), "Equilibrium Phase Properties of the Hydrogen-Methane-Carbon Dioxide, Hydrogen-Carbon Dioxide-n-Pentane Systems" *Fluid Phase Equilibria*, Vol. 31, pp. 183-201.

Galicia-Luna, L, Richon, D and Renon, H, (1994), "New Loading Technique for a Vibrating Tube Densimeter and Measurements of Liquid Densities up to 39.5 MPa for Binary and Ternary Mixtures of Carbon-Dioxide-Methanol-Propane system" J. *Chem. Eng. Data*, Vol. 24, pp. 424-431.

Guadalupe Silva-Olivier, Gaudenico Eliosa-Jiménez, Fernando Garcia-sànchez and Juan R Avendano-Gomez, (2006) "High-Pressure Vapour-Liquid Equilibria in the nitrogen-n pentane system", *Fluid Phase Equilibria*, Vol. 20, pp. 37-48.

Guibot P, Valtz A, Legendre H and Richon D, (2000), "Rapid Online Sampler-Injector- A reliable Tool for HT-HP Sampling and Online Analysis". Analysis, 28, 426-431.

Madani H, Valtz, Coquelet, C, Hassem, A, Richon, D, (2008), "Vapour-liquid equilibrium data for the (hexafluoroethane +1, 1, 1, 2-tetrafluoroethane) system at temperatures from 263 to 353 K and pressures up to 4.16 MPa", *Fluid Phase Equilibria*, Vol. 268, pp. 68-73.

Heyen, G, (1981), "A cubic Equation of State with Extended range of Application", Neuman, S, (ed.), *Second world congress on Chemical Engineering*, Canada, Montreal, pp. 41-46.

Inomata, H, Kondo, T, Hirohama, S, Arai, K, Suzuki, Y and Konno, M, (1989), "Vapour-Liquid Equilibrium for Binary Mixtures of carbon Dioxide and Fatty Acid Methyl Esters," *Fluid Phase equilibria*, Vol. 165, pp. 23-40.

Jong Sun Lim, Youm Geun Jung and Ki-Pung Yoo, (2007), "High-Pressure Vapour-Liquid Equilibria for the Binary Mixtures of carbon dioxide + isopropanol (IPA)", *J.Chem. Eng. Data,* ASAP Article.

Karla, H and Robinson, D B, (1979), "Vapour-liquid Equilibrium in a six-Component Simulated Sour Natural Gas System at Sub-Ambient Temperatures," *Fluid Phase Equilibria*, Vol. 3, pp. 133-144.

Kim, K –H, Vimalchand, P and Donohue, M D, (1986), "Vapour-Liquid Equibria for Binary Mixtures of Carbon Dioxide with Benzene, Toluene and p-Xylene", *Fluid Phase Equilibria*, Vol. 31, pp. 299-311.

Kissun, S, (2001), "A Static Equilibrium Cell for Low Temperature Vapour-Liquid Equilibrium Measurements", MSc. Eng. Dissertation, University of Natal, Durban, South Africa.

Klink, A E, Cheh, H Y and Amick, E H Jr, (1975), "The Vapour-Liquid equilibrium of the Hydrogen n-Butane Systems at Elevated Pressures", *AIChE J.*, Vol. 21(6), pp. 1142-1148.

Kojima, K, Moon, H M and Ochi, K, (1990), "Thermodynamic Consistency Test of Vapour-Liquid equilibrium Data", *Fluid Phase Equilibria*, Vol. 56 pp. 269-284.

Kubota, W L, Inatome, H, Tanaka, Y and Makita, T, (1993), "Vapour-Liquid Equilibria of the Ethylene-Propylene System under High Pressure", *J. Chem. Eng. Jpn*., Vol. 16 (2), pp.99-103.

Legret, D, Richon, D and Renon, H, (1980), "Static Still for Measuring Vapour-Liquid Equilibria up to 50 Bar", *Ind. Eng. Chem. Fundam*., Vol. 19, pp. 122-126.

Legret, D, Richon, D and Renon, H, (1981), "vapour-Liquid Equilibria up to 100 MPa", *AIChE J*, Vol. 27(2), pp. 203-207.

Mathias, P M and Copeman, T W, (1983), "Extension of the Peng-Robinson Equation of State to Polar Fluids and Fluids Mixtures", *Fluid Phase Equilibria*, Vol. 13, pp. 91-108.

Matos, H A, de Azevedo, E G, Simoes P C Carrondo, M T and Numes da Ponte, M, (1989), "Phase Equilibria of Natural Flavours and Supercritical Solvents", *Fluid Phase Equilibria*, Vol. 52, pp. 357-364.

McHugh, M and Krukonis, V J, (1986), "Supercritical Fluid Extraction Principles and Practice", Butterworths, Stoneham.

Michael, M Abbott, (1986), "Low-Pressure Phase Equilibria: Measurement of VLE", *Fluid Phase Equilibria,* Vol. 29 pp. 193-207.

Michael F Doherty and Michael F Malone, (2001), "Conceptual Design of Distillation system", Boston: McGraw.

Molina, M J and Rowland F S, (1974) "Stratospheric sink for chlorofluoromethanes: chlorine atomc-atalysed destruction of ozone", *Nature*, 249, 810.

Moodley, K, (2002), "High-pressure Vapour-Liquid Equilibrium Studies at Low Temperatures", PhD thesis, University of Natal, Durban, South Africa.

Mühlbauer, A L, (1990), "Measurement and Thermodynamic Interpretation of High-Pressure Vapour-Liquid Equilibrium Data", PhD thesis, University of Natal, Durban, South Africa.

Mühlbauer, A L and Raal J D, (1991), "Measurement and Thermodynamic Interpretation of High-Pressure Vapour-Liquid Equilibria in the toluene-CO2 system", *Fluid Phase Equilibria,* Vol. 64, pp. 213-236.

Muirbrook, N K and Prausnitz, J M, (1965), "Multicomponent Vapour-Liquid Equilibria at High Pressures: Part1. Experimental Study of the Nitrogen-Oxygen-Carbon Dioxide System at 0 °C", *AIChE J.*, Vol. 11 (6), pp. 1092-1096.

Naidoo, P, (2004), "High-Pressure Vapour-Liquid Equilibrium Studies", PhD thesis, University of Kwa-Zulu Natal, Durban, South Africa.

Nakayama, T, Sagara, H, Arai, K and Saito, S, (1987), "High-Pressure Liquid-Liquid Equilibria for the System of Water, Ethanol and 1, 1-Difluoroethane at 323.2 K", *Fluid Phase Equilibria*, Vol. 38: 109-127.

Nasir, P, Martin, R J and Kobayashi, R, (1981), "A Novel Apparatus for the Measurement of Phase and Volumetric Behaviour at High Temperatures and Pressures and its Application to Study VLE in the Hydrogen-Tetralin System", *Fluid Phase equilibria*, Vol. 5, pp. 279-288.

Naidoo, P, Ramjugernath, D and Raal, J D, (2008), "A New High-Pressure Vapour-Liquid Equilibrium Apparatus", *Fluid Phase Equilibria*, Vol. 269, pp. 104-112.

Panagiotopoulos, A Z, and Reid, R C, (1986b). "Equations of State-Theories and Applications", Chao, K C and Robinson, R (Eds.), ACS Symp. Ser. No. 300, American Chemical Society, Washington, DC.

Peng, D-Yu and Robinson, D B, (1976), "A new Two-Constant Equation of State", *Ind. Eng. Chem. Fundam.*, Vol. 15 (1), pp. 59-64.

Perry, R J and Green, D, (1984), "Perry's Chemical Engineer's Handbook, 6th Ed., McGraw-Hill, Singapore.

Pitzer, K S and Curl, R F, Jr., (1957), "The Volumetric and Thermodynamic Properties of Fluids. III, Empirical Equation for the Second Virial Coefficient", *J. Am. Chem. Soc*., Vol. 70, pp. 2369-2370.

Raal, J D and Mühlbauer, A L, (1994), "The Measurement of High Pressure Vapour-Liquid Equilibria", *Dev. Chem. Eng. Mineral Process*, Vol. 2, pp. 69-105.

Raal, J D and Mühlbauer, A L, (1995), "Computation and Thermodynamic Interpretation of High-pressure Vapour-Liquid Equilibrium- A review", *The Chemical Engineering journal and the Biochemical Engineering journal*, Vol. 60, number1 pp. 1-29.

Raal, J D. and Mühlbauer, A L, (1998), "Phase Equilibria: Measurement and Computation", Taylor and Francis, Bristol, PA.

Ramjugernath, D, (2000), "High pressure Vapour-Liquid Equilibrium Studies", PhD thesis, university of KwaZulu Natal, Durban, South Africa.

Renon, H and Prausnitz, J M, (1968), "Liquid-Liquid and Vapour-Liquid for Binary and Ternary Systems with Dibutyl Ketone, Dimethyl Sulfoxide, n-Hexane, and 1-Hexene", *Ind. Eng. Chem. Process. Des. Dev*, Vol. 7(2), pp. 220-225.

Rivolet F, Chapoy, A, Coquelet, C, Richon, D., (2004), "Vapour-liquid equilibrium data for the carbon dioxide ($C0_2$) + difluoromethane (R32) system at temperatures from 283.12 to 343 K and pressures up to 7.46 MPa", *Fluid Phase Equilibria*, 218, pp. 95-101.

Rogers, B L and Prausnitz, J M, (1970), "Sample-Extrusion Apparatus for High-Pressure Vapour-Liquid equilibria", *Ind. Eng. Chem. Fundam*., Vol. 9(1), pp. 292-293.

Sagara, H, Arai, Y and Saito, S, (1972), "Vapour-Liquid Equilibria of Binary and Ternary Systems Containing Hydrogen and Light Hydrocarbons", *J. Chem. Eng. Jpn*., Vol. 5(4), pp. 339-348.

Sandler, S I, Orbey, H and Lee, B I, (1994), "Equation of State in Models for Thermodynamic and Phase Equilibria Calculations", Sandler, S.I. (Ed), Marcel Deckert, Inc., New York, pp. 87-186.

Sandler, S I, (1997), "Chemical and Engineering Thermodynamics", 3rd edition, New York, John Wiley & sons, Inc.

Shibata, S K and Sandler, S I, (1989), "High-Pressure Vapour-Liquid Equilibria Involving mixtures of Nitrogen, Carbon Dioxide, and n-Butane", *J. Chem. Eng. Data*, Vol. 34, pp. 291-298.

Shimawaki, K Fujii and Higashi, Y, (2002), "Precise Measurements of the Vapour-Liquid equilibria (VLE) of HFC-32/134a Mixtures using a New Apparatus", *International journal of Thermodynamics,* Vol. 23, pp. 801-808.

Silvia-Olivier G and Galacia-Luna, L A, (2002), "Vapour-liquid equilibrium data for CO_2 + 1, 1, 1, 2-tetrafluoroethane (R-134a) systems at temperatures from 329 to 354 k and pressures up to 7.37 MPa", *Fluid Phase Equilibria*, Vol. 199, pp. 213-22.

Smith, J M, Van Ness, H C and Abbott, M M, (2005), "Introduction to Chemical Engineering Thermodynamics", 7th edition, Mc Graw international Edition, chemical Engineering series, Singapore.

Staby, A and Mollerup, J, (1991), "Measurement and Solubilities of 1-Pentanol in Supercritical Ethene", *J. Supercritical Fluids*, Vol. 4, pp. 223-237.

Stein, F P, Stener, C J and Geist, J M, (1962), "Vapour-Liquid Equilibrium Apparatus for Cryogenic Systems", *Chem. Eng. Progr.,* Vol. 58, pp. 70-73.

Tanaka, H, Yamaki, Y and kato, M, (1993), "Solubility of Carbon Dioxide in Pentadecane, Hexadecane, and Pentadecane + Hexadecane" *J. Chem. Eng. Data*, Vol. 38, pp. 386-388.

Tsonopoulos, C, (1974), "An empirical correlation of second Virial coefficients", *AIChE J.*, Vol. 20, pp. 263-272.

Uusi-Kyyny, P, (2004), "Vapour-Liquid Equilibrium Measurements for Process Design", Chemical Engineering report Series, Helsinki University of Technology.

Valtz, A, Coquelet, C, Baba-Ahmed, A and Richon D, (2002), "Vapour-Liquid Equilibrium data for the propane + 1,1,1,2,3,3,3-heptafluoropropane (227ea) system at temperatures from 293.16 to 353.18 K and pressures up to 3.4 MPa", *Fluid Phase Equilibria*, Vol. 202, pp. 29-47.

Van Ness, H C, Byers, S M and Gibbs, R E, (1973), "Vapour-Liquid equilibrium: An apparatus of Data Reduction Methods" *AIChE J.,* Vol. 19 (1), pp. 238-244.

Vetere, A, (2000), "A Simple Modification of the NRTL Equation", *Fluid Phase Equilibria*, Vol. 173, pp. 57-64.

Viera de Melo, S A B, Pallado, P, Guarise G B and Bertucoo, A, (1999) "High-Pressure Vapour-Liquid Equilibrium Data for Binary and Ternary Systems formed by supercritical CO2, LIMONENE AND LINALOOL", *Braz. J. Chem. Eng*, Vol. 16 n.1.

Wagner, Z and Wichterle, I (1987), "High-Pressure Vapour-Liquid Equilibrium in Systems Containing Carbon Dioxide, 1-Hexene, and N-Hexene", *Fluid Phase Equilibria*, Vol. 33, pp. 109-123.

Walas, S M, (1985), "Phase Equilibria in Chemical Engineering", Butterworth Publishers, Stoneham, MA.

Weber, W, Zeck, S and Knapp, H, (1984), "Gas Solubilities in Liquid Solvents at High-Pressures: Apparatus and Results for Binary and Ternary Systems of N_2, CO_2 and CH_3OH", *Fluid Phase Equilibria,* Vol. 18, pp. 253-278.

Wichterle, I, (1978a), "High-Pressure Vapour-Liquid Equilibria. IV-quantitative Description. Part 2", *Fluid Phase equilibria*, Vol. 2, pp. 59-78.

Wichterle, I, (1978b) "High-Pressure Vapour-Liquid Equilibria. V-Quantitative Description. Part 3," *Fluid Phase equilibria*, Vol. 2, pp. 143-159.

Won K W and Prausnitz, J M, (1973), "High-Pressure Vapour-Liquid Equilibria Calculation of Partial Pressures from Total Pressure Data. Thermodynamic Consistency", *Ind. Eng. Chem. Fundam*., Vol. 12, pp. 459-463.

Wong, D S H and Sandler, S I, (1992), "A Theoretically Correct Mixing Rule for Cubic Equations of State", *AIChE J*., Vol. 38(5), pp. 671-680.

APPENDICES

APPENDIX A

A.1 GC calibration

The GC calibration was undertaken using the direct method. This is justified since binary systems being investigated are made of volatile components. Thus, standards solutions containing a mixture of both components of the binary systems could not be prepared. The direct method is based on an idea such as the number of moles of any component introduced into the GC is directly proportional to the GC peak area generated. The results may be regressed using either a linear or a polynomial equation depending on what gives a better a representation.

Linear regression: $A_i = C_i * n_i + D_i$

Polynomial regression (second order): $A_i = C_{1,i} * n_i^2 + C_{2,i} * n_i + D_i$

GC calibrations for propane, hexafluoroethane (R116), octafluoropropane (R218), ethane and hexafluoropropylene oxide (HFPO) were performed. Since all components were gaseous, the GC calibration procedure was similar. However, only the GC calibration procedure for propane will be presented.

GC calibration for propane

Different volumes of the gas propane injected into the GC were withdrawn directly from the bottle using a syringe. The bottle was equipped with a regulator in connection with a tube whereby a septum was attached at one end. The pressure on the regulator was set to a constant value (0.2 MPa) during the entire calibration. Two syringes of a total volume of 100 µl and 1 ml manufactured by SGE were at our disposal. Before withdrawing the final sample, syringes were flushed out five times with the propane gas sample. Afterwards, each volume within the range of the syringes was injected several times and only results that correlated to within 1% was considered. A careful note of temperature and atmospheric pressure was taken at each injection. This helped in the calculation of the number of moles of each volume injected.

The conversion of the volume injected into the number of moles was possible using the iterative virial EoS whereby the second virial coefficient was calculated from the Tsonopoulos correlation. An iteration procedure was required to get the molar volume. Knowing the volume

injected, one could easily work out the number of moles. One could also use the perfect gas equation to calculate the number of moles. This is justified since the pressure of the gas sample within the syringe is equal to the atmospheric pressure once withdrawn.

Iterative virial EoS:

$$V_i = \frac{RT}{P}\left(1 + \frac{B}{V_{i+1}}\right)$$

Where V_i -Molar volume of the component i [cm^3]

R-Universal gas constant [$KPa.cm^3/mol.K$]

T-Room temperature [K]

P-Atmospheric pressure [KPa]

B-second virial coefficient [cm^3]

Tsonopoulos correlation

$$B = \left(\frac{RT_C}{P_C}\right) * f_0(T_r) + \omega * f_1(T_r) + f_2(T_r)$$

$$f_0(T_r) = 0.1445 - \left(\frac{0.330}{T_r}\right) - \left(\frac{0.1385}{T_r^2}\right) - \left(\frac{0.121}{T_r^3}\right) - \left(\frac{0.000607}{T_r^8}\right)$$

$$f_1(T_r) = 0.0637 + \left(\frac{0.331}{T_r^2}\right) - \left(\frac{0.423}{T_r^3}\right) - \left(\frac{0.008}{T_r^8}\right)$$

$$f_2(T_r) = \frac{a}{T_r^6}$$

$$a = -2.188 * 10^{-11} * U_r^4 - 7.831 * 10^{-21} * U_r^8$$

$$U_r = \left(\frac{U^2 * P_C}{1.01325 * T_C^2}\right)$$

Where R-Universal gas constant [$KPa.cm^3/mol.K$]

T_c- Critical temperature [K]

P_c- Critical pressure [KPa]

T_r-Reduced temperature [K]

ω- Acentric factor

U- Dipole moment [cm]

U_r-Reduced dipole moment

Perfect gas equation

$$PV = nRT$$

Where P-Atmospheric pressure [KPa]

V-Molar volume [cm^3]

n-Number of moles

R-Universal gas constant [$KPa.cm^3/K.mol$]

T-Room temperature [K]

Calculation of number of moles

$$n = \frac{V}{V'}$$

Where V and V' are respectively the volume and the molar volume of the gas injected in the same condition of temperature and pressure. Both volumes are expressed in cm^3.

A.2 Physical properties of components investigated

The physical properties of components investigated are presented in this section. These properties are imperative in the prediction and correlation of VLE data. However, only properties that are required in the VLE data calculation are presented. These properties were obtained from the Component plus software, Thermopack software and the Dortmund Data Bank software.

Table A-1 Physical properties of chemicals used

Components	**T_C (K)**	**P_C (MPa)**	**ω**	**Z_C**
Ethane	305.4	4.884	0.098	0.285
Propane	369.95	4.246	0.152	0.28
Octafluoropropane	345.05	2.68	0.325	0.279
Hexafluoroethane	293.04	3.042	0.229	
HFPO	358.93	3.136	0.353	0.272